Doctoral Thesis

Social Factors in Motion: Quantifying the Dynamics of Dyad–Individual Collision Avoidance

GREGORJ Adrien Thibaud Marie

Division of Industrial Innovation Sciences
Graduate School of Natural Science and Technology
Okayama University

March 2025

Abstract

Analyzing the dynamics of human motion within social contexts is essential for advancing our understanding of pedestrian behavior, with broad applications in urban planning, robotics, and virtual reality. This thesis examines how social factors—encompassing both interactions and relationships—shape the collision avoidance behavior of two-person groups (dyads) encountering a single individual. Through quantifying deviations and elucidating the interplay between group and individual behaviors, this research provides novel insights into the mechanisms governing human movement in shared spaces.

The thesis begins with the development of a method to identify arm gestures in pedestrian dyads from video data. Employing signal processing techniques grounded in pitch detection, this approach reliably captures arm movement patterns, offering a foundation for understanding the role of non-verbal communication in pedestrian behavior.

Subsequently, the focus shifts to the influence of social interaction on dyad-individual encounters. The findings demonstrate that when the dyads are engaged in higher levels of interaction, mutual deviation during avoidance maneuvers of the two parties is increased. Conversely, non-interacting dyads are more susceptible to be intruded on, underscoring the dual role of interaction intensity in shaping avoidance dynamics.

Building on these results, the study incorporates social relationships into the analysis. Using a novel modeling framework inspired by the scattering problem in physics, mutual deviations are represented through a potential function. This potential exhibits a steeper gradient for strongly bonded dyads, reflecting the pronounced influence of social ties on collision avoidance strategies.

The investigation then explores asymmetries in the contributions of dyads and individuals to the collision avoidance process. Initial results reveal that individuals contribute more significantly to deviation behaviors than dyads. Further analysis, employing diverse deviation metrics and comparisons to undisturbed baseline conditions, confirms this asymmetry.

Dyads engaged in social interaction exhibit reduced responsiveness in avoidance scenarios, while pedestrians as a whole demonstrate more pronounced deviations in high-risk collision contexts, highlighting the adaptive nature of human motion.

By integrating behavioral analysis, signal processing methodologies, and theoretical modeling, this thesis constructs a comprehensive framework for understanding the impact of social factors on pedestrian collision avoidance. These findings hold significant implications for the design of socially aware systems and environments capable of accommodating the complexities of human interactions.

Contents

List of Figures

List of Tables

Chapter 1

Introduction

Present in all aspects of our lives, human motion is a particularly complex phenomenon that is shaped by a multitude of factors, including but not limited to environmental conditions, individual characteristics, and social settings. Understanding the dynamics of human movement is crucial for a wide range of applications, from designing pedestrian-friendly urban spaces [1, 2] to developing autonomous systems capable of navigating shared environments [3, 4]. In particular, the study of pedestrian behavior has garnered significant interest in recent years, driven by the need to optimize crowd flows with always increasing urbanization and the rise of autonomous vehicles.

The study of pedestrian motion spans multiple scales, each offering unique insights into the underlying dynamics. At the smallest scale, the focus lies on the biomechanics of individual motion, such as the movement of limbs, motor control, postural adjustments, and balance mechanisms that enable stable locomotion [5, 6]. At the microscopic scale, research examines the behaviors of individual pedestrians and small groups, exploring patterns of gait, path selection, and the intricacies of collision avoidance in dynamic environments [7, 8]. At the macroscopic scale, the attention shifts to crowd dynamics, where the collective movement of large groups reveals emergent behaviors influenced by density, flow, and social interactions [9]. These interconnected scales provide a comprehensive framework for understanding pedestrian motion in its entirety.

Modeling the dynamics of pedestrians at these scales is a challenging task, requiring a multidisciplinary approach that integrates insights from physics, psychology, computer science, and engineering. Physics-inspired models, such as floor fields and force-based models, offer a theoretical foundation for understanding crowd dynamics [10], emphasizing collective motion and interaction forces that guide pedestrian flow. On the other hand, agent-based models focus on the cognitive and decision-making aspects of pedestrian behavior, simulating individuals as autonomous agents with goals and reactive capabilities [11]. Data-driven approaches have also gained prominence, leveraging advances in computer vision and machine learning to analyze pedestrian trajectories and train models that predict motion [12, 13].

Social factors have been recognized as key determinants of pedestrian behavior, influencing group dynamics [14, 15]. Social interactions, such as conversations, gestures, and shared attention and social relationships, such as friendship, trust, and familiarity, can influence the dynamics of group behaviors, affecting the cohesion and responsiveness of pedestrians in shared spaces. By quantifying the effects of these social factors on pedestrian motion, we can gain valuable insights into the mechanisms governing human behavior and inform the design of socially aware systems and environments.

Collision avoidance is a fundamental aspect of pedestrian behavior, essential for ensuring safe and efficient movement in shared spaces. The ability to navigate around obstacles, avoid collisions with other pedestrians, and maintain a clear path is a critical skill that pedestrians must master to move through crowded environments. By studying the dynamics of collision avoidance, we can gain insights into the strategies pedestrians employ and the factors that influence their decisions.

This thesis focuses on investigating the effects of social factors on collision avoidance behaviors, particularly in scenarios involving two-person groups (dyads) and single pedestrians. By analyzing deviations in trajectories and the interplay of individual and group behaviors, this work aims to shed light on the role of social interactions and relationships in shaping avoidance strategies. The research combines behavioral studies, signal processing techniques, and theoretical modeling to provide a comprehensive view of these dynamics.

In Chapter 2, the research begins with a preliminary study on detecting arm gestures in pedestrian dyads, as a first step towards quantifying the intensity of social interactions in groups. Arm gestures are a common form of non-verbal communication that can convey information, emotions, and intentions, playing a crucial role in social interactions. By identifying arm gestures in pedestrian dyads, we can gain insights into the dynamics of non-verbal communication and its impact on group behaviors. Using signal processing techniques inspired by pitch detection, the proposed approach decouples arm oscillations from gestures, enabling the detection of non-verbal communication patterns. The results demonstrate the

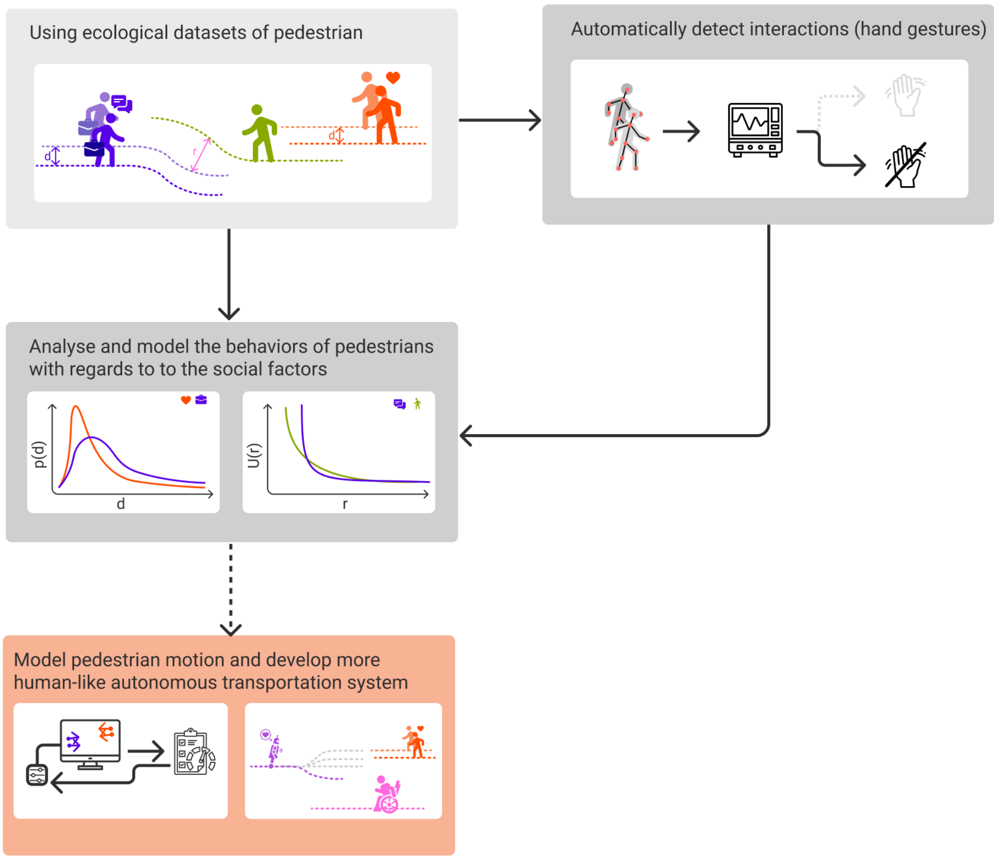

Figure 1.1: Overview of the research flow.

robustness of the method and its potential applications in studying group dynamics.

In Chapter 3, the focus shifts to the impact of social interaction on dyad-individual encounters. It is shown that dyads engaged in more intense interactions exhibit greater mutual deviations during collision avoidance maneuvers. Conversely, dyads with lower levels of interaction are more prone to intrusive behaviors, revealing a dual influence of interaction intensity on avoidance dynamics.

Chapter 4 extends on this idea to include an analysis of the effect of social relationships. A novel modeling framework inspired by the scattering problem in physics is employed to describe mutual deviations using a potential function. The analysis reveals that strongly bonded dyads exhibit steeper potential gradients, indicating a higher degree of coordination and cohesion in their avoidance behaviors. The probabilities of intrusion (i.e., the likelihood of one pedestrian going through a dyad) are also quantified, showing that social relationships play a significant role in shaping these probabilities.

Chapter 5 investigates asymmetries in the contributions of dyads and individuals to the collision avoidance process. Initial findings suggest that individuals contribute more significantly to deviation behaviors than dyads.

In Chapter 6, this asymmetry is further quantified using multiple deviation measures and comparisons to undisturbed baseline conditions. The results confirm that individuals play a more active role in avoidance maneuvers and that dyads engaged in social interaction demonstrate reduced responsiveness. Additional insights are gained into the adaptive nature of human motion, with pedestrians demonstrating more pronounced deviations in high-risk collision contexts.

Finally, in the concluding chapter, the findings are synthesized, highlighting their implications for the broader understanding of pedestrian dynamics. By integrating diverse methodologies and perspectives, this thesis provides a robust framework for analyzing the influence of social factors on collision avoidance. The insights gained have practical applications in designing socially aware environments and systems, from autonomous vehicles to public space planning.

Through its multidisciplinary approach, this research advances the field of pedestrian behavior analysis, offering valuable contributions

Chapter 2

Identification of arm gestures in pedestrian groups

2.1 Introduction and motivation

Nonverbal communication is a very complex and important part of human-human interaction, which relates facial expressions, postures, gestures etc. [16]. Among those, this study focuses on gestures, which may refer to different actions or behaviors in different research fields. Namely, taking a *purely mechanical standpoint*, gestures can be defined as the deployment of -upper- limbs in interaction. On the contrary, taking a *social signal processing standpoint*, gestures can be dealt in regard to their implications [17][1]. Nevertheless, irrespective of the definition (being expressive or not), some of the most prominent body parts in gesture portrayal emerge as hands and arms [18]. These fundamental components of nonverbal interaction may serve for various purposes, e.g. drawing attention (of listeners); or conveying feelings, expectations, intentions etc. [19, 20, 21].

Therefore, hand and arm gestures are studied in human-robot interaction (HRI) in a long time [22, 23, 24]. Specifically, human-robot collaboration treats gestures in a cooperation scenario. For instance, [25] examines common hand configurations of co-workers for ultimately building robots that work in collaboration with humans. Similar to [25], most human-robot collaboration studies address face-to-face communication in stationary settings (e.g. assembly line).

[1]For instance, a hand waving gesture can refer to acceptance or rejection depending on the affective state or attitude of the performer.

In this respect, we address a complex and dynamical interaction setting in a continuously evolving environment. Namely, we consider an outdoor scenario, where a robot-human pair interacts while walking. Such an interaction requires a complex coordination, where the peers stay in each other's field of view, avoid obstacles without breaking group composition and sustain their joint attention [26].

For achieving these goals, gestures are regarded to serve very useful [27]. Namely, Yucel et. al. demostrate that pedestrian groups, which perform gestures along with their interaction, move in closer proximity, with a lower speed and sustain a firm configuration as compared to no-gesture groups [27]. In other words, for avoiding an obstacle no-gesture groups tend to interrupt their interaction, re-arrange for avoiding and subsequently recover the former arrangement, whereas gesture performing groups are more conservative.

In the light of these findings, we propose a method for identification of such gestures by a robot. We first assume that -manual- gestures involve the movement of the arms for making fine-grained parts (e.g. fingers) visible to the peer. Thus, as a first step in recognition of manual gestures, we propose decoupling inherent oscillations of the arms, i.e. arm swings, and gesture periods. To that end, we investigate common gesture and no-gesture arm motion patterns of human-human pedestrian pairs. We detect gestures by exploiting the fact that the oscillatory motion of upper limbs is not affected by the view angle or distance of the human to the camera[2]. Thanks to this independence, gestures can easily be identified as a disturbance on this oscillation. In testing, we employ a video data set recorded in uncontrolled settings and show that we achieve a detection rate of 0.80.

2.2 Background and related work

It is important to understand the dynamics of walking oscillations, to decouple arm gestures and arm swings. Arm swings are suggested to be an integral part of gait, possibly driven by central pattern generators arising from natural passive dynamics sustained with little active torque [28][3].

[2]Although the amplitude of the oscillations vary with the view angle, we expect their frequency to be reasonably stable, provided that there is not significant (self)occlusion.

[3]Specifically, benefits of arm swings to gait economy involve decreasing shoulder and elbow joint torques, offsetting motion of the legs, reducing vertical ground reaction moments and attendant muscle forces, thereby reducing metabolic energy expenditure [29]. They also produce counter-rotations of the pelvis and thorax to maintain stability and a steady visual platform by minimizing head movements [30, 31].

Despite their simplicity, arm swings are studied in a diverse range of research fields such as neuroscience [32], medicine and biomechanics [33], computer vision [34] etc. In humanoid robotics, gait is often analyzed for generating stable and natural biped locomotion focusing particularly on the oscillations of the lower body (i.e. hip, knee, foot) and representing upper body motion in a simple manner [35, 36, 37]. Moreover, gait issues are actively discussed in operator-exoskeleton interaction as well as programming of walking robots [38, 39]. However, in human-robot social interaction, impact of hand/arm gestures is subject to a detailed treatment [22]. Most studies take a robot stand-point and address face-to-face communication between a robot and a human in stationary settings such as around a table [23]. In such scenarios, the aim is often recognizing and interpreting human gestures [25].

In this respect, Salem et al. differ from the mainstream studies by considering a more dynamical interaction, where the human-robot pair moves around in a domestic environment or classroom [40]. They show that a robot, which employs gestures along with speech, is perceived by humans as more friendly, engaged, and competent. Such effects of gestures are assumed to be pertinent in mobile human-robot interaction as well [41]. However, to the best of our knowledge there is yet no work on gesture recognition in mobile interaction. Therefore, this chapter tries to fill a void in literature initially by decoupling arm swings and arm gestures, which may then be recognized at a finer level (i.e. by distinguishing pointing, waving etc.)

2.3 Data set

Although methodological experiments or simulations are very useful to test new tracking or detection algorithms, they do not provide workable data in studying social interaction [42]. Namely, target models or instructed subjects (acting deliberately) fail to interact in a natural way [43]. Therefore, the characteristic of human-human interaction is considered to be best depicted when the actors are observed in their ecological environment [44].

Therefore, we examined various pedestrian video data sets [45] and regarded the freely available DukeMTMC data set to be a well-match for our purposes due to several reasons [46]. Namely, DukeMTMC is filmed in the campus of Duke University depicting naturally interacting pedestrians at oblique view and involves a large quantity of data[4]. In addition, it

[4] 85 minutes of 1080p and 60 fps video from 8 cameras with more than 2700 identities

provides several ground truth values including OpenPose estimations regarding each individual[5].

In addition, a subset of DukeMTMC is annotated for pedestrian groups and the DukeMTMC-Groups data set is introduced by [34], where 64 groups are tracked across 4 cameras for an average of ~ 400 frames per group (see fig. 2.1).

Figure 2.1: Frames from DukeMTMC-Groups. Group members are marked in yellow.

In order to obtain a ground truth for the arm gestures in the DukeMTMC-Groups set, we carried out an additional annotation. Here, it is important to note that we do not contain ourselves to some well-defined symbolic gestures (e.g. waving) or deictic gestures (e.g. pointing) but also consider lexical gestures [47], which may be firmly interwoven with arm swings (see open palm pointing upwards in fig. 2.5-(c)).

Two coders watched the clips and annotated such gestures for each individual in a group. We evaluated the reliability of the annotation process using an inter-rater agreement analysis based on Krippendorff's α coefficient[48], and found $\alpha = 0.80$, which indicates a substantial agreement (see [49] for significance of α).

2.4 Method

Principally, two kinds of joints play role in arm gestures[6], i.e. elbows and shoulders. The configuration of these joints is reflected by the four angles depicted in fig. 2.2-(a). Therefore, we particularly focus on the limbs, which connect to these joints in the OpenPose estimations [50] provided as ground truth in [51].

[5]In addition, trajectories on image plane are provided in a piece-wise linear manner and relating real-world coordinates can be computed using homography matrices.

[6]Here, we exclude fine-grained gestures arising from finger and wrist motion.

(a) (b) (c) (d)

Figure 2.2: (a) Skeleton representation of OpenPose together with elbow and shoulder angles; (b-d) Several examples of pose estimations.

We then compute the relative orientation of those limbs at every frame for each pedestrian in each group. As an example, fig. 2.3 shows elbow and shoulder angles for a pedestrian, who does not perform any arm gestures. It appears that -sole- walking motion (i.e. without gestures) causes a certain periodicity in the signal and that is exactly what is intended to be identified. In addition, the values depicted in fig. 2.3 are found to be in line with characteristics of common gait motion. Namely, in agreement with Van Emerik et al., shoulder flexion and extension is observed to vary roughly between 5 and 30 degrees [30].

However, we also notice a certain instability in the estimation of the articulations, which are probably due to the errors in estimation of the joint coordinates (see fig. 2.3-(a)). In order to eliminate such inconsistencies, we first perform a pre-processing operation as detailed in section 2.4.1 and then apply a pitch detection algorithm to identify oscillatory motion as explained in section 2.4.2.

2.4.1 Pre-processing

Suppose that $\alpha[n]$ denotes the articulation of an arbitrary joint (right or left elbow or shoulder) at frame n. For eliminating the noise or instability in the estimation of α, we apply a median filter

$$\bar{\alpha}[n] = m(\alpha[n-T], \ldots, \alpha[n], \ldots, \alpha[n+T]),$$

where $\bar{\alpha}$ denotes the pre-processed signal, $m(\cdot)$ stands for the median operator and $2T+1$ is the size of the filter[7].

[7] $T = 1$ is considered to give satisfactory results.

Obviously, due to the relative position of the pedestrians with respect to the camera or their partner, and occlusions with obstacles, some joints or limbs may not be visible at all frames. Thus, α is often defined as a piece-wise linear function. Should α be defined at some intervals shorter than the window size, we do not apply pre-processing to those intervals.

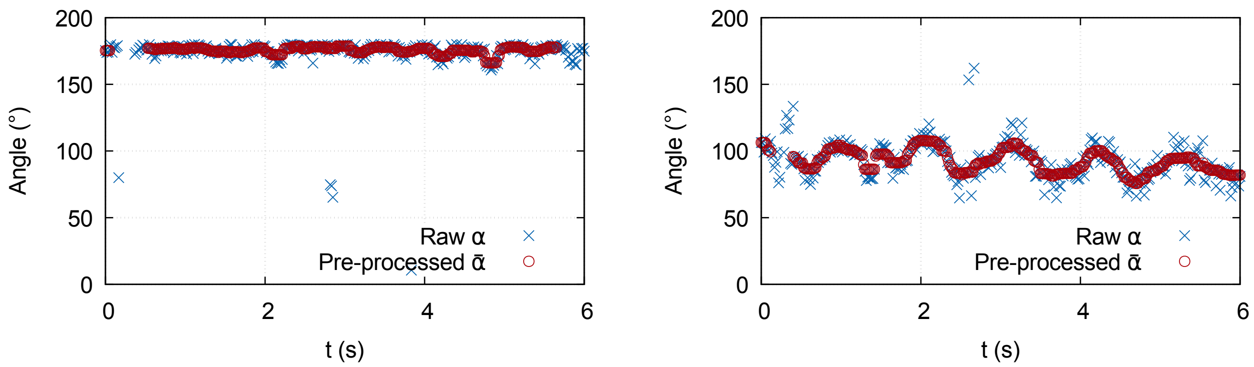

(a) (b)

Figure 2.3: (a) Elbow and (b) shoulder angles before pre-processing (in blue plus)and after pre-processing (in red cross).

Note that this also introduces the need to deal with deficiencies due to missing data. So as to address this problem, we introduce an upper limit to the permissible rate of missing samples and consider only those joints with less than 15% missing estimations.

Figure 2.3 illustrates the outcome of the median filtering operation for a couple of elbow and shoulder joints. After carefully examining such pre-processed angles regarding all pedestrians, we decided to focus on elbow joints in our analysis for three reasons. Firstly, as seen in fig. 2.3-(a) and (b), flexion and extension are inherently more pronounced for shoulders than elbows in gesture-free walking. Thus, gestures are easier to identify in terms of elbow angles, which are not subject to a variation as large as shoulder angles. Secondly, most gestures encountered in -pedestrian- interaction (e.g. metaphorical gestures) involve forearm motion to a more prominent degree than upper arm motion [18], which puts a bigger importance on elbow angles. Thirdly, since the region of the shoulder is broader than the region of the elbow, estimations of OpenPose are observed to vary more from one frame to the next regarding shoulders. This is particularly true since the footage is recorded outdoors in winter season and pedestrians often wear heavy clothes, which makes accurate identification of shoulders challenging.

2.4.2 Pitch detection

Essentially, retireval of the oscillations due to gait is very similar to pitch detection, where the goal is also to identify a low frequency periodicity from a noisy signal. Different methods exist to perform such tasks and in this study we opt for the average magnitude difference function (AMDF) introduced in [52]. AMDF concerning a discrete waveform $x[n]$ is defined as,

$$D[\tau] = \frac{1}{N - \tau - 1} \sum_{n=0}^{N-\tau-1} |x[n] - x[n+\tau]|,$$

where τ is the lag number and N is the number of samples. For mere walking action, $D[\tau]$ should be similar to a sine wave. Therefore, it is expected to have minimas at lags corresponding to the period of the walking oscillations and its multiples (see fig. 2.4-(b)).

Based on this inference, we fit a sinusoidal waveform $y[\tau]$ to the obtained AMDF curve $D[\tau]$,

$$y[\tau] = A \sin[\omega\tau + \phi] + c,$$

where A is the amplitude, ω is the frequency, ϕ is the phase and c is the offset. In particular, we minimize the sum of squared error between D and y, i.e. ε

$$\varepsilon = \sum_{\tau} (D[\tau] - y[\tau])^2$$

using the Levenberg-Marquardt optimization algorithm. If the outcome of this optimization process is positive (i.e. there exist a solution), the underlying motion is considered to be periodic.

On the other hand, for walking actions involving arm gestures, oscillations are expected to have a disruption and the periodicity of $D[\tau]$ is supposed to be lost for a certain duration of time (see fig. 2.4-(c)). In that case, overall periodicity is assumed to disrupted and an arm gesture is said to be performed.

2.5 Results and discussion

Running the proposed method on DukeMTMC-Groups data set, we obtained the results given in table 2.1. Specifically, the proposed method achieves a precision of 0.65, a recall of 0.89, and an accuracy of 0.80. Considering the challenging nature of the set, these results are

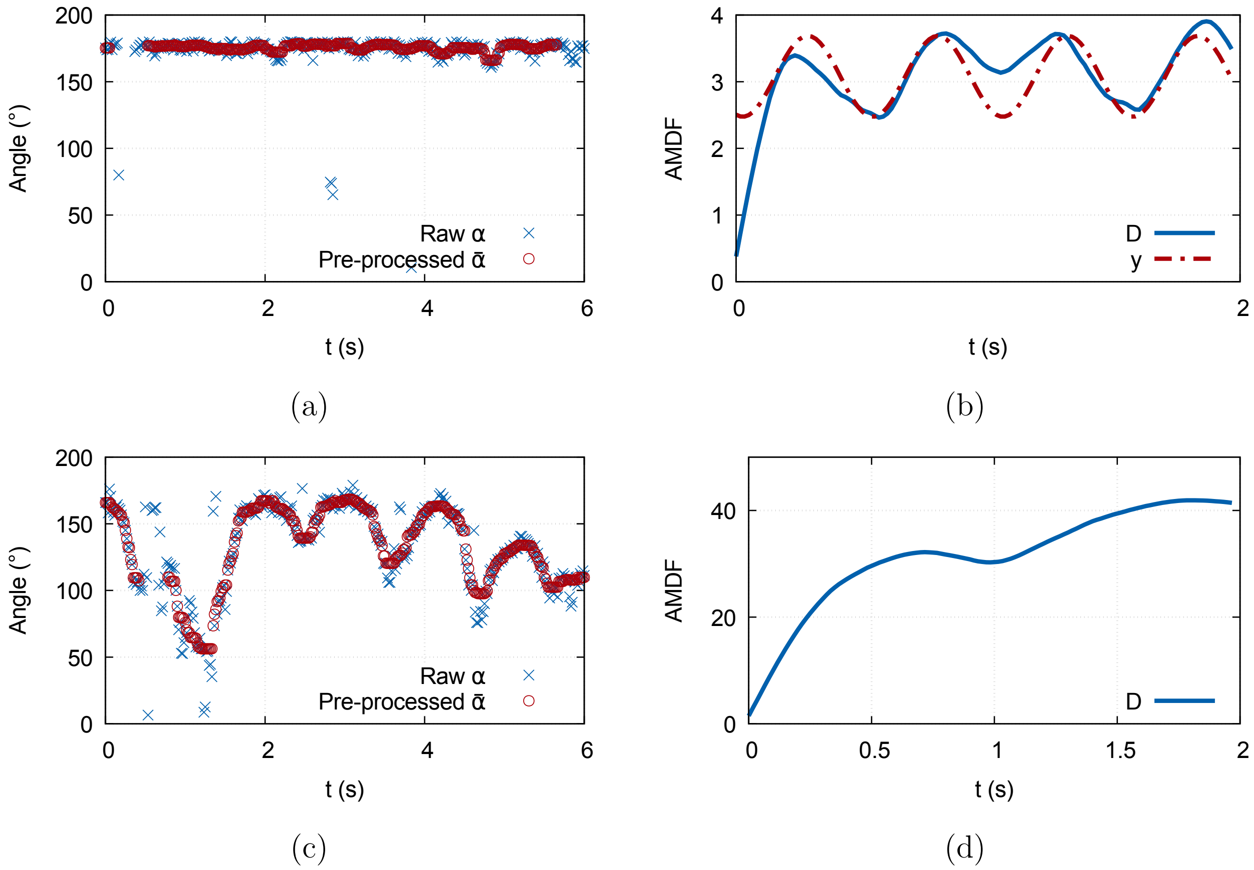

Figure 2.4: (a) Elbow angles and (b) AMDF and corresponding sinusoidal model for a no-gesture case.(c) Elbow angles and (d) AMDF for a gesture case.

considered to be a promising start for the decoupling of walking oscillations and gestures. In what follows, we provide a discussion on possible sources of error and future work.

The principal cause of mistakes is considered to be the failures in accurate estimation of poses. Moreover, missing estimations due to occlusion (by objects, peers or other pedestrians) (see fig. 2.5) are somehow an inevitable reason.

In addition, various pedestrians perform arm movements different than gestures (e.g. switch a cup from one hand to the other). Although the coders did not consider such movements as gestures, the proposed method identifies them as a disturbance on walking oscillations, which may explain the relatively high rate of false positives in table 2.1.

There are also several fundamental challenges arising from the collection of the set. First of all, certain cameras provide a frontal view (see fig. 2.1-(b)), where pedestrians have a

Table 2.1: Gesture detection results (in %).

		Estimation	
		Gesture	No gesture
Ground truth	Gesture	89	11
	No gesture	24	76

change in depth more than 20 meters. Obviously, as explained in section 2.1, the proposed method is indifferent to changes in depth but OpenPose relies on identification of body parts, which suffer from the low resolution views of targets when they are very far away from the camera.

Moreover, since the set is recorded in winter season, lots of pedestrians walk with their hands in pocket or with umbrellas (see fig. 2.5-(b,d)), which limits the oscillations of the arms and makes it more difficult to identify an oscillatory pattern, even when no gesture is present.

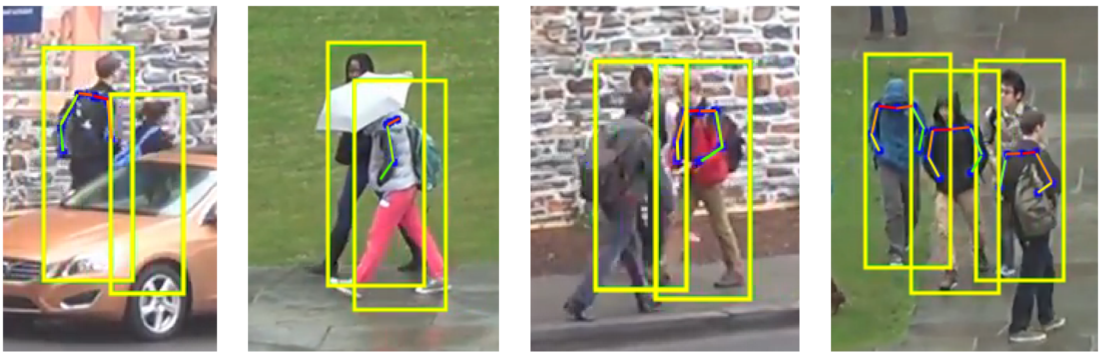

(a) (b) (c) (d)

Figure 2.5: Occlusion due to (a) an object, (b) the partner (in the same group) and (c, d) other pedestrians (outside the group).

Future work includes improving pose estimations to correct errors and interpolate missing data. Graph convolutional neural networks, which generalize the convolution operation on 1D and 2D arrays to graph data structure, is a promising tool for skeleton pose estimations. The Spatio-Temporal Graph Convolutional Network by Yan et al. seem particularly beneficial in action classification, where the classier employs a graph model of the skeleton at multiple successive frames, each joint being linked to its detection on the preceding and succeeding frames [53]. Using this method, given a set of detections, it may be possible to estimate the locations of some missing joints. In addition, for the pitch detection step using a cepstrum analysis is considered to improve the results.

2.6 Conclusion

This chapter focuses on gesture recognition in mobile interaction settings, i.e. when the interacting partners are pedestrians. Here, the problem is that the pedestrians move their arms as part of their walking activity. Thus, a first step in recognition, would be to decouple this inherent oscillatory movement and gestures. To that end, we use a pitch detection method, identify the oscillatory motions and model them using a sinusoidal waveform. The signals which cannot be represented with this model, are assumed to involve a gesture action.

The proposed method achieves a considerable accuracy of 0.80. Besides, being based on video, it is noninvasive, which is very desirable in interaction studies. In addition, the oscillatory actions of the arms can be observed independent of the view angle or distance to the camera, which makes it independent of camera configurations. Moreover, video input is particularly favorable, since it can easily be collected and integrated into existing systems (e.g. security surveillance) in a large variety of environments (indoor or outdoor)[8].

[8] With current depth sensors, observing the environments at the scale of the ones in fig. 2.1 is perhaps not possible, if not with some very expensive equipment.

Chapter 3

The impact of social interaction on intrusive behaviours

3.1 Introduction and Objectives

A crowd is defined as a large group of people that are gathered or considered together [54]. It has a heterogeneous structure and is composed of various components with distinct dynamics, with individuals and groups commonly regarded as its building blocks. Indeed, more than a bare collection of individuals, group motion is shaped by numerous factors, such as individual factors (e.g, age, gender, height), group factors (e.g, social relation, intensity of interaction, gestures), environmental factors (e.g, density, obstacles, flow direction) or social factors (e.g, manners, social acceptability) [44].

As a matter of fact, some of our previous studies are focused on characterising the effect of social bonding on group dynamics, especially in the case of two-people groups (i.e. dyads). In particular, it was shown that social relation and social interaction have a significant impact on the dyad's motion, with, for instance, members of strongly bonded groups (i.e. couples, friends, or people interacting strongly) being found to walk slower and closer to one another.

Nonetheless, the impact that the internal parameters of the group has on the dynamics of other pedestrians that move in its vicinity (i.e. close enough to require collision avoidance manoeuvres) has yet to be investigated. To shed some light on this matter, we propose to analyze the particular situation of non-groups (i.e. pedestrians that are alone and not part of any group) frontally encountering dyads, by using trajectory data of uninstructed, free-moving pedestrians.

In particular, we study the relation between the intensity of interaction inside the group and the deviation/intrusion behaviour of the non-group. To that end, we compute the *undisturbed minimum distance*, i.e. the distance between the dyad and the non-group assuming that they will walk in a straight line without performing any collision avoidance. Then, we compare it to the actual observed minimum distance. This allows quantifying the effective mutual avoidance performed and correlating it with the intensity of interaction inside the dyad.

3.2 Related Work

The problem of generating socially compliant trajectories, for instance for autonomous agents capable of averting collisions with other agents or pedestrians, is essential. Physics-based methods, such as the classic Social Force Model [10], propose to solve this by using repulsive forces to reproduce collision avoidance. More recently, data-driven methods, such as [12, 13] used neural networks to predict socially plausible trajectories by training them on publicly available trajectory data sets.

Various works have examined the influence that social groups have on the dynamics of the crowd, particularly in the case of evacuation scenarios [55, 56, 57]. Their effect on unidirectional [58], bidirectional [59, 60] or multi-directional flows of pedestrians [61] has also been recently studied. It was found that social groups keep a larger distance from other pedestrians, overtake less often [58] and make fewer detours when walking toward a defined goal [62]. In [60], the authors studied various collision avoidance strategies with regard to the size of the groups and pedestrian density. They notably showed that bigger groups are more likely to split into subgroups to accommodate conflicting pedestrians.

Nonetheless, to the best of your knowledge, no study has yet considered the impact of the social bonding of the group on the avoidance dynamics with non-groups, which we propose to do here.

3.3 Data Set

We use the DIAMOR data set, which contains pedestrian trajectories recorded over 8 days in an underground pedestrian street network in Osaka, Japan [14]. In this experimental campaign, we collected trajectories of uninstructed pedestrians[1] and were walking freely in a 200 m^2 environment, allowing continuous tracking for approximately 50 m. Depth data was collected with laser range finders and video data was simultaneously captured for annotation of social groups [63] and their intensity of social interaction. This intensity was annotated on a scale ranging from 0 (i.e. no interaction) to 3 (i.e. strong interaction).

The trajectories are first processed to ensure that they are suitable for our study. First of all, for the sake of simplicity, the trajectories of the dyad members are reduced to a single mobile agent (as average positions the members). We then consider trajectories for which the number of observations is deemed sufficient, i.e. with more than 16 points[2]. Additionally, we only retain the trajectories for which the velocity is between realistic boundaries for walking motion, i.e. [0.5, 3] m/s.

Besides, since we are interested in studying the effect of the intensity of interaction on collision avoidance dynamics, we require that the dyad d and non-group n get close enough so that such an effect might sensibly be detected. Specifically, we consider encounters, for which the instantaneous distance between d and n gets smaller than 4 m.

Finally, we confine our analysis to *frontal encounters*, where d and n walk in opposite directions such that n can acquire sufficient information about the intensity of social interaction of d. This condition can be enforced by measuring the unsigned angle between the velocity vectors of d and n, $\alpha = |\angle \vec{v}_d, \vec{v}_n|$, and retaining those encounters, where α is (on average) between $3\pi/4$ and π.

Since d and n are mobile, the (static) environment reference frame is not the most suited to study their relative positions. Thus, for the sake of clarity and ease of interpretation, we adopt a *dyad-centred reference frame*. In particular, (i) we translate the trajectories of d and n such that d is positioned at the origin at all times and (ii) we rotate them such that the velocity of the dyad $\vec{v}_d$ lies along x^+ at all times.

[1]A sign board informed pedestrians that they were being recorded as part of an experiment. The experimentation is reviewed and approved for studies involving human participants by ATR ethics board (document number 10-502-1).

[2]The sampling interval Δt is 500 ms, and, thus, 16 samples correspond to 8 seconds of observation.

3.4 Trajectory Deviation and Intrusion

Our analysis relies on the hypothesis that, in the vicinity of d (specifically, a 4×4 ^{2} m area around it), n would follow an effortless straight-line trajectory, would there be no d on its path[3]. Consequently, the deviation from this straight line can be attributed to an effort for collision avoidance.

To measure this deviation, we compute two distances, (i) the *straight-line distance* r_b and (ii) the *observed minimum distance* r_0. The straight-line distance r_b is defined as the distance between the theoretical straight-line trajectory of n and the origin (i.e. the position of d in the *dyad-centred reference frame*). We compute this as the straight line connecting the positions of n where it enters and exits d's vicinity. On the other hand, the observed minimum distance r_0 is simply the actual smallest distance between d and n. It can simply be computed as the minimum distance between pairs of trajectory samples. However, since the sampling interval is relatively large (i.e. $\Delta t = 500\,\text{ms}$) we interpolate the position of n between consecutive time steps using its velocity $\vec{v}_n$ to refine the accuracy of the computation[4]. This procedure allows us to detect minimum distances not only exactly at sampling instants but also at intermediate time points between consecutive samples, which yields a more accurate estimation of r_0. Comparing r_b and r_0, we can quantify the deviation due to collision avoidance.

In addition to quantifying the deviation with regard to social interaction, studying these distances allows us to investigate the particular case of *intrusions*, i.e. when the non-group n passes between the two members of the dyad d.

However, note that while dealing with intrusions, one needs to be careful with the group breadth. In [15] we showed that there is a strong relationship between the intensity of interaction of d and the interpersonal distance between its members. Namely, higher levels of interaction correspond to smaller interpersonal distances, while lower levels correspond to larger distances. Therefore, the preference of n to intrude into d or not depends also on the available space between the members of d. To alleviate this effect, we normalise r_b and r_0 by the average interpersonal distance for groups with the same intensity of interaction.

[3] Vice-versa is valid too. In addition, pedestrian trajectories are, in general, not perfectly straight, but over relatively small distances and for the geometry of the environment in focus (a straight corridor), we argue that this assumption is reasonable.

[4] We check whether the distance between the origin and the line, which passes through the position of n at t_k, $p_n(t_k)$ and is directed along its velocity $\vec{v}_n(t_k)$, is smaller than the distance between the origin and $p_n(t_k)$. In order for that new distance to be acceptable as the smallest distance between n and d, n must reach the position on the line that verifies this distance in a time shorter than the sampling interval Δt.

Henceforth, these normalised values are referred to as $\bar{r}_b$ and $\bar{r}_0$, respectively.

Given the previously described normalisation, we point out that values of r_0 smaller than 1 indicate that n is at a distance from the centre of mass of d smaller than the distance between the two members of this dyad. This is likely to correspond to n passing through d. To determine whether this likelihood is conditioned on the intensity of interaction of d, we study the proportion of cases where $\bar{r}_0 < 1$. Specifically, we compute the probability

$$P(\bar{r}_0 < 1|I) = \frac{|e \in \mathcal{E}_{\bar{r}_b \in I} : \bar{r}_0 < 1|}{|\mathcal{E}_{\bar{r}_b \in I}|}, \tag{3.1}$$

where I is a given interval for the distance $\bar{r}_b$ and $\mathcal{E}_{\bar{r}_b \in I}$ is the set of encounters such that $\bar{r}_b$ is in that interval. In practice, we compute this probability for quantised values of $\bar{r}_b$, i.e. the intervals I are non-overlapping bins of equal size.

3.5 Results and Discussion

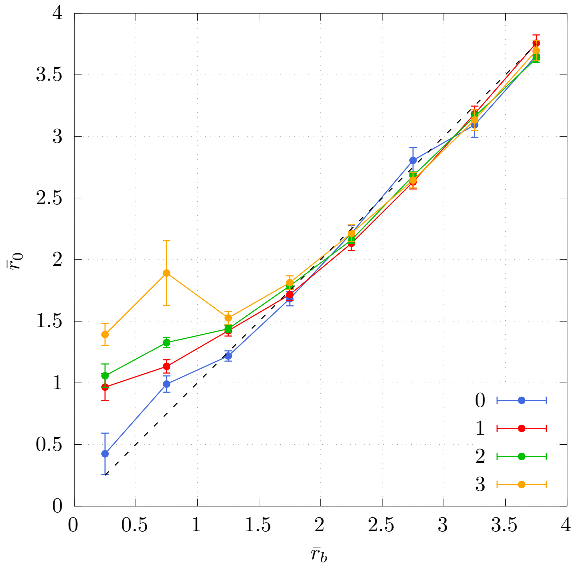

(a)

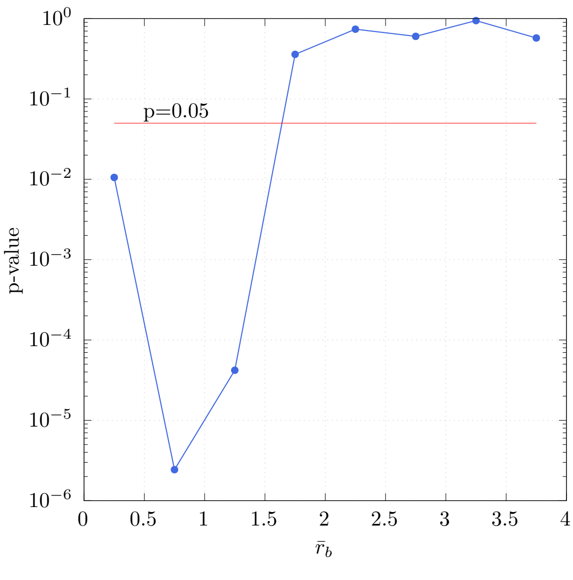

(b)

Figure 3.1: (a) $\bar{r}_0$ against $\bar{r}_b$ for various intensities of interaction. (b) Corresponding ANOVA p-values (in logarithmic scale).

section 3.5-(a) shows the average value of $\bar{r}_0$ over quantised values of $\bar{r}_b$, for different intensities of interaction of d. On the right part of the graph ($\bar{r}_b > 2$), all curves follow closely the $y = x$ line (in black dashes). This means that, when n's straight-line trajectory would bring it at a distance $\bar{r}_b$, which is larger than twice the size of the group, it does not undergo any additional avoidance, regardless of the intensity of interaction of d. In other words, groups' social interaction does not affect collision avoidance dynamics, when the trajectories are separated by a large enough distance (more than twice the size of the group).

On the other hand, observing the left part of the graph ($\bar{r}_b < 2$), the curves are seen to drift from the $y = x$ line, as avoidance behaviours take place. Even more remarkably, the intensity of this deviation seems to be conditioned on the level of interaction of d. As a matter of fact, increasing levels of interaction correspond to more pronounced avoidance dynamics. The significance of this result can be assessed by observing the p-values shown in section 3.5-(b) for $\bar{r}_b < 1.5$, indicating that the null hypothesis (that the mean values are all equal) can be safely rejected.

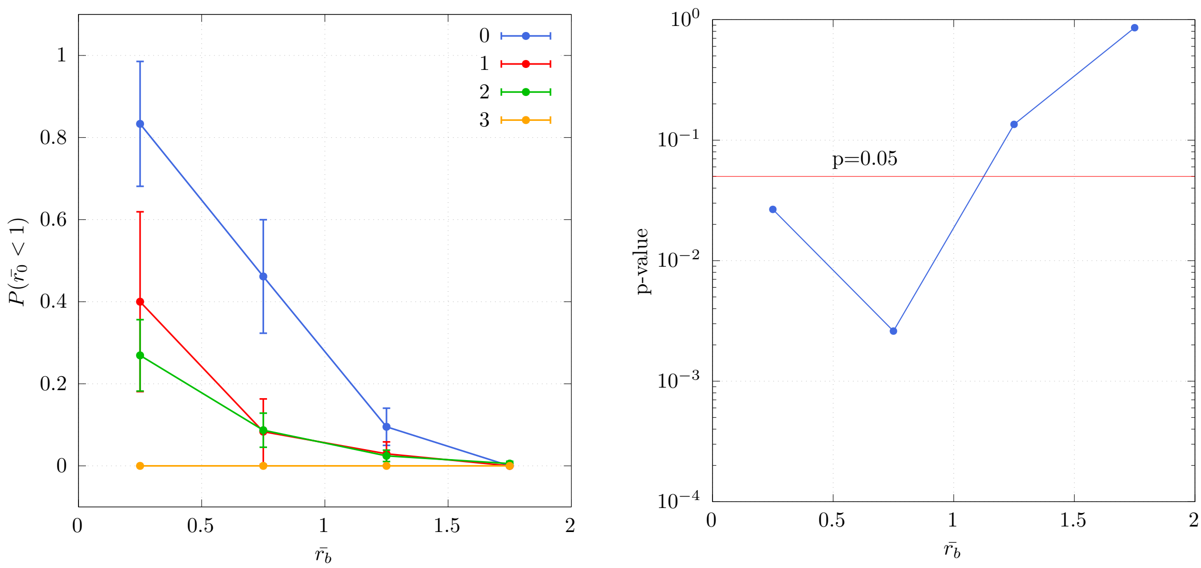

(a) (b)

Figure 3.2: (a) Probability for $\bar{r}_0 < 1$ for various intensities of interaction of the dyad d. (b) Corresponding p-values from Pearson's χ^2 test (in logarithmic scale).

Regarding intrusive behaviours, section 3.5-(a) shows the probability of $\bar{r}_0$ being lower than 1, $P(\bar{r}_0 < 1)$, for quantised values of $\bar{r}_b$. Remarkably, we see that there is a direct link between the intensity of interaction of d and the probability that n intrudes into d.

Namely, non-groups are more likely to intrude into dyads with lower levels of interaction. In section 3.5-(b), we show the p-values obtained from Pearson's χ^2 test corresponding to a null hypothesis that the proportion of values of $\bar{r}_0$ smaller than 1 are not significantly different across intensities of interaction. We see that these p-values are smaller than 0.05 for $\bar{r}_b < 1.5$, confirming the statistical significance of the difference observed in $P(\bar{r}_0 < 1)$.

Similar to the deviation distance, we believe that this might possibly be an unconscious behaviour causing pedestrians to judge more acceptable to pass through non-interacting groups, as it might be considered as causing less disturbance than for an interacting group.

3.6 Conclusion

In this chapter, we studied the effect of the intensity of interaction of dyads d on their collision avoidance with non-groups n. Remarkably, we found that, when d and n are in a colliding path, the magnitude of the deviation of the non-group is contingent on the intensity of interaction of the dyad. As a matter of fact, the deviation is shown to increase with intensifying levels of interaction. What is more, we found that the probability of intruding into a dyad was also correlated with social interactions. Namely, the more the dyad interacts, the less likely the non-group is to intrude into it.

We believe that these findings can be explained by social norms and conventions. It seems that it is regarded as more acceptable to come closer, or even intrude into, groups not engaged in strong social interaction.

We argue that these findings are strengthening our understanding of pedestrian dynamics and specifically of the unspoken social conventions characteristic of human locomotion. They could be applied to help in developing more realistic crowd simulation models (such as social force models) with a wide variety of applications (infrastructure design, disease spread predictions, etc.). Additionally, autonomous agents (i.e. guiding robots, autonomous wheelchairs, etc.) could benefit from navigation algorithms implementing rules derived from our results. Beyond the ability to plan and follow paths among moving, interacting pedestrian, following social conventions is a requirement when conceiving mobile devices that will make human users feel comfortable.

Chapter 4

Social aspects of collision avoidance

4.1 Introduction

Groups represent an important component of pedestrian crowds [64, 65], and lately they have been the subject of many studies, focusing on such themes as their effect on crowd dynamics [58], the observation of their shape and velocity [64, 66, 14, 67, 68, 69, 70], mathematical and computational modeling of interaction dynamics [71, 72, 14, 73, 74, 75, 76], and dependence on social structure and interaction level [44, 15, 77, 78]. Many works are based on ecological observations [79, 11, 66, 64, 14, 73, 67, 44, 78, 15, 77], which may be argued to be indispensable in dealing with social aspects of human behavior [80, 81, 82, 83, 84, 85, 66].

To plan safe buildings [86, 87, 2, 88, 89] and manage crowds in busy public places (i.e. transportation hubs) and events [90], it is important to consider group behavior in crowd simulators and monitoring/predicting tools [91, 92, 76, 93]. This includes taking into account factors such as the structure of different types of groups, their social relations [94], and cultural differences [95, 96] for more accurate simulations. It is also crucial to model not only the internal dynamics of the group, but also their reaction to the external environment, such as the presence of other pedestrians, while keeping in mind the aforementioned characteristics of each group. Furthermore, it is essential to consider the impact of the group on other pedestrians and how their behavior may be influenced by the presence of the group.

However, the majority of the studies mentioned above concentrate solely on the collective behavior of groups, i.e. the dynamics that drive the group to move as one cohesive unit. Mathematically oriented works on group dynamics may introduce the concept of a "group potential" and examine it by assuming that interactions with pedestrians outside the group can be approximated as white noise [14] or as an external "mean-field" potential [73] on average. Similarly, observation-based works [67, 77, 44, 78] often describe group properties using probability density functions defined by an average process that neglects the specifics of the environment.

On the other hand, when introducing group behavior into a microscopic simulator, it is essential to incorporate specific rules that describe interactions between the group and the environment, particularly with surrounding pedestrians. Introducing in-group dynamical rules is a logical starting point, and these can simply be added to the collision-avoidance rules used for individuals. For instance, if a two-person group encounters a single-walking pedestrian in an acceleration-based or "Social Force" model [26, 10, 97], the acceleration terms of the group's pedestrians can be obtained by summing the individual-individual collision avoidance term and those resulting from in-group interaction [59]. The behavior of the lone pedestrian can be modeled by adding the two avoidance terms with respect to the pedestrians in the group. In other words, collision avoidance is treated as a one-to-one behavior, group dynamics are regarded as an exclusively in-group phenomenon, and the overall dynamics is the sum of these distinct components.

This is the (classical) linear superposition principle [98], which is typically assumed (and verified) in mechanics and simplifies physical models and their dynamics to a great extent. However, this principle does not necessarily apply to pedestrian dynamics. For instance, when a single walking pedestrian encounters a two-person group walking side by side, particularly if they are socially interacting, he or she may choose to avoid walking through them, even if it seems like the best choice from a pure collision-avoidance perspective. This intrusion decision would be likely, should the two pedestrians be perceived as independent. In this work, we investigate a relatively unexplored aspect of pedestrian behavior and crowd dynamics: collision avoidance of (or against) groups, and in particular, its dependence on the groups' "social attributes", which refer specifically to social relation and intensity of interaction.

In doing that, we use two data sets of pedestrian trajectory including annotations of groups' *social attributes* to investigate the nature of individual-group collision avoidance. Moreover, we focus particularly on groups composed of 2 people (i.e. dyads), since they are much more common than larger ones and they actually constitute their fundamental building block together with triads (i.e. for an easy navigation and social interaction, large groups break into sub-groups of 2 or 3 people) [66]. In addition, larger groups (of 3 or more people) may require a categorization of pair-wise social relations or interactions, which may be very complex to formulate or generalize. In that respect, we use the word *group* to refer simply to dyads. As groups' counterpart in collision avoidance, we focus on *individuals*, which is a term we use to refer to people not appertaining to a group.

4.2 Methods

4.2.1 Data sets

In this chapter, we used two data sets, namely the ATC data set and DIAMOR data set, both of which are reviewed and approved for studies involving human participants by the ATR ethics board [67, 14], are publicly available and contain trajectories derived from range data [99, 100, 101]. From these trajectories, we computed the normalized cumulative density maps of the experiment environments shown in fig. 4.1.

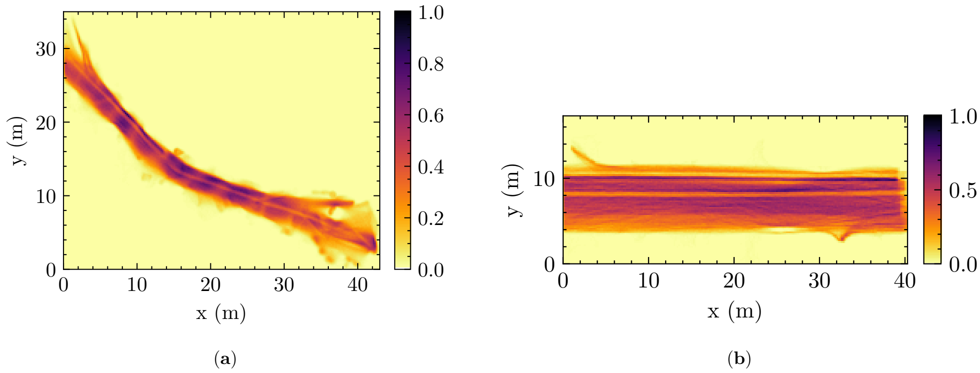

Figure 4.1: The normalized cumulative density maps for (a) the ATC data set and (b) DIAMOR data set. The environment is discretized as a 2D mesh with a grid cell size of 10 cm by 10 cm, and the number of observations is counted in each grid cell. Normalization refers to the scaling of this histogram with its maximum value.

The data sets are annotated based on video footage for different social attributes of groups. Specifically, the ATC data set is annotated from the viewpoint of social relations, whereas the DIAMOR data set is annotated from the viewpoint of the intensity of interaction.

For the ATC data set, possible options for social relation are couples, colleagues, family and friends, which are determined through the domain-based approach of Bugental [102] and correspond to the domains of mating, coalitional, attachment and reciprocal, respectively. This annotation process yields the values presented in table 4.1-(a).

For the DIAMOR data set, the intensity of interaction is evaluated at 4 degrees, 0 representing no-interaction and 1, 2, and 3 representing weak, mild and strong interaction, respectively. This annotation process yields the values presented in table 4.1-(b). Note that in order not to bias the coders' assessment, we only defined the number of interaction levels as 4, but we did not give any guidelines on what can be considered as weak, mild or strong interaction [103]. Instead, we let the coders grasp a feeling about different intensities of interaction through a free-viewing task (i.e. letting them watch the videos for 3 hours before giving any labels, see Supplementary Information Section 1 for further details.)

Table 4.1: Number of groups annotated with each (a) social relation (in ATC data set) and (b) intensity of interaction (in DIAMOR data set).

(a)

Social relation	# of annotations
Couples	69
Colleagues	314
Family	180
Friends	253
Total	817

(b)

Intensity of interaction	# of annotations
0 (no interaction)	140
1	159
2	460
3 (strong interaction)	100
Total	859

4.2.2 Approach

Provided that the group and the individual do not perform any collision avoidance, we can expect their (relative) motion to be approximated by a straight line. We are aware that this assumption requires implicitly the environment to be sufficiently straight and wide (e.g. like DIAMOR, see fig. 4.1-(b) and the discussion in Supplementary Information Section 7) and is valid up to a reasonable range (i.e. over a few meters). Namely, in environments with complex geometries (curved or with many obstacles, intersections etc.), the pedestrians need to deviate as part of their interaction with the boundaries. Similarly, over long distances, they will eventually meet some walls, or divert towards different goals, making their relative motion bent. Nevertheless, in a sufficiently straight corridor and on a scale of few meters, we can expect it to be a good approximation.

This trivial assumption can be considered to serve as a hypothesis, opposite to what we actually anticipate. Based on such a hypothesis, the deviation of (relative) motion from a straight line can be attributed to group-individual collision avoidance. Specifically, by measuring this deviation with respect to different social relations or intensities of interaction (of the group), we may understand the reflections of such group attributes on collision avoidance.

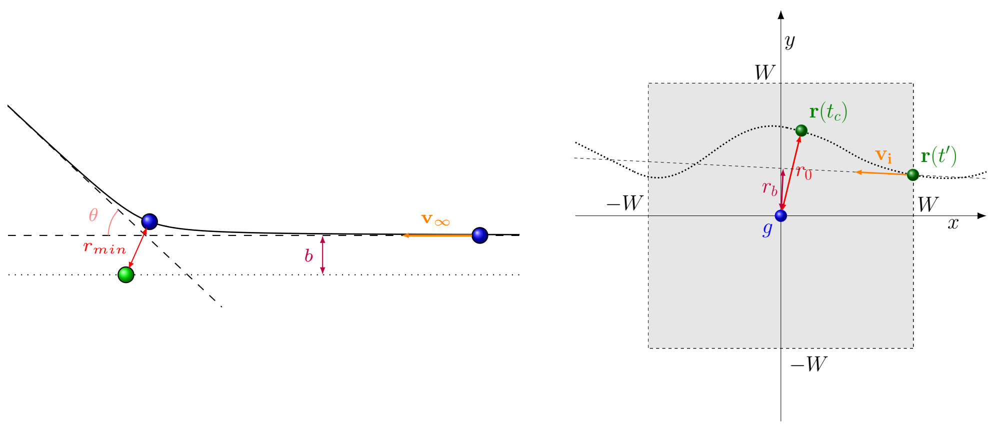

(a) (b)

Figure 4.2: (a) Illustration of the scattering problem in physics. A mobile particle (in blue) is projected toward a fixed particle (in green). The impact parameter, b, is the straight-line distance between the particles, and r_{min} is the closest approach. The particle is deflected with an angle θ. (b) A typical pedestrian avoidance situation in the *group-centered reference frame*. The individual enters the vicinity of the group (gray region) at time t' with velocity $\mathbf{v}_i$. The straight-line distance from the individual to the group is denoted by r_b. At time t_c, the individual is closest to the group at a distance of r_0.

This formulation presents a striking resemblance to one of the fundamental problems of Physics, namely, the "scattering problem", where a "particle" (blue ball in fig. 4.2-(a)) is shot on a "target" (green ball), and its deviation from the straight line motion is used to study the interaction potential. In the original scattering problem (see fig. 4.2), this deviation is assessed by accounting for the straight-line distance b (called the impact parameter) and closest approach $r_{\min}$, which is derived from the scattering angle θ, as an accurate measurement of particles' location is very difficult. By repeating the experiment with different impact parameters and estimating the corresponding closest approach $r_{\min}$, one can get an approximation for the potential acting on the particle.

In this chapter, we establish a simple duality relation between the above-mentioned problem and our group-individual collision avoidance scenario. Namely, the impact parameter b is replaced with a *straight-line distance* r_b and the closest approach can simply be measured as the shortest distance r_0 between pairs of trajectory data points of the group and the individual. In section 4.2.3 we elaborate in detail on how we define these observable quantities.

Using this approach from physical sciences to describe human behavior represents obviously a strong approximation, not only because human behavior is too complex to be modeled through simple physical forces, but also because it completely ignores the effect of the environment, which, in physical parlance, is equivalent to a strong and non-uniform external force. Nevertheless, as we will see, this approach still allows us to grasp the fundamentals of the collision dynamics between groups and individuals and to quantify the interaction. At this point, it is also worth stressing that the proposed model in section 4.2.4 is aimed at assessing the effect of different social attributes in a qualitative way, rather than reproducing quantitatively human behavior.

4.2.3 Observables

Data preparation and transformation

We first carry out a data preparation step by (i) removing atypical/non-characterizing motion (waiting, running etc.), (ii) representing the group as a single unit (its geometrical center) and (iii) focusing on frontal encounters of groups and individuals, for which we expect the pedestrians to be able to judge the social attributes of the incoming party.

Subsequently, we transform trajectories of the group g and the individual i to a reference frame, which is co-moving with the group. Namely, at each time instant (i) the positions of the group and the individual $\mathbf{r}_{g,i}$ are translated such that the group (center of mass) is positioned at the origin and (ii) their velocities $\mathbf{v}_{g,i}$ are rotated such that the velocity of the group is directed towards x^+. Finally, the velocities $\mathbf{v}_{g,i}$ are translated by $-\mathbf{v}_g$, rendering the group immobile. The main purpose of this transformation is to provide an easier visualization of relative position in 2D, which represents the position of the individual with respect to the group center, while having the group motion as a preferential direction. On the other hand, most of our analysis is based on the absolute value of the relative distance between the group center and the individual, which is rotationally invariant and independent of frame choice.

Relative distance r

Our analysis is based on $\mathbf{r}$, the relative position between the group center and the individual,

$$\mathbf{r}(t) = \mathbf{r}_i(t) - \mathbf{r}_g(t). \tag{4.1}$$

Its time derivative is the relative velocity $\mathbf{v}$,

$$\mathbf{v}(t) = \mathbf{v}_i(t) - \mathbf{v}_g(t). \tag{4.2}$$

The absolute value (norm) of $\mathbf{r}$ is simply denoted as r.

Straight-line distance r_b

The straight-line distance r_b is computed as the shortest distance from the origin (i.e. translated position of the group) to the line, which passes through the point at which the individual enters a pre-defined vicinity around the group termed as *window of observation*. This refers to the area in the group-centered reference frame from $-W$ to W meters both along x and y axes (i.e. along the group's motion direction and the direction orthogonal to that). Empirically a W of 4 m is seen to contain the most significant part of the group-individual collision avoidance (see fig. 4.2-(b) for an illustration. Refer to previous literature [104, 105] and Supplementary Information Section 3 for details on the choice of W).

Let t' be the time instant at which the individual enters W and let $\mathbf{r}(t')$ be its relative position at that instant. According to the hypothesis mentioned in section 4.2, provided that there is no collision avoidance the individual will follow a path starting at $\mathbf{r}(t')$ and move along its velocity vector at that instant $\mathbf{v}(t')$. In this case, the straight-line distance r_b can be computed as the shortest distance between this line and the origin (i.e. translated position of the group),

$$r_b = \frac{||\mathbf{r}(t') \times \mathbf{v}(t')||}{||\mathbf{v}(t')||}. \tag{4.3}$$

In the analysis, in order to alleviate the impact of orientation noise on the velocity of the individual, we averaged its velocity vector over 4 time instants (before t') and used this mean velocity in eq. (4.3) instead of $\mathbf{v}(t')$.

Observed minimum distance r_0

The observed (i.e. actual) minimum distance r_0 between the group and the individual is simply,

$$r_0 = \min_t \big(r(t)\big) = r(t_c), \tag{4.4}$$

where t_c is the time instant at which the individual is closest to the group. The time steps, at which pedestrian positions are recorded, are obviously discrete. Nevertheless, in order to have a more accurate estimation of r_0, one can also interpolate $\mathbf{r}(t)$ between two consecutive time steps t_k and t_{k+1} by using the velocity vector at time t_k,

$$\mathbf{r}(t) \approx \mathbf{r}(t_k) + (t - t_k)\mathbf{v}(t_k),\ t \in [t_k, t_{k+1}). \tag{4.5}$$

This procedure allows detecting minimum distances not only *exactly at sampling instants*, but also *at intermediate time points* between consecutive samples, which yields a much more accurate estimation of r_0 (refer to Supplementary Information Section 4 for details).

Scaled distances

Groups' interpersonal distance is shown to depend on their social relation and interaction intensity [77, 15]. Thus, we represent the distances defined above in two ways: in a group-independent way (in meters) and in a group-dependent way, in which the unit of distance is the average interpersonal distance of dyads with the given social bonding [44]). In the text, we denote distances measured in meters with the normal font (e.g. r) and scaled distances measured in interpersonal distance units with a bar (e.g. $\bar{r}$). Since we observed that results concerning scaled values are in general easier to interpret, in the main text we mostly report those (for further details, refer to Supplementary Information Section 5).

4.2.4 Analysis of collision avoidance

As mentioned in section 4.2, our study of the collision avoidance dynamics between groups and individuals is fundamentally based on examining the relation between r_b and r_0. To that end, in what follows we define two different methods to analyze this relation and then propose a method to model it.

Empirical relation between r_b and r_0 and its statistical analysis

To examine the distribution of r_b versus r_0, the values of $\bar{r}_b$ are quantized into bins of 0.5 unit and for each bin, the average and standard error of the corresponding values of $\bar{r}_0$ are computed. The choice of 0.5 as bin size was primarily driven by empirical observations. For certain combinations of distance r_b (or $\bar{r}_b$) and bonding (social relation or interaction level), setting a smaller bin size results in having bins with little or no data. Conversely, using a larger bin size decreases the resolution. In that respect, we consider a bin size of 0.5 to strike a balance between these competing factors. The results will be presented and discussed in section 4.3.2.

Intrusions

Small groups, such as dyads, have been shown to usually prefer deviating to avoid splitting [60]. Nonetheless, we found situations where the individual passes through the group (i.e. between group members), and we refer to them as “intrusion”. For simplicity's sake, we define the probability of intrusion as the probability of having r_0 smaller than the group interpersonal distance (see section 4.2.3). We perform a statistical analysis to investigate the dependence of intrusion on the social attributes of the group. The results will be shown and discussed in section 4.3.3, whereas the details of the computational procedure can be found in Supplementary Information Section 6.

Modeling

Many models of pedestrian collision avoidance are based on “Social Forces” [26, 10, 97], which may be defined through a potential. It has been reported that using position-dependent potentials in modeling of pedestrian collision avoidance fails to reproduce detailed behavior. Even if we assume that a “Social Force” approach may reproduce actual human behavior, the corresponding potential should at least be velocity-dependent and based not on current distance but on future distance at the moment of predicted closest approach [97, 74]. Nevertheless, determining a potential that may, at least qualitatively, describe the collision avoidance between groups and individuals, represent an important first step towards a more realistic quantitative modeling.

Let us first review how we can study the potential energy between two *interacting* bodies in physics (note that while discussing the physical model, we use the word “interaction” to refer to the effect that the bodies exert on each other.). The study of such a “scattering” problem is obviously a cornerstone of physics, and the non-Quantum formalism analyzed in this section was used to study such important problems as the structure of atoms [106] and gravitational lens effect due to space-time curvature [107] among others. In general, the “bodies” in focus are very complex and composed of many particles (e.g. planets, stars). Nevertheless, due to the scale of the problem, they may be treated as point particles themselves (in our “pedestrian scenario”, the group will be represented with a single point).

Their interaction is determined by a potential energy $U(\mathbf{r})$, which is in general a function of only relative position (a result connected to invariance under space translations and equivalent to Newton’s third law [108]). Nevertheless, in many important applications, the potential is central, i.e. rotationally invariant, and depends only on the magnitude of the distance, $U(r)$.

In such a case, it is shown that the interesting (potential-dependent) dynamics is studied in the r variable [106]. Defining the reduced mass μ as

$$\mu = \frac{m_1 m_2}{m_1 + m_2}, \tag{4.6}$$

where m_1 and m_2 are the masses of the two bodies, the angular momentum $\mathbf{L}$ and energy E result to be constants of motion,

$$E = \frac{\mu}{2}\dot{r}^2 + \frac{||\mathbf{L}||^2}{2\mu r^2} + U(r). \tag{4.7}$$

In a scattering problem, the system is not bound and r diverges for $t \to \pm\infty$. In most physical applications, we can only measure the scattering angle and the velocity far before/after the interaction. We can then compare the measured angle with a theoretical result involving an integral. However, if the full trajectory is known, a simpler way to study the system is available.

We study the system far before interaction, i.e. for $t \to -\infty$ and $r \to +\infty$, and call the corresponding asymptotic speed v_∞. We see that the absolute value of angular momentum can be written as

$$L \equiv ||\mathbf{L}|| = \mu v_\infty b, \tag{4.8}$$

where the impact parameter b is the minimum value of r assumed in case of straight motion (i.e. no interaction). Assuming $\lim_{r \to +\infty} U(r) = 0$, we obtain

$$E_\infty = \frac{\mu}{2} v_\infty^2. \tag{4.9}$$

On the other hand, since we actually have interaction, the minimum distance $r_{\min}$ in the observed trajectory turns out to be different than b, i.e. $r_{\min} \neq b$. At $r = r_{\min}$, having a minimum, we have $\dot{r} = 0$ and the corresponding energy is

$$E_0 = \frac{\mu v_\infty^2 b^2}{2 r_{\min}^2} + U(r_{\min}). \tag{4.10}$$

Conservation of energy implies $E_\infty = E_0$ and provides the following relation for the value of $U(r)$ at $r = r_{\min}$

$$U(r = r_{\min}) = \frac{\mu v_\infty^2}{2} \frac{r_{\min}^2 - b^2}{r_{\min}^2}. \tag{4.11}$$

This relation enables studying the potential $U(r)$, provided that v_∞, b and $r_{\min}$ are measured. In modeling collision avoidance between pedestrians based on the above framework, we assume that

$$\frac{\mathrm{d}U(r)}{\mathrm{d}r} < 0 \ \forall r \Rightarrow U(r) > 0 \ \forall r. \tag{4.12}$$

In other words, the force is assumed to be repulsive. Namely, denoting $\mathbf{F}_1$ as the force acting on body 1, and recalling the usual definition $\mathbf{r} = \mathbf{r}_1 - \mathbf{r}_2$, we have

$$\mathbf{F}_1 = -\boldsymbol{\nabla} U(r) = -\frac{\mathrm{d}U(r)}{\mathrm{d}r} \frac{\mathbf{r}}{r}. \tag{4.13}$$

We apply these physical concepts in a pedestrian scenario to model the "collision avoidance potential" between groups and individuals. As mentioned in section 4.2, r_b is inspired by the impact parameter b, whereas r_0 corresponds to the closest approach $r_{\min}$. Thus, the term v_∞ in eq. (4.11) should be approximated by using the relative velocity when r_b is computed. But since pedestrian velocities have a small variation, we may consider it to be almost constant. In a similar way, as usual when studying "forces" that determine the pedestrians' cognitive decisions, all masses are considered to be equal (to one) [26] and we may remove μ from the equation. Finally, since the approach is completely of a qualitative nature, we opt for ignoring the overall constant in eq. (4.11) and study the following simplified version,

$$U'(r = r_0) = \frac{r_0^2 - r_b^2}{r_0^2}, \tag{4.14}$$

to which we will refer to as the "collision avoidance potential" (defined as a dimensionless pure number).

A comment on eq. (4.14) is probably needed. This equation does not represent the functional form of the dependence of the potential on r. Instead, it shows which is the value of U attained at r_0 given that the straight-line distance is r_b. Different values of r_b allow us to probe different values of U, where the smaller b is, the higher U' is. Nevertheless, eq. (4.14) clearly allows us only to probe values $U' < 1$. This is due to the fact that in the computation of U' the value of the initial kinetic energy

$$\frac{\mu v_\infty^2}{2} \tag{4.15}$$

is taken as fixed, and we are measuring the probed values of the collision avoidance potential as multiples of such kinetic energy. Note that in particle physics short distances are indeed probed by using very high kinetic energies.

The results are shown and discussed in section 4.3.4, whereas the details of the computational procedure are described in Supplementary Information Section 7. In addition, in section 4.3.5 we also show the results concerning a similarly defined potential describing individual-individual collision avoidance.

4.3 Results and discussion

4.3.1 Results on relative frame pdfs

The *group-centered reference frame* is particularly suitable to study the 2D distribution of $\mathbf{r}$, i.e. of the position of the individual around the group. Figures 3 and 4 show the 2D distributions in relation to different social relations and interaction intensities of the group, respectively, using as a distance unit the groups' average interpersonal distance. Note that, in order to highlight the specificities of each social attribute *as compared to the whole*, we depict the difference between a given attribute and the overall 2D average, which is computed as an unweighted average of the distributions of all relating cases. Therefore, positive values depict an increased likeliness of presence for the individual, while, reciprocally, negative values depict a decreased likeliness.

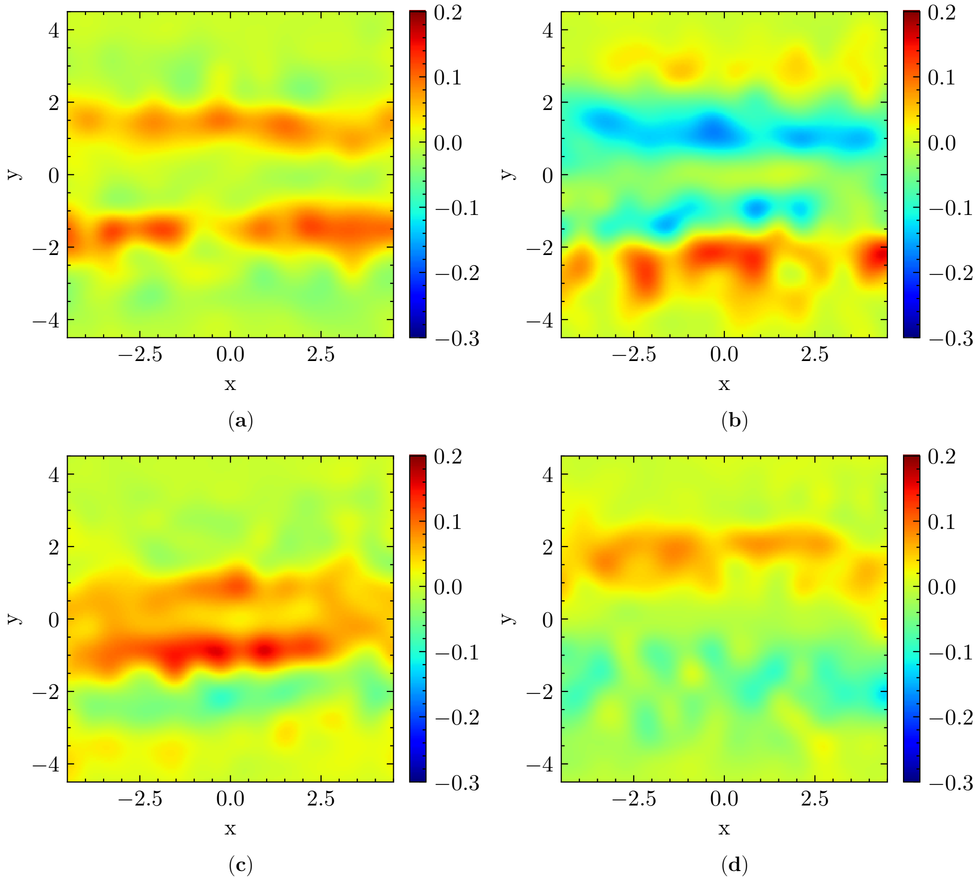

Figure 4.3: 2D probability distribution of individuals' position $\bar{\mathbf{r}}$ relative to overall average. Positions are shown in the group-centered reference frame and the x axis is aligned with the direction of motion of the group. Each sub-figure depicts the difference between the distribution relating to a certain social relation and an unweighted average concerning all social relations. (a) Colleagues, (b) couples, (c) families, (d) friends. The color scales are adjusted for highlighting the differences.

The effects of varying social relations are presented in fig. 4.3. Comparing fig. 4.3-(a) with fig. 4.3-(b) and (d), one may notice that individuals do not have a prominent preference to pass on the right or left side of colleagues, whereas they prefer to pass more on the right for couples and on the left for friends (as compared to the overall average). In addition, they pass with a very small distance ($r \approx 0$) more often for families (see fig. 4.3-(c)) than for other kinds of social relations, which may be due to a more dispersed configuration of family group members [77]. On the other hand, in fig. 4.3-(b) we see very clearly two low probability horizontal stripes, roughly located around $y = \pm 1$. As these stripes correspond more or less to group members' positions, they suggest that the group's abreast formation is rarely disturbed in couples.

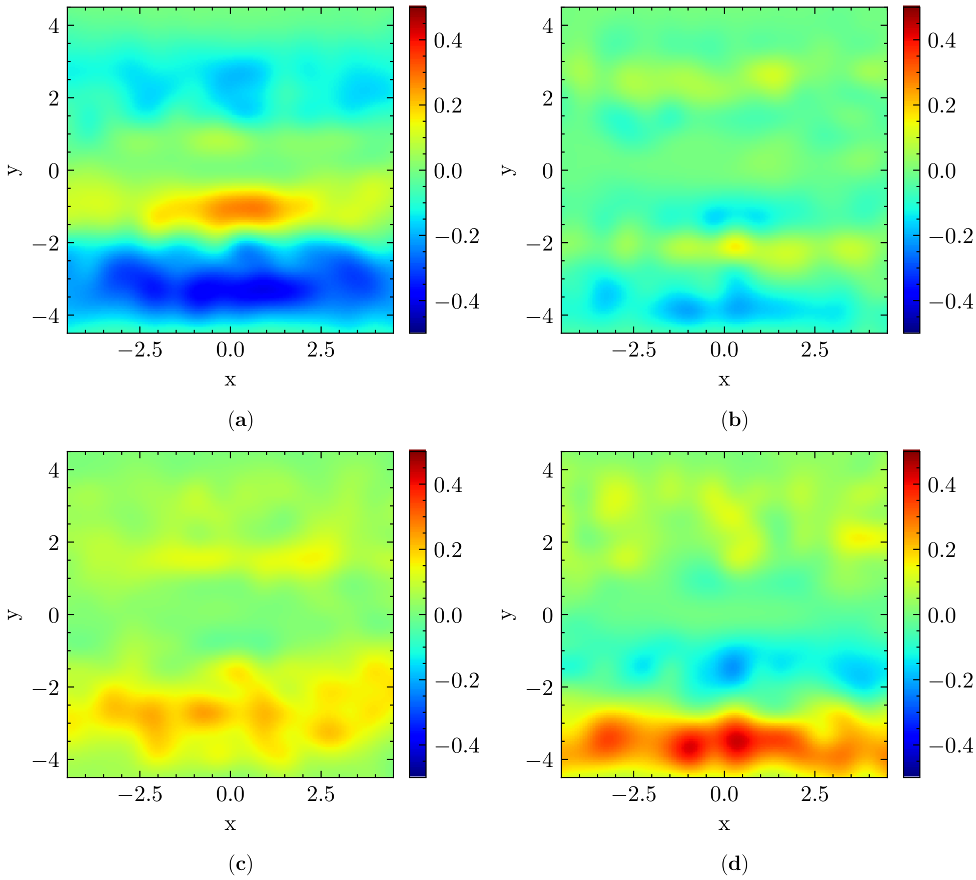

Figure 4.4: 2D distribution of individuals' position $\bar{\mathbf{r}}$ relative to overall average. Positions are shown in the group-centered reference frame and the x axis is aligned with the direction of motion of the group.
Each sub-figure depicts the difference between the distribution relating to a certain intensity of interaction and an unweighted average of all intensities. (a) 0, (b) 1, (c) 2, (d) 3. The color scales are adjusted for highlighting the differences.

Concerning social interaction, the difference with respect to varying intensities is much more noticeable, the most interesting one being between 0 and 3 (see Figures 4-(a) and (d)).

Namely, concerning groups annotated as non-interacting (i.e. with 0 intensity of interaction), the center stripe presents positive values, while the lower and upper stripes $y \approx \pm 2.5$ present negative values, indicating that individuals are more likely to maintain a trajectory directly facing the group (possibly even intruding it) (see fig. 4.4-(a)). Reciprocally, from fig. 4.4-(d) we can see that individuals are less likely to position themselves on a colliding trajectory with the group and prefer to place themselves on its side, when it has a high intensity of interaction. There are interesting left/right asymmetries in fig. 4.4, which may be related to the tendency of Japanese pedestrians to move mainly on the left, and overtake on the right [109]. This tendency may cause low-interaction groups, when they are not intruded on, to have a relatively higher possibility to be passed on their left than on their right, since they are expected to have a higher speed than highly interacting ones. We do not have a clear interpretation for the right/left asymmetry between the couples distribution in fig. 4.3-(b) and the friends distribution in fig. 4.3-(d).

4.3.2 Results on the relation between $\bar{r}_0$ and $\bar{r}_b$

We divide the range of $\bar{r}_b$ into bins of 0.5 unit and compute the mean and standard error of $\bar{r}_0$ corresponding to each bin. The results are depicted in Figures 5-(a) and (b). Smaller values of $\bar{r}_b$ indicate that the straight line trajectory of the individuals would require them to pass very close to the group. In addition, $\bar{r}_b < 0.5$ signifies a distance smaller than half of the group interpersonal distance, which means that the individual would need to *intrude on the group* (if moving straight).

Concerning social relations, we observe that when $\bar{r}_b < 0.5$, the average value of $\bar{r}_0$ is considerably larger for couples and friends than for colleagues and families (see fig. 4.5-(a)). In other words, there is a strong resistance against intruding on groups with the former social relations. Concerning intensity of interaction, we have a similar observation for higher intensities of interaction (from 1 to 3, see fig. 4.5-(b)), while for 0 intensity we have $\bar{r}_0 \approx \bar{r}_b$ for all $\bar{r}_b$ values.

These observations make us believe that the social attributes of the group do impact group-individual collision avoidance. Specifically, there is larger avoidance, when there is a strongly-bonded group involved (i.e. couples, friends or with high intensity of interaction).

The statistical significance of these results can be assessed through an ANOVA (see Supplementary Information Section 8 for considerations regarding the necessary assumptions).

To that end, we compute the p values concerning each bin shown in Figures 5-(a) and (b) and demonstrate the results in Figures 5-(c) and (d), respectively. Regarding lower values of $\bar{r}_b$ (i.e. $\bar{r}_b < 1.5$), we observe statistical significance (i.e. $p < 0.05$) concerning both social relation and intensity of interaction. Regarding larger values of $\bar{r}_b$ (i.e. $\bar{r}_b > 2$), there is no statistically significant difference, as it can be expected observing the overlapping curves in the corresponding regions of Figures 5-(a) and (b).

Let us also notice that in fig. 4.5-(b) concerning the DIAMOR data set, for $\bar{r}_b \gg 1$, we have $\bar{r}_b \approx \bar{r}_0$ regardless of intensity of interaction, in agreement with the hypothesis that collision avoidance can be ignored for such values (eq. (4.14)). The fact that this is not the case in ATC, where we actually observe $\bar{r}_b > \bar{r}_0$ for $\bar{r}_b \gg 1$, is considered to be an effect of the ATC environment being less straight and narrower (see Figure1-(a)).

To compensate for this effect in the computation of the potential, we perform a linear correction in the computation of $\bar{r}_b$ in section 4.3.4. The details of this correction are presented in Supplementary Information Section 7. In addition, results concerning the relation between r_b and r_0, i.e. values measured in meters and not scaled with group interpersonal distance, are shown in section 4.3.5.

4.3.3 Intrusion

It is noticeable that the observed minimum distance $\bar{r}_0$ reaches particularly low values in some encounters. For instance, the first bin in fig. 4.5-(b) for intensity of interaction 0 presents an average value of $\bar{r}_0$ smaller than 1. This means that the distance from the center of mass of the group to the individual gets smaller than the group interpersonal distance (see Supplementary Information Section 5). In such cases, it is likely that the individual is actually intruding on the group instead of deviating, essentially following the straight line trajectory.

To quantify the frequency of such intrusions, we computed the probability of $\bar{r}_0$ being smaller than 1. Specifically, this is an empirical probability computed as the ratio of the number of observations with $\bar{r}_0 < 1$ to the total number of observations (for a given bin of $\bar{r}_b$). The results are shown in Figures 6-(a) and (b). Here, we see that there is indeed a correlation between the probability of intrusion and the social bonding of the group being intruded on. Namely, individuals have a higher probability to intrude on loosely-bonded groups (i.e. colleagues, families and non- or slightly-interacting groups) than strongly-bonded groups (couples, friends and strongly interacting groups).

The statistical significance of this observation is assessed through Pearson's χ^2 test and the relating p-values are presented in Figures 6-(c) and (d). The difference in probability of intrusion concerning different social relations is significant ($p < 0.05$), when $\bar{r}_b$ is smaller than 1.5. On the other hand, for the intensity of interaction we have a significant difference of intrusion for $\bar{r}_b < 1$.

Actually, the average distance of a group member from the group center is $\bar{r}_0 = 0.5$. The corresponding analysis for the probability of having $\bar{r}_0 < 0.5$ is shown in Supplementary Information Section 6.

4.3.4 Potential

As described in section 4.2.4, we study $U'(r_0)$ (see eq. (4.14)) to model the "potential" representing the interaction between the group and the individual. To that end, we again quantize the values of $\bar{r}_b$ and compute the corresponding mean values of $\bar{r}_0$ before calculating the values of the potential $U'(\bar{r}_0)$ for each bin. Figures 7-(a) and (b) show the relating values. Additionally, to extrapolate outside the range available, a function of the form k/r^{β} is fitted to the data using non-linear least squares, illustrated with dashed lines in Figures 7-(a) and (b).

Interestingly, the potential is shown to be affected by the nature of the social bonding of the group. As a matter of fact, stronger bondings (e.g. couples, high intensity of interaction) generate a "stronger potential" (i.e. with a steeper negative derivative) which, as seen in section 4.3.2 and section 4.3.3 "causes" individuals to deviate more, and significantly decreases their probability to intrude on the group. On the other hand, loosely-bonded groups (e.g. colleagues and non- or slightly-interacting groups) generate a weaker potential, resulting in a smaller deviation and a higher chance of intrusion.

The discussion above concerns results obtained using distances scaled with the group interpersonal distance; results concerning computations performed using distances measured in meters are shown in section 4.3.5.

4.3.5 Comparison to individual-individual collision avoidance

Many practitioners simulate crowds on the basis of individuals. Thus, it is interesting to compare the above-mentioned potentials with results obtained for individual-individual interaction. The results (using distances measured in meters, i.e. not scaled by group interpersonal distance) are shown in Figures 7-(c) and (d).

Note that groups are larger (than individuals) and expected to exert a stronger "social force", but they are also susceptible to being disrupted and intruded on (passed at ≈ 0 distance to their geometrical center). Also, while it is expected (statistically) that collision avoidance between individuals is symmetric, it may be that groups interact less than individuals by deviating very little. These effects seem to balance and potentials for collision avoidance between individuals are quite similar to those with groups.

Nevertheless, it may be seen that potentials describing low intensity social interactions, colleagues and families have typically a less steep derivative than the one for individual-individual encounters, while the opposite is observed for high-intensity social interactions and (in particular) for couples.

4.4 Conclusion

In this work, we analyzed how group-individual pedestrian collision avoidance depends on the group's social relation and social interaction intensity.

In detail, we verified that when straight motion (i.e. absence of collision avoidance) would lead to a possible collision, the actual minimum distance r_0 between the individual and the group is a growing function of social interaction intensity, and assumes a higher value for couples and friends. Similarly, individuals have a stronger tendency to "intrude" or "disrupt" a group by passing at a distance comparable to the group interpersonal distance when they face groups with low interaction intensity and colleagues and families, as can be verified both by studying 2D distance probability distributions, and by performing a statistical analysis on the probability that the minimum distance becomes smaller than the group interpersonal distance.

We also introduced a "potential" to study the dependence of "intensity of collision avoidance" on relative distance, by mimicking the theoretical modeling of two-body scattering in classical mechanics. This approach, which may be used as a guiding light in the development of a "social force model" of individual-group interaction, shows again that the potential determining collision avoidance tends to grow much faster with decreasing distance values (i.e. it has a steeper negative derivative) for strongly interacting groups, couples and families.

The latter result is particularly clear when studied using the group's average interpersonal distance as a length unit. A further comment on this result may be necessary, since the tendency of individuals not to pass through "strongly bonded dyads" (such as couples, friends and strongly interacting dyads) may be due not only to some kind of "social rule", but also to the fact that passing through these groups is actually harder due to the narrower space between them.

To this respect, we should finally comment also on the results concerning families, which may be a little counter-intuitive by suggesting that families are somehow perceived as weakly interacting and are often "intruded" [110]. It should be stressed that, as reported by Zanlungo et al. [44], the families in the ATC data set are mostly composed of parent-child pairs, that often do not walk abreast, or at least have a weaker tendency to walk abreast. The authors of the original study justify this tendency by referring to "the erratic behavior of children", but it may also be related to a stronger hierarchical structure in a parent-child dyad with respect to couples, friends and colleagues [44]. It may thus be argued that the tendency of individuals to approach families at a shorter distance may depend on families being less spatially structured, or correspondingly having a higher tendency to change their spatial structure. Such role of group spatial structure in individual-group interaction could be the subject of future studies, possibly when larger data sets collected in more suitable environments will be available.

We believe that our results and inferences point out interesting variabilities in pedestrian motion due to social aspects of human navigation [111]. A valuable implication of our study is that infrastructure design could be adapted to the nature of the social bonding of its users. We can speculate that, for instance, if a particular environment is known to be frequented mostly by strongly bonded groups, such as an amusement park, providing additional space (e.g. by widening corridors or walkways) to allow for collision avoidance may make it more comfortable. Nevertheless, these qualitative considerations should ultimately be corroborated with quantitative simulation models that include our findings. By taking into account the social dynamics of the people using a particular space, designers and architects could create environments that are more conducive to safe and efficient movement. This could help to reduce the risk of accidents and improve the overall user experience. We also hope that using models which account for the expected social composition of the crowd may help in improving the performance of tracking and simulation systems [112].

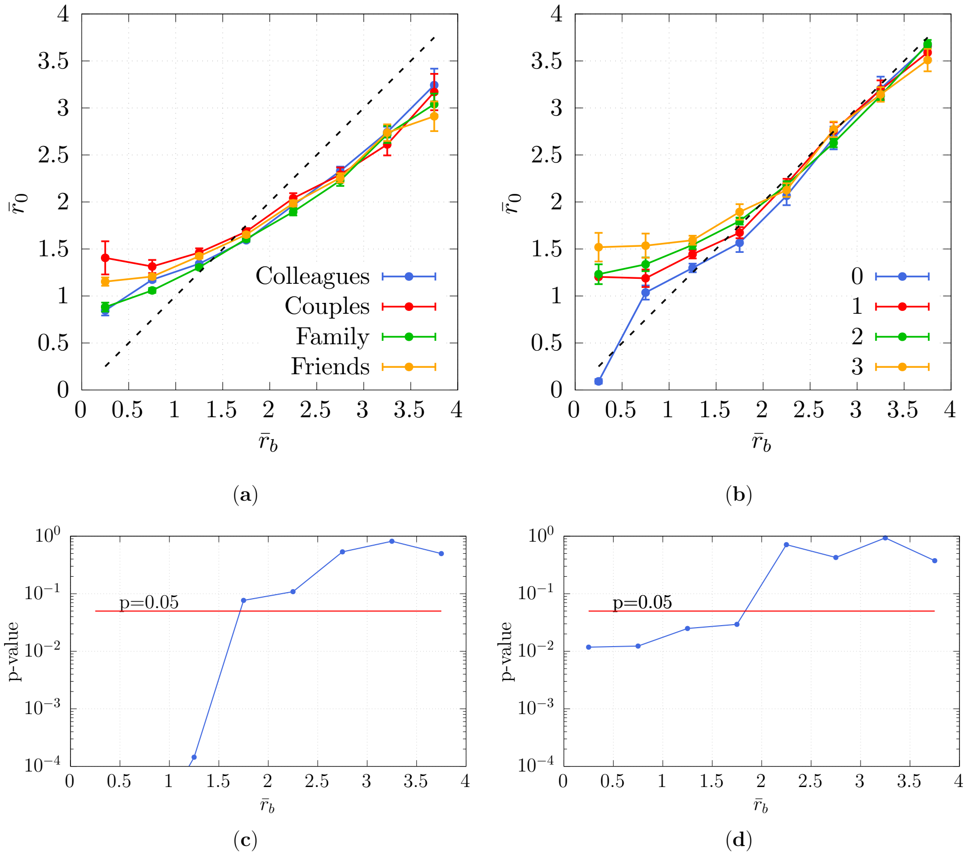

Figure 4.5: Observed minimum distance $\bar{r}_0$ as a function of the undisturbed straight-line distance $\bar{r}_b$ (a) for various social relations and (b) intensities of interaction of the group. Error bars report standard error intervals. The dashed line corresponds to the $\bar{r}_0 = \bar{r}_b$ linear dependence. p-values for the ANOVA of $\bar{r}_0$ (c) for various social relations and (d) intensities of interaction of the dyad. In (c), results for $\bar{r}_b < 1$ are not displayed as very low values were obtained ($p < 10^{-6}$).

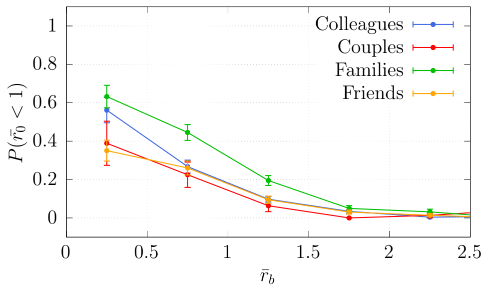

(a)

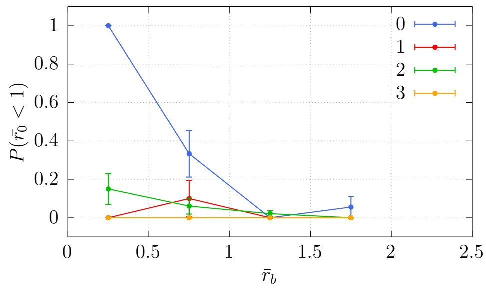

(b)

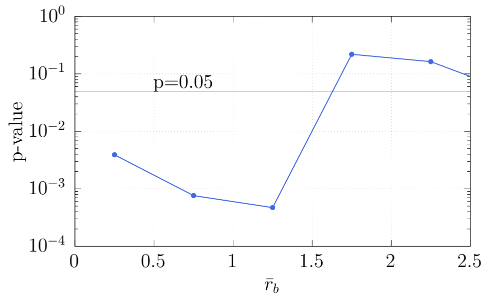

(c)

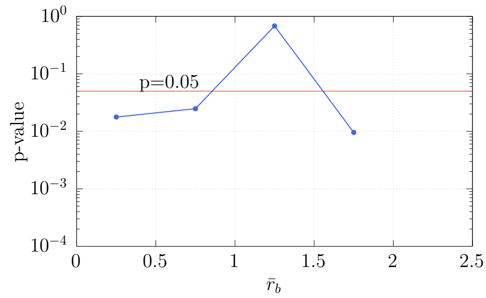

(d)

Figure 4.6: Probability that the distance $\bar{r}_0$ is smaller than 1 for (a) for various social relations and (b) intensities of interaction of the dyad. Pearson's χ^2 p-values for the hypothesis of independence of the frequencies of samples verifying $\bar{r}_0 < 1$ for (c) for various social relations and (d) intensities of interaction (of the group).

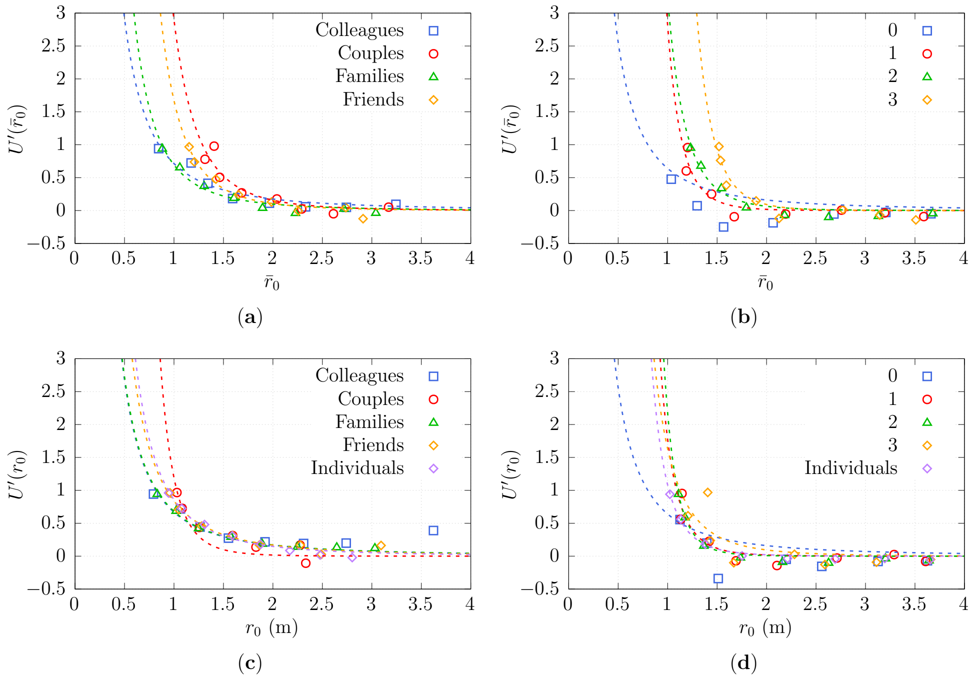

Figure 4.7: Collision avoidance potential $U'(\bar{r}_0)$ (a) for various social relations and (b) intensities of interaction of the group. Dashed lines correspond to a power function fit of the quantized data. Collision avoidance potential $U'(r_0)$ (c) for various social relations and (d) intensities of interaction of the group. Dashed lines correspond to an exponential fit of the quantized data. (c) and (d) report a comparison to individual-individual (non-group) interaction using non-scaled distances.

Chapter 5

Asymmetries in collision avoidance due to social factors

5.1 Introduction

With the progress of autonomous navigating agents for smart vehicles, assistive robots and drones and the pursuit of more accurate model of crowds, research attention towards collision avoidance has increased rapidly in recent years [104, 113, 114, 115]. Researchers have explored different approaches to model this capability [116, 117, 118]. In the early stages, the Social Force Model [10] introduced a repulsive force between particles (representing pedestrians) to account for collision avoidance. These models have demonstrated promising results, particularly when coupled with path-finding algorithms for navigating autonomous agents [3].

Recent studies have delved into the specifics of pairwise avoidance during face-to-face encounters among pedestrians, leveraging trajectory data from uninstructed individuals [119, 120, 9]. These investigations have studied the deviations exhibited by pedestrians from their initially projected, undisturbed paths when coming into contact with others, examining both one-on-one and one-versus-many scenarios. The findings of these studies were compared with those of a Langevin-like physics model, revealing, for instance, that interactions involving multiple approaching pedestrians are more accurately characterized by the non-linear combination of short-range contact avoidance forces.

In order to improve our comprehension of the impact of groups on the broader crowd dynamics, it is also necessary to study the specifics of collision avoidance between groups and

individuals. In particular, our recent works have revealed that collision avoidance between dyads and individuals is more pronounced when the dyad has a stronger social bond (e.g, couples or friends over colleagues, or engagement in a conversation) [3, 2, 123].
However, these conclusions were drawn based on an analysis that focused solely on the relative distance between the dyad and the individual. Therefore, this approach does not provide insight into the specific contributions of each party involved to the observed collision avoidance, since pedestrians do not necessarily follow the action-reaction principle of Physics [124]. It is plausible to assume that the dyads may become absorbed in their own social interaction, potentially making them less attentive to the pedestrians around them. As a result, individuals might need to be more proactive in avoiding collisions, either to compensate for this or due to adherence to a social norm. To put this hypothesis to the test, our study examines natural trajectories of uninstructed pedestrians.

5.2 Data and Methods

The data set used in this work is the DIAMOR data set [14]. It contains trajectories of uninstructed pedestrians recorded in an underground pedestrian street network of a commercial district of Osaka, in Japan. Trajectories are derived from depth information recorded using multiple laser ranger finders. The recording duration spans two weekdays for a total of eight hours of data, encompassing approximately 200 m^2 and allowing continuous tracking along a stretch of about 50 meters. The trajectories contain the position of each pedestrian and we compute the velocity by taking a first order derivative of the position.
Furthermore, video data was captured and employed for annotating social parameters. Human coders were tasked with annotating both groups and individuals (those not affiliated with a group). These coders also marked whether or not dyad members were involved in interaction (verbal communication, potentially accompanied by non-verbal cues like gestures or eye contact, as defined by Knapp et al. [103]), as well as gauging the intensity of the interaction on a scale of four levels, ranging from 0, denoting no interaction, to 3, indicating strong interaction. Previous works using this data set [15] have generally focused on quantifying and modeling the impact of social interaction on the dynamics and spatial properties of social groups.

5.2.1 Data preparation

Given that the data is gathered in an ecological environment, the tracked trajectories may encompass various behaviors such as waiting or running which are not pertinent to this study. To filter out atypical or non-characteristic observations, each trajectory is processed in the following manner.

We focus particularly on two-person groups, i.e. dyads, since they are the most represented groups in the data set, and because they have been shown to generally have stable spatial structures [125]. Formally, let a dyad be defined as an unordered pair consisting of two members, denoted as p and q, i.e., $d = (p, q)$, and let i represent an individual. For simplification purposes, we condense a dyad to a single mobile agent during the data preparation phase. Specifically, the dyad's location is denoted by the center of mass of the group, while its velocity is represented by the dyad velocity $\mathbf{v_d}$. More precisely, $\mathbf{r_d}$ and $\mathbf{v_d}$ denote the average positions and velocities of p and q at each time step, respectively.

Consequently, we handle both a dyad d and an individual i in a similar manner, initially assessing the adequacy of the number of trajectory data points. If there are more than 8 seconds of observation, we deem the trajectories to possess a satisfactory amount of data for characterizing locomotion while trajectory with fewer samples are excluded.

Furthermore, due to our focus on studying collision avoidance behaviors, we require that the dyad and the individual approach sufficiently close to each other. Therefore, we only consider trajectories where the following condition is verified: $\exists t \mid d_{di}(t) \leq 4$ m, where t denotes time and d_{di} is the instantaneous distance. The choice of a 4 m threshold is motivated by previous research on collision avoidance. Cinelli and Patla discovered that the "safety zone", which is the area in which individuals allow a moving object to approach before initiating an avoidance behavior, averages around 3.73 meters [104]. Additionally, Kitazawa et al. demonstrated that pedestrians focus their gaze most intensely on other approaching individuals when they are, on average, approximately 3.97 meters away, rarely directing their attention to pedestrians at greater distances [105].

Lastly, as our focus centers on understanding how the social attributes of the dyad influence collision avoidance, it is crucial that the pedestrians involved have sufficient visual access to each other. Thus, we stipulate that the dyad and the individual must have a frontal view of each other, indicating that they are moving in opposing directions. In this arrangement, they will be able to observe the approaching party and discern its social characteristics.

To guarantee a frontal view, we determined the relative motion direction of d and i, only considering those pairs that are moving in opposite directions. Let ϕ denote the angle between the velocity vectors $\mathbf{v_d}$ and $\mathbf{v_i}$ at a given moment, $\phi = arccos\frac{(\mathbf{v_d} \cdot \mathbf{v_i})}{(||\mathbf{v_d}||||\mathbf{v_i}||)}$. Then, d and i are regarded as moving in opposite directions, if $3\pi/4 \leq \phi < \pi$.
It is possible that other pedestrians may be present in the vicinity of the dyad and the individual, potentially influencing their behavior but we do not filter these to avoid reducing the sample size. We argue that such effects are likely to be averaged out and that most of the deviation will be due to the actual encounter between dyad and the individual.

5.2.2 Maximum lateral deviation

In a previous study [113], Huber et al. studied the adjustments of path and speed made by a pedestrian when crossing with a non-reacting interferer at varying angles. Although the present study differs in purpose and nature of data/experiments, we expect to find similar behaviors in real world data, with pedestrians deflecting laterally to avoid a collision.
In quantifying the level of such adjustments, Huber et al. define the "lateral deviation" from the planned path of pedestrians, when avoiding collision with an "interferer" (an instructed pedestrian walking on a straight path, intersecting with the subject's path). In particular, this deviation is defined as the maximum Euclidean distance between the points on the actual (i.e. observed) trajectory and the straight line passing through its initial and final points. Nonetheless, in real world trajectories, it can be expected that after deviation from their initial trajectory, pedestrians stay on the new lateral position rather than returning to their original position. This assumption is validated in the work of Corbetta et al. [119], where pedestrians are shown to maintain their lateral distance even after avoidance is ensured.
Consequently, we compute our "maximum lateral deviation" δ by measuring the maximum distance between the points on the trajectory during the encounter (i.e. when the dyad and the individuals are less than 4 m apart) and the line directed by the velocity of the individual (resp. dyad) at the beginning of the encounter, i.e. 4 m away from the incoming dyad (resp. individual) (see fig. 5.1). We argue that this line constitutes a better approximation of the intended trajectory than the line going through the first and last point of the trajectory, since it does not make any assumptions on what happens after the avoidance phenomenon.
To make the computation of this distance more robust against instantaneous fluctuations of

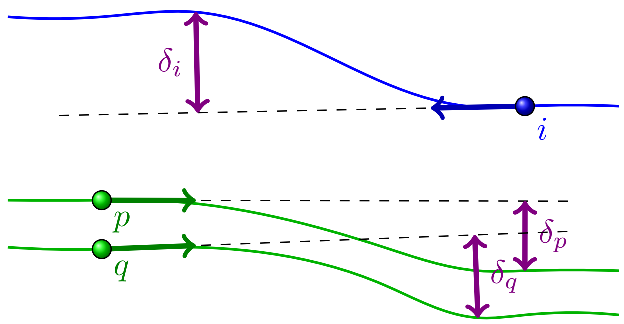

Figure 5.1: Illustration of the computation of the maximum lateral deviation δ for an encounter between a dyad $d = (p, q)$ and an individual i

the direction of the velocity vector of the pedestrian(s) that can arise from gait dynamics, we measure the velocity before the encounter by averaging the instantaneous velocities over 2 seconds.

It is important to note that the values for the dyads correspond to the average of the individual deviation of the dyad's members, i.e. $\delta_d = \frac{\delta_p+\delta_q}{2}$. Using the center of mass of the dyad, as defined and used in section 5.2.1, to compute the deviation would result in artificially lower values, since it would tend to smooth the trajectories.

5.3 Results and Discussion

table 5.1 shows the average maximum lateral deviation of individuals and dyads for various levels of intensity of interaction, as well as the average deviation for all individuals and dyads.

One first interesting result is that, based on the cumulated values, it is clear that individuals deviate more than dyads during frontal encounters. The statistical significance of the difference seen in lateral deviation values is demonstrated by the low p-value obtained from the two-sample Welch's t-tests for the equality of means ($\ll 10^{-3}$).

Moreover, it appears that this difference in deviation between individual and dyad depends on the intensity of interaction of the dyad. As a matter of fact, higher levels of interaction of the dyad (annotated as 2 and 3) are consistent with more significant deviations between individual and dyad (both p-values $< 10^{-3}$). On the other hand, for lower levels of interaction (0 and 1), the statistical significance is lost and the deviations present less pronounced

Table 5.1: Average maximum lateral deviation δ of individuals and dyads annotated with each intensity of interaction of the encountered dyad. p-value for the two-sample Welch's t-tests for the equality of means are also shown.

Intensity of interaction	# encounters	δ_i (mm)	δ_d (mm)	T-test p-value
0 (no interaction)	75	383 ± 236	382 ± 300	0.98
1	161	387 ± 287	326 ± 220	0.20
2	771	396 ± 305	334 ± 252	$< 10^{-3}$
3 (strong interaction)	208	450 ± 333	359 ± 250	$< 10^{-3}$
all	1215	403 ± 304	340 ± 251	$< 10^{-3}$

disparities.

Finally, we observe that a higher level of interaction of the dyad is consistently associated with a stronger deviation of the individual. In other words, people tend to, perhaps unconsciously, give more space to incoming groups when they are strongly interacting. One may argue that individuals gauge their avoidance based on their expectation of how much the groups will act to avoid them, as previously modeled in [8]. Nevertheless, such relation could not be found for the dyad itself though, as the smaller deviations are found for the intermediate levels of interaction (1 and 2).

5.4 Conclusion and Limits

This chapter delved into the intricacies of frontal encounters between dyads and individuals, with a focus on quantifying each participant's role in collision avoidance based on their deviation from their intended path. By establishing the intended trajectory for each party, considering their pre-encounter walking direction, we identified the maximum lateral deviation as a key metric.

Unlike our previous works on the topic [2, 3], we did not limit ourselves to studying only relative distances but analyzed the position of each pedestrian involved in the collision avoidance, in the reference frame of the world. This decision was made to ensure that a direct comparison of the contributions of both parties to the collision avoidance dynamics was feasible. It also allowed computing separate deviations for both members of the dyad to prevent any collateral smoothing resulting from using the center of mass of the group.

Our findings revealed a substantial discrepancy in deviation between group members and individuals during these encounters. Moreover, we conducted a thorough analysis of how the intensity of interaction among group members influences collision avoidance dynamics. Notably, the contrast in deviation between individuals and group members was most pronounced when the level of interaction within the dyad was high. Finally, our results demonstrated that higher levels of interaction between the members of the dyad led to more significant deviations in the trajectories of encountered individuals, but that no such relation could be found for the dyad itself.

This research underscores the pivotal role of social dynamics in shaping pedestrian behavior during face-to-face encounters, offering valuable insights for understanding and potentially improving collision avoidance strategies in various contexts, such as autonomous navigation and crowd management.

Nevertheless, there are certain limitations within the scope of this study. Firstly, we focused on encounter scenarios, but it would be valuable to contrast the deviations observed in these cases with a baseline of undisturbed situations, when neither dyads nor individuals are in proximity to any other pedestrian. Additionally, alternative metrics for quantifying the extent of deviation between the two parties could be explored. For instance, the straightness index, calculated as the ratio of the straight-line distance to the actual traveled distance, presents another viable option. Addressing these limitations will be a focal point in forthcoming works.

Chapter 6

Imbalances in collision avoidance due to social interaction

6.1 Introduction

Human walking motion is studied across various disciplines, each offering a unique perspective, ranging from event safety [1, 126, 127], and public space design [128, 129, 130]to visuo-motor coordination [131]. In this chapter, we focus on walking as the most fundamental means of transportation [132] and as an essential activity for independent living. In such settings, people navigate among fellow pedestrians and obstacles, with a focus on safety and fluidity, a concept referred to as human–human collision avoidance. These localised interactions are thought to give rise to self-organization within a local-to-global framework [133, 134].

To capture the essence of this navigation behaviour, a large variety of computational models have been proposed [135, 136]. Early models, inspired by physics, employed repulsive forces to simulate human–human collision avoidance [10]. Although these models have been successful in generating coherent patterns at the collective level and have greatly contributed to our understanding of pedestrian motion [10], they often fall short in accurately capturing the realistic attributes of human trajectories [133], namely the ones arising from the very fact that humans are social beings, with a theory of mind. For example, it is not unreasonable to assume that pedestrians may adjust their collision avoidance strategies based on social cues from others, an aspect often overlooked in traditional models. More problematically, we believe that there is a shortage of research quantifying the effect of social interaction on pedestrian dynamics in real-world settings.

A typical manifestation of the social nature of humans is group formation. In this chapter, *groups* refer to 2 or more pedestrians travelling together in the same direction, engaged in a social relationship [54, 102]. Conversely, pedestrians not part of a group are termed *singles*[1]. We build on the findings of [3, 4] that illustrate the effect of social interaction on human–human collision avoidance. Carrying this forward, we investigate the extent of each party's contribution to the collision avoidance and how social interaction affects this contribution by analysing pedestrians' behaviour in their ecological environment. To dissociate the attentional demands of groups from their size and hierarchy, we choose to focus on two-people groups, known as *dyads*[2]. We argue that this approach is not oversimplified, as most groups in crowds consist of two people [138] and larger groups often break down into sub-groups of two or three people, making dyads a fundamental building block of crowds [139, 125]. By categorising these dyads according to their level of social interaction [15], we can address the variability in attentional demands and potentially approximate the gradation of mental workload[3].

6.2 Literature review

6.2.1 Community ambulation

The concept of "community ambulation" in the literature refers to an individuals' ability to move independently in public spaces [140][4]. By definition, community ambulation requires the capacity to integrate walking with various demands arising from the dynamic nature of public environments. Patla et al. precisely identify factors contributing to this integration,

[1]While each group member can navigate independently, their group affiliation significantly influences their movement. Therefore, we identify and analyze them based on their group dynamics throughout the research.

[2]A dyad specifically refers to a group of exactly two pedestrians. In particular, a pair of pedestrians in a larger group is not considered a dyad in this study.

[3]We would like to clarify that we use the term *interaction* in a specific context, referring exclusively to social interaction characterised by verbal communication, gestures, gaze, physical contact and other forms of engagement within the dyad. Importantly, we distinguish social interaction from the reactive collision avoidance strategies that pedestrians employ during encounters.

[4]A more precise definition provided in [141] specifies that community ambulation entails walking a defined distance (such as 800 m) and navigating stairs without assistance.

including walking distance and speed, ambient conditions, physical load, terrain variations, postural transitions, traffic density, and attentional demands [142].

To meet these demands, individuals must constantly navigate decision-making processes while engaged in ongoing activities [143]. These embodied decisions necessitate the rapid and continuous processing of multimodal sensory information [144] as well as the evaluation of all possibilities in parallel, leading to the execution of the anticipated optimal choice. Although there is ongoing debate regarding the exact mechanisms underlying these decision-making processes [145, 146], the complexity of this cognitive process is widely acknowledged.

While navigating in public environments, pedestrians need to allocate attentional resources to observe their surroundings, identify potential hazards (like stairs and static obstacles) and remain vigilant to changes [147]. Nevertheless, the underlying principles of anticipatory locomotor adaptations used to circumvent such challenges are not completely understood [148]. Shumway-Cook et al. identify three key factors influencing attentional demands during community ambulation: familiarity with the trip location, environmental distractions, and the presence or absence of travel companions [141].

6.2.2 Allocation of attention during community ambulation

Humans generally possess a highly effective ability to perceive and interpret the visual world [144], despite certain limitations in our vision [149]. During community ambulation, visual information is processed in real time [131]. This processing is influenced by visual conspicuity (i.e. how easily objects or obstacles stand out in the environment [150, 144]) and by the specific demands of the task [151]. The principal role of the vision in locomotion is to provide an understanding of the location of oneself, the goal, and the environment (e.g. dimensions, terrain features, etc.), which are essential for adaptive locomotion [152]. This has been demonstrated in studies contrasting open-loop obstacle avoidance to full visual sampling [131].

Studies [153, 154] have demonstrated that pedestrians rely on visual cues for efficient path planning around static obstacles. This entails utilising visual information to locate the target destination and assess the surrounding path, as well as evaluating the magnitude of the deviation necessary to effectively navigate obstacles, ensuring seamless progression toward their intended destination.

Beyond static obstacles, pedestrians must also be aware of moving targets (e.g. other pedestrians, bicycles, cars, etc.) and anticipate potential collisions, which present greater challenges compared to stationary obstacles due to their momentum and potentially erratic motion [155].

Pedestrians use visual information not only to anticipate the paths of others, but also to make fine-tuned path adjustments based on perceived apparent personal features of others. For instance, role-dependent strategies in human–human collision avoidance have been shown to vary with factors such as gender, attractiveness, height, and group relationships [156, 157]. Conversely, the lack of visual information can increase anxiety during encounters with other pedestrians[158]. In addition, pedestrians navigating around stationary individuals maintain greater distances from males than females, from groups rather than individuals, and from attractive rather than unattractive people [157]. Nevertheless, to the best of our knowledge, no study has examined whether pedestrians perceive social interactions within groups or whether they adjust their collision avoidance strategies based on such perceptions. This chapter provides compelling evidence that pedestrians perceive these interactions and adjust their behaviour accordingly, although the extent of this adjustment depends on the attentional resources available to the parties involved, possibly influenced by a theory of mind model.

6.2.3 Theory of Mind Model

In addition to the factors discussed, pedestrians' gaze direction is a crucial cue for understanding their intentions and attentional focus [159]. In the context of community ambulation, eye gaze is a key component of social interaction, serving as a communicative tool for signaling intentions and coordinating behaviour [160, 161]. A study on pedestrian navigation in urban settings by Nummenmaa et al. demonstrated that pedestrians use gaze aversion to signal their intended path, prompting others to steer in the opposite direction to avoid collisions [161]. This chapter highlights the communicative efficacy of gaze aversion and the role of eye gaze in understanding others' intentions.

The Theory of Mind Model suggests that eye gaze plays a crucial role in understanding others' intentions [159]. The absence of gaze alternation can lead to failures in anticipating others' attentional focus and intentions in static scenarios, a phenomenon known as "mind blindness" [162]. Beyond gaze direction, head orientation indicates focus of attention [163] and serves as a cue for path selection, while body orientation suggests a "potential to move" [164]. These findings imply that the brain, responsible for orchestrating swift and successful behaviour in such settings, relies not only on spontaneous sensory inputs but also on internal representations of surrounding pedestrians to fulfill this role effectively [165].

6.2.4 Social interaction and cognitive load

To effectively navigate their environment and avoid collisions with others, group members must not only maintain situational awareness but also observe their partners. This attentiveness is essential to promote group cohesion and facilitate social interactions within the group. This monitoring process often relies on visual and auditory channels, akin to a dual-task mobility scenario.

Specifically, social interaction in a group typically requires visual resources for tracking the focus of attention (e.g. gaze on partner or a mutual gaze on a target) and eliciting emotions (e.g. facial expression, gestures), etc. [166]. In addition, the audio channel is essential for understanding speech, detecting changes in pitch, loudness, and intonation of the interlocutor, and managing conversational turns (signaling turn taking, holding, giving or skipping). It also plays a vital role in communicating feedback (e.g. agreement, surprise, etc.) and providing acknowledgement (i.e. back-channeling).

Given that humans have limited attentional resources and group members may already need to devote part of those to the afore-mentioned commitments towards their partners, they are likely to be left with less resources for navigation planning compared to individuals [167, 168, 169][5].

6.2.5 Ecological studies and modeling of pedestrian dynamics

Pedestrian dynamics have been extensively studied through various models [9] designed to replicate pedestrian behaviour as they navigate toward goals while avoiding both static (e.g. walls, pillars) and dynamic (e.g. other pedestrians) obstacles. Prominent approaches in this field include particle-based simulations [10] and agent-based models [170].

One of the early models, the social force model [10], uses attractive and repulsive forces to simulate movement, where particles are "pushed" away from obstacles and other pedes-

[5]This scenario might also require them to maintain larger personal space to make the trajectory adjustments necessary for collision avoidance [148].

trians, and "pulled" toward their destination. Parameters for these models may be obtained from real-world observations of pedestrians [14, 74], enabling these models to more closely mirror actual movement patterns. Recent developments in pedestrian modeling have integrated more complex decision-making processes, inspired by game theory strategies [171] or cognitive heuristics [172, 173].

Data-driven models have gained significant momentum, fueled by the availability of large-scale trajectory datasets captured using increasingly advanced tracking technologies [174, 175]. Their rich datasets enable researchers to refine models for better accuracy in capturing real-world pedestrian behaviours, particularly in various scenarios such as navigating along curved paths [176] or avoiding collisions with others [119].

Human–human collision avoidance remains a central focus in pedestrian dynamics research, often studied in experimental settings involving static obstacles [177] or pairwise encounters [148, 113]. These analyses typically involve measuring how much pedestrians deviate from a straight path when navigating around obstacles or others.

Additionally, works such as [178, 119] have utilised ecological data, applying methods similar to impact parameter analysis in physics to model pedestrian deviations in both 1-1 and 1-N encounters. Our framework aligns with these studies, but we further incorporate the intensity of interaction as a significant factor. This approach helps capture the influence of social dynamics on collision avoidance behaviour more comprehensively. While our study does not aim to model pedestrian behaviour, it focuses on quantifying deviations during pedestrian encounters.

6.3 Material and methods

6.3.1 Dataset

The dataset utilised in this chapter is the DIAMOR dataset [179], which was previously employed for the purpose of group recognition and pedestrian dynamics modeling [101, 15]. These data were collected in an underground pedestrian street network located in a commercial district of Osaka, Japan. They comprise recordings from two straight corridors within this street network, and our focus centres on one of these. A photograph of the recording area is shown in fig. 6.1a. The location, surrounded by several train stations, business centers, and shopping malls, offers diverse pedestrian profiles. The recording area covers roughly 200 m^2 and allows continuous tracking along approximately 50 m and the recording spans eight hours in a weekday.

This dataset is particularly valuable as it captures uninstructed pedestrians in their natural environment, providing insights into naturalistic behaviour. The experiment was reviewed and approved by the ATR ethics board with document number 10-502-1 and was conducted with posters informing passersby about the pedestrian tracking experiment. The data, containing anonymous trajectories derived from range data [180], is publicly available [179].

Notably, studies on nonhuman animals have revealed differences in behaviour between constrained tasks and natural settings [181, 182, 183]. Similarly, in human studies, the phenomenon of modifying one's behaviour in response to the awareness of being observed has even been given a name, i.e. the "Hawthorne effect"[6]. This effect has been observed in various settings, including when assessing the quality of care provided by trained practitioners [186], or the energy awareness of consumers [187]. In human locomotion, it was shown that observed participants exhibit lower variability in gait parameters [188], and that locomotion parameters (e.g. speed, step length) were impacted by the number of researchers present in the room [189, 188]. In this respect, the ecological data studied in the upcoming sections minimise experimental or behavioural bias, or subconscious alterations in behaviour, or is at least minimally affected by such factors. Note that with these arguments, we by no means intend to assert that the outcomes derived from traditional, meticulously controlled experimental paradigms are inaccurate or invalid. These approaches, which are proficient at dissecting intricate behaviours into their single components, have significantly contributed to our understanding of the fundamental processes that govern behaviour. Nonetheless, this reductionist approach may constrain the ability to elucidate naturalistic behaviour. In real-world settings, pristine experiences are more of an exception than the norm and it is essential to study naturalistic behaviour to effectively explain real-world actions [190].

The data include both depth and video information. The depth information is utilised to derive pedestrian trajectories [180], which can be freely downloaded [179]. From this tracking process, we obtain the normalised cumulative density map shown in fig. 6.1b. The map is obtained by dividing the recording area into a grid of 10 cm $\times$ 10 cm cells and counting the number of pedestrians that have been in each cell over time. The counts are then normalised by dividing by the maximum count in the grid, with darker areas indicating

[6]Although it is now largely agreed that such effect was less significant than originally thought in the scenario from which it takes its name [184, 185]

higher pedestrian density.

(a)

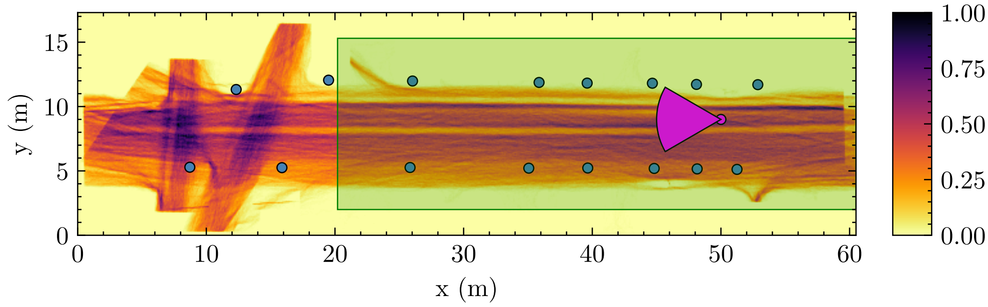

(b)

Figure 6.1: (a) Photograph of the underground pedestrian street network where the DIAMOR dataset was recorded. The sensors used for pedestrian tracking are highlighted in blue. (b) Normalised cumulative density map for the DIAMOR dataset. It is obtained by dividing the recording area into a grid of 10 cm × 10 cm cells and counting the number of pedestrians that have been in each cell at any point in time. The counts are then normalised by the maximum count in the grid. Darker areas indicate higher pedestrian density. The green rectangle indicates the portion of the recording area used in this study (a corridor of approximately 40 m), the blue dots represent the sensors used for tracking pedestrians, and the magenta wedge indicates the field of view of the camera used for the video data.

The video data served as the basis for establishing the ground truth regarding dyads and their intensity of interaction. To assess errors arising from coding fatigue and coder bias, each relationship (group membership and interaction intensity) was labeled by two different coders. Initially, coders observed factors such as walking patterns, age, gender, and clothing to determine which pedestrians formed a group (with sizes ranging from two to as many as seven people). In the second stage, coders focused on dyads identified in the first stage to assess interaction intensity. We then used the labels provided by one of the coders as the ground truth. This reduced the amount of data each coder had to view, thus enhancing coding efficiency. Coders were asked to rate the intensity of interaction on a subjective scale from 0 to 3 (0: no interaction, 1: weak interaction, 2: mild interaction, 3: strong interaction). To avoid bias in their assessments, only the resolution (i.e. the number of interaction levels) was predefined (four levels), with no guidelines provided on what constituted weak, mild, or strong interaction intensity. Instead, coders engaged in free-viewing of three hours of dyad video footage to intuitively grasp variations in interaction intensity before starting the actual coding task. A key reason for this approach is that social interactions are inherently fluid and can vary greatly depending on the context, making it difficult to establish strict boundaries for each intensity level. By observing the natural flow of interactions, coders were able to make judgments based on the overall impression, rather than following rigid criteria that might overlook the complexity of social behaviour. The agreement between coders for group relation labeling was evaluated using Cohen's κ coefficient, which showed a high value of $\kappa = 0.96$, indicating strong agreement[191]. For interaction intensity labeling, reliability was assessed using Krippendorff's α coefficient, yielding a value of $\alpha = 0.67$, usually considered sufficiently high[49].

6.3.2 Data preparation

The raw trajectories in the DIAMOR dataset were sampled at a non-uniform rate, with frequencies ranging from 20 to 50 Hz [179] owing to occlusions or tracking errors. To prevent these inconsistencies from impacting the analysis, we resample the trajectories at a constant rate f_s of 33 Hz using cubic spline interpolation [192].

As mentioned in section 6.1, this chapter focuses on understanding the dynamics of typical single-dyad collision avoidance in public settings. To achieve this, we retain only the trajectories that align with typical walking speeds in public spaces, excluding anomalies. Based on literature on human locomotion [14], we consider trajectories with an average velocity falling within the range of $[0.5, 3]$ m/sec as representative of typical urban walking motion while others are associated with different states (such as standing, running, or tracking artifacts).

To address the impact of sensing noise and natural swaying resulting from human gait, we applied filtering to the trajectories. Low-pass filtering is a common method for this [193, 194, 133], and in this chapter we opted for a Savitzky–Golay filter [195], which is well-suited for smoothing noisy data. Specifically, we adjusted the polynomial order to 2 and the filter window length to 3 s based on the typical gait cycle duration of 1 to 2 s [196, 197].

In this chapter, we use the notation $\mathbf{p}(t)$ to denote the position of a pedestrian at time t, and $\mathbf{v}(t)$ to denote the velocity of the pedestrian at time t. We will also use the notation $\mathbf{p}_i(t)$ and $\mathbf{v}_i(t)$ to denote the position and velocity of the single i at time t, and $\mathbf{p}_d(t)$ and $\mathbf{v}_d(t)$ to denote the position and velocity of the dyad d at time t[7].

A *trajectory* T is defined as the sequence of positions $\mathbf{p}(t_k)$ and velocities $\mathbf{v}(t_k)$ of a pedestrian, where t_k is the time at which the positions are recorded, with $k \in [0, N-1]$ and N denoting the number of samples.

The velocity $\mathbf{v}(t_k)$ is derived from the positions using a simple forward Euler difference, i.e.

$$\mathbf{v}(t_k) = \begin{cases} \dfrac{\mathbf{p}(t_{k+1}) - \mathbf{p}(t_k)}{t_{k+1} - t_k} & \text{if } k < N-1 \\ \mathbf{v}(t_{k-1}) & \text{if } k = N-1 \end{cases} \tag{6.1}$$

$$T = \left[(\mathbf{p}(t_0), \mathbf{v}(t_0)), (\mathbf{p}(t_1), \mathbf{v}(t_1)), \ldots, (\mathbf{p}(t_{N-1}), \mathbf{v}(t_{N-1}))\right]. \tag{6.2}$$

6.3.3 Intended direction of motion

Our primary assumption in assessing the trajectory deviation is that pedestrians aim to minimise the distance traveled, selecting the straightest path to reach their destination whenever possible. This assumption, notably introduced by Hoogendoorn et al. [7] and adopted by numerous other studies [140, 198], posits that at the tactical level, where pedestrians make decisions about their desired area and route, they do so by minimising a cost function. This function considers factors such as the distance traveled, trajectory comfort, or anticipated encounters with other pedestrians [7]. In a straight corridor, such as the one

[7] When this notation is used, we consider the dyad as a single entity and use the average position and velocity of the dyad members. In other situations, we will consider the dyad members separately to avoid biases from artificial smoothing caused by averaging.

examined in our study, a straight line is reasonably the optimal route to cross the corridor (assuming that the pedestrian does not intend to exit the corridor through a side passage). If the corridor is sufficiently wide, the optimal path may still be straight, but not perfectly aligned with the corridor axis, as pedestrians may cross it diagonally.

To compute the straight line trajectory, we first need to identify the *intended direction of motion* of the pedestrian. We define it as the line going through $\mathbf{p}(t_0)$ and guided by $\mathbf{v_0}$ which is the average velocity vector[8] over a 0.5 s window starting at t_0 (the first time point of the trajectory). At a sampling frequency of 33 Hz, this corresponds to $N_e = \lfloor 33 \times 0.5 \rfloor = 16$ samples and

$$\mathbf{v_0} = \frac{1}{N_e} \sum_{k=0}^{N_e-1} \mathbf{v}(t_k). \tag{6.3}$$

We believe a 0.5 s window size to be appropriate for this analysis. This duration corresponds to the time it takes for a pedestrian to complete a single step, allowing it to effectively capture the overall direction of motion, while being small enough to avoid incorporating the effects of collision avoidance behaviour.

The intended direction of motion L_0 is formally defined as follows:

$$L_0 = \{\mathbf{p}(t_0) + \lambda \mathbf{v_0} \mid \lambda \in \mathbb{R}\}. \tag{6.4}$$

We argue that this line better represents the intended motion of the pedestrian than one formed by connecting $\mathbf{p}(t_0)$ and $\mathbf{p}(t_{N-1})$, as the latter is influenced by the trajectory deviations that we aim to quantify, particularly if the pedestrian does not return to their original intended path after deviating.

In addition, the *straight line trajectory* T_0 is defined as the trajectory that the pedestrian would follow, should they maintain their intended direction while walking at a constant speed. The points of the straight line trajectory are all on the line L_0 and verify

$$\begin{cases} \tilde{\mathbf{p}}(t_k) = \mathbf{p}(t_0) + \mathbf{v_0} t_k \\ \tilde{\mathbf{v}}(t_k) = \mathbf{v_0} \end{cases} \quad \forall k \in [0, N-1] \tag{6.5}$$

We emphasise that the straight line trajectory, composed of a sequence of N discrete positions and velocities, differs from the desired direction of motion, which represents a line with an infinite number of points.

[8]Since the velocity vectors are computed using a forward Euler difference, the velocity at time t_k points from $\mathbf{p}(t_k)$ to $\mathbf{p}(t_{k+1})$. Therefore, the average velocity vector $\mathbf{v_0}$ points from $\mathbf{p}(t_0)$ to $\mathbf{p}(t_{N_e})$.

6.3.4 Situations of interest

Drawing from the terminology introduced in [7], at the operational level, where pedestrians execute their selected route, they may deviate from the straight line trajectory, possibly influenced by factors such as gait characteristics [199] and the presence of other pedestrians or obstacles. This chapter aims to quantify and compare trajectory deviations between singles and dyads, emphasising the impact of social interaction within groups (which we assume may influence the group's mental workload and attentional resources available for navigation planning, although we do not measure them directly), we examine two scenarios: (1) undisturbed segments, where singles or dyads move freely without encountering other pedestrians within a reasonably large area, allowing them to move freely without needing to perform avoidance behaviour, and (2) encounters, where a dyad and a single are on a frontal collision or close-to-collision course.

Undisturbed situations

As discussed in section 6.3.3, although pedestrians generally aim to minimise the traveled distance by selecting the straightest possible path, it is unrealistic to expect perfectly straight walking even in the absence of other pedestrians. This natural meandering [199] can be attributed to the natural swaying resulting from human gait and the impact of factors such as the cognitive load [200] and has been modeled using a Langevin-like model [178].

To establish a baseline of straightness for both individuals and dyads when not forced to avoid collisions, we define undisturbed segments as parts of a trajectory where no other pedestrian is located within 4 m away, consistent with the window size adopted in the computation of trajectory deviation during encounters.

Unlike encounters, which are spatially constrained (typically 3 to 4 m, depending on lateral distance and speed) as defined in section 6.3.4, undisturbed segments can be arbitrarily long.

To enable comparability between segments from the two scenarios, we must select undisturbed segments with lengths similar to the spatially constrained encounter cases. We extract undisturbed segments of 4 m [104, 74], ensuring there are no overlaps between them. In addition, the motion direction at the beginning and end of the segment must align with the horizontal axis. This is ensured by verifying that the absolute angles of the velocity vector in 0.5 s windows at the segment's beginning and end, wrapped within the range $[-\pi, \pi]$ are less than $\frac{\pi}{8}$ or greater than $\frac{7\pi}{8}$ in more than 90% of all N_e time steps in these windows. This ensures that the pedestrian is not turning at the beginning or end of the segment.

According to the above, a single or dyad may have multiple undisturbed segments (in particular if they are observed for a long time and if there are few other pedestrians around). Since these segments might not be independent, given that the pedestrians' behaviour in one segment may be influenced by the behaviour in the previous one, we consider the average deviation across all undisturbed segments of a single or dyad as a unique data point in the analysis. In the "Undisturbed" column table 6.1, we list the number of singles and dyads in undisturbed situations. In the "Encounters" column, we provide a breakdown of the number of undisturbed dyads based on the intensity of interaction of the dyad. We note that the number of observations for encounters involving a dyad with an interaction level of 2 is significantly higher than the other levels. This may be partially explained by the "central tendency bias"[201], where coders tend to assign the middle value of the scale more frequently than the extreme values. Nonetheless, we believe that the dataset is sufficiently diverse to draw meaningful conclusions.

Table 6.1: Trajectory statistics. Breakdown of the number of analyzed trajectories. For undisturbed segments, the number of singles and dyad members are shown. Dyads are further broken down according to the intensity of interaction. For encounters, the numbers of situations are shown (each situation involves three trajectories: one for the single and two for the dyad members). The encounters are further broken down according to the intensity of interaction of the dyads. A total of 2768 unique pedestrians were analyzed.

Intensity of interaction	Undisturbed		Encounters
	Dyad members	Singles	
0	18	NA	45
1	60		88
2	299		380
3	80		96
All	457	1966	609

Encounters

We define encounters as situations where a dyad d and a single i move toward each other on a collision or close-to-collision course. In these scenarios, it is likely that one or both parties will engage in collision avoidance behaviour to ensure a comfortable passage. Despite the common use of the superposition assumption in many models (such as the social force model [10]), which suggests that the collective effects on a pedestrian from multiple neighbors can be linearly combined [133], there is ongoing debate regarding whether neighborhood is determined by metric or topological distances (e.g. degree of neighborhood). In this work, we have chosen to use metric distance since the density in our dataset is not high enough to induce collective behaviour [202]. In that respect, we consider only those dyads and singles, who approach each other closely. Specifically, we require that $\exists t \mid d_{di}(t) \leq 4\text{m}$, where d_{di} denotes the instantaneous distance between the dyad and the single.

The choice of a 4 m threshold is grounded in prior research on human–human collision avoidance. Cinelli and Patla found that the "safety zone", or the distance at which individuals begin to avoid a moving object, averages around 3.73 m [104]. In addition, Gérin–Lajoie et al. showed that the anticipatory locomotor phase starts with an initial path deviation which occurs approximately 4.5 m from an obstacle [148]. It has also been demonstrated that pedestrians focus their gaze most intensely on approaching individuals when they are, on average, approximately 3.97 m away, rarely paying attention to pedestrians at greater distances [105].

Among the instances where dyads and singles come sufficiently close, we solely consider those engaging in *frontal encounters*, meaning they are moving in opposite directions. There are two main reasons for this selective approach. First, given our focus on human–human collision avoidance within an environment characterised by predominantly bi-directional flow, we argue that encounters involving pedestrians from opposite directions are more pertinent than those moving in the same direction. Second, to understand the implications of social interaction levels (allowing us to speculate on the allocation of attentional demands), we consider only scenarios where the involved parties can visually examine each other (this is crucial for an individual pedestrian to judge group dynamics and assess dyad's interaction level) [192, 157]. Non-frontal encounters are omitted, since collision avoidance is less prominent for such encounters within low-density bi-directional flow settings, and singles are not likely to react to dyads' characteristics owing to limited observation capabilities.

To address this, we compute the predominant relative motion direction of d and i at the beginning of the encounter by calculating the cosine of the angle between their velocity vectors,

$$c_{di}(t) = \frac{\mathbf{v}_d(t) \cdot \mathbf{v}_i(t)}{||\mathbf{v}_d(t)||||\mathbf{v}_i(t)||}. \tag{6.6}$$

We classify an encounter as frontal if, during a 0.5 s window starting at t_0, the cosine of the angle between the velocity vectors is smaller than $-\cos\left(\frac{\pi}{8}\right)$ for at least 90% of all N_e time steps (indicating an angle range of $[\frac{7\pi}{8}, \frac{9\pi}{8}]$). This condition is formally expressed as

$$\frac{1}{N_e} \sum_{k=0}^{N_e-1} \mathbb{1}_{\{c_{di}(t_k) < -\cos\left(\frac{\pi}{8}\right)\}} \geq 0.9, \tag{6.7}$$

where $\mathbb{1}$ is the indicator function that is equal to 1 if the condition inside the brackets is true and 0 otherwise.

To further ensure anticipatory locomotor adjustments during frontal encounters, we calculated extrapolated straight line trajectories (see eq. (6.5)) at the initial instant of the encounter and require the closest approach distance on these paths to be less than 2 m. This is because, even when an encounter begins at a distance of 4 m, the dyad and the single might still have sufficient lateral distance to pass each other comfortably, rendering such encounters irrelevant for the scope of this work.

Finally, we ensure that the behaviours of both the dyad and the single are captured even after they have laterally passed each other. This conditioning is motivated by the findings reported by Corbetta et al. [119], who showed that in very close encounters, lateral distance continues to increase even after avoidance is achieved. To ensure effective clearance between individuals, both the single pedestrian and the dyad must completely move past each other, with sufficiently long trajectories both before and after passing. Specifically, we require them to maintain a distance of at least 3 m apart at the beginning and end of the encounter, indicating an initial approach followed by a subsequent distancing. After applying the conditions described above, the number of encounters subject to an analysis in the upcoming sections, is illustrated in table 6.1.

6.3.5 Measures of deviation

In this section, we define a set of measures for quantifying the deviation of an actual trajectory from an intended straight line trajectory (or, equivalently, its dissimilarity to such a path) along with a discussion on their specifications. For an extensive collection of measures and examples demonstrating how deviation values vary across different types of trajectories, readers can refer to the extended version of this article [203].

When computing the deviation of a dyad, we consider the deviation of each member separately. This ensures that the deviation of the dyad is not artificially reduced by averaging the positions of the two members.

Lockstep maximum deviation

In human–human collision avoidance literature, avoidance behaviour is often assessed by measuring deviation from a straight line. In studies with controlled experimental settings, such as frontal encounters in a corridor [177, 113, 204], this straight line is considered directly as the axis of the environment and deviation is measured along the orthogonal direction (typically denoted as y-axis). In our case, rather than using the axis of the corridor, we derive an *intended direction of motion* for each single and dyad (see eqs. (6.4) and (6.5)).

The lockstep maximum deviation δ_{max} is defined as the maximum distance between the simultaneous pairs of points of the observed trajectory T and the straight line trajectory T_0. Formally,

$$\delta_{max} = \max_{k \in [0, N-1]} ||\mathbf{p}(t_k) - \tilde{\mathbf{p}}(t_k)||. \tag{6.8}$$

Notably, this measure is sometimes called the lockstep Euclidean distance in the literature [205]. In fig. 6.2, we show an example for computing the lockstep maximum deviation.

Maximum cumulative turning angle θ_{max}

In addition to the position-based measure δ_{max}, we introduce a measure that quantifies the trajectory deviation of a pedestrian from a straight line trajectory based on the orientation of the velocity vectors, i.e. the direction of motion.

To deviate from their intended trajectory, pedestrians must naturally turn. We can quantify this deviation by examining the amount of turning performed. The cumulative turning

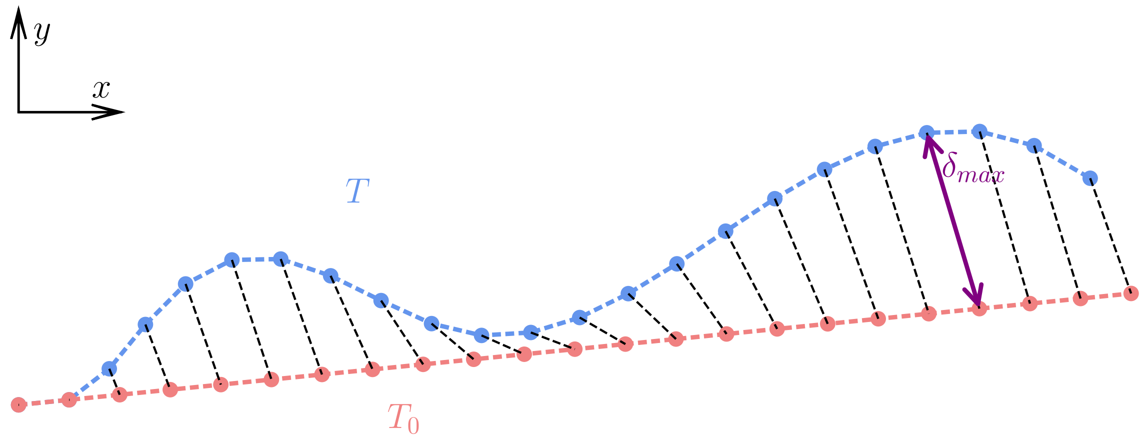

Figure 6.2: Illustration of the lockstep maximum deviation, defined as the maximum distance between the simultaneous pairs of points of the observed trajectory T and the straight line trajectory T_0.

angle until time t_k is defined as the sum of the turning angles between consecutive velocity vectors until time t_k[9].

Formally, it is defined as

$$\theta_k = \sum_{j=0}^{k-1} d\theta_j, \tag{6.9}$$

where $d\theta_j$ is the signed angle between the velocity vectors $\mathbf{v}(t_j)$ and $\mathbf{v}(t_{j+1})$, $d\theta_j = \angle(\mathbf{v}(t_j), \mathbf{v}(t_{j+1}))$.

The turning angles are signed, meaning that the cumulative turning angle can be positive or negative, depending on the turning direction (see fig. 6.3). We are interested in the maximum cumulative turning angle θ_{max}, which is the maximum of the absolute value of the cumulative turning angles over the trajectory.

$$\theta_{max} = \max_{k\in[0,N-3]} |\theta_k|. \tag{6.10}$$

In fig. 6.3, we illustrate the computation of the maximum cumulative turning angle. The left panel of the figure shows the turning angles $d\theta_j$ and the trajectory segment where the cumulative turning angle is maximum. The right part displays a graph of the turning angles $d\theta_j$, the cumulative turning angles θ_k, $|\theta_k|$, and the maximum cumulative turning angle θ_{max}.

[9] It is worth noting that this calculation is not the same as simply measuring the angle between $\mathbf{v}(t_0)$ and $\mathbf{v}(t_k)$. In theory, a pedestrian could achieve an angle larger than 2π if they make a full turn. Nonetheless, such situations are unlikely to occur in practice.

Notably, unlike the lockstep maximum deviation, the maximum cumulative turning angle serves as an early indicator of trajectory deviation. Typically, this maximum is reached earlier in the trajectory than δ_{max}. Specifically, as the pedestrian begins to turn back toward their intended motion direction, the cumulative turning angle starts to decrease.

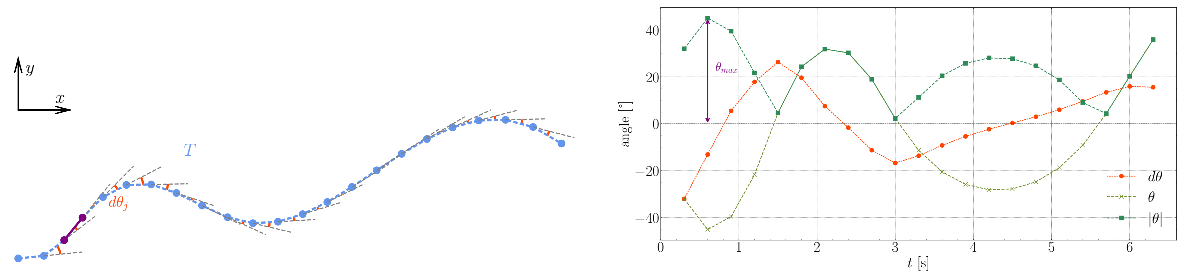

(a) (b)

Figure 6.3: (a) Turning angles $d\theta$ are shown in red. The trajectory segment for which the cumulative turning angle is maximum is drawn in purple. (b) Corresponding values of the turning angles $d\theta$, the cumulative turning angles θ, their absolute values $|\theta|$ and the maximum cumulative turning angle θ_{max}.

Turn intensity I

Some studies have proposed measures that combine position and orientation information to quantify a trajectory's deviation. In this section, we present one such measure, namely the turn intensity.

Turn intensity was introduced in [134]. In the authors' experiment, participants moved and crossed paths along a straight elongated path (x-axis). The authors considered instants at which the motion along the orthogonal axis (y-axis) changes direction, referred to as "turning" instants. A "step" is defined as the motion between two consecutive turning instants, with the "step length" being the y component of a step and the "step angle" the absolute angle deviation from the horizontal axis. Turn intensity is then defined as the product of the step length and the step angle.

In our study, since pedestrians might not be moving along the environment axis (i.e. x axis), we adapt the definitions of turning instants and steps to account for deviation from the intended direction of motion. In particular, we consider the signed angle ψ_k between the initial velocity vector $\mathbf{v_0}$ and the velocity vector $\mathbf{v}(t_k)$ at each time step t_k, $\psi_k = \angle(\mathbf{v_0}, \mathbf{v}(t_k))$. Turning instants t_s are then defined as the moments at which ψ_k changes sign.

We define the s-th step angle ω_s as the absolute value of the angle deviation of a step from the intended motion direction and the step length λ_s as the orthogonal distance between the pedestrian's position at the end of the step and the intended motion direction.

$$\omega_s = \left|\angle(\mathbf{v_0}, (\mathbf{p_{s+1}} - \mathbf{p_s}))\right|, \tag{6.11}$$

$$\lambda_s = \frac{||(\mathbf{p_{s+1}} - \mathbf{p_s}) \times \mathbf{v_0}||}{||\mathbf{v_0}||}. \tag{6.12}$$

The turn intensity is then defined as the average value of the product of the step lengths and step angles,

$$I = \frac{\sum_{s=0}^{N_S-1} \omega_s \lambda_s}{N_S}, \tag{6.13}$$

where N_S is the number of steps.

In fig. 6.4, we illustrate the variables used in computing the turn intensity I.

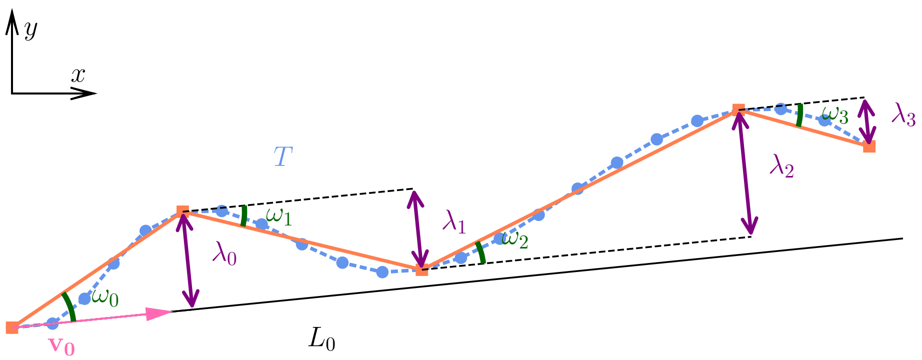

Figure 6.4: Illustration of the variables used in computing the turn intensity I. The steps are shown in orange, the step angles ω are depicted in green, and the step lengths λ are illustrated in purple.

6.3.6 Impact parameter

In this section, we briefly introduce the concept of the impact parameter, which has been used in previous analyses of human–human collision avoidance behaviour [3].

In physics, the impact parameter refers to the distance between the path of an incoming particle and a target particle. Applying this concept to pedestrian trajectories, we treat the deviation of a single from a dyad as a scattering event. To do so, we transform the trajectories of both the dyad d and the single i into a reference frame moving with the dyad. Specifically, at each time instant, the positions of the dyad and the single are translated so that the dyad's center of mass is positioned at the origin, and their velocities are rotated to align the dyad's movement with the positive x-axis. We denote the position of a single in the reference frame as $\hat{\mathbf{p}}_i$ and its velocity as $\hat{\mathbf{v}}_i$.

In this reference frame, the impact parameter r_b is computed as the distance from the dyad (positioned at the origin) to the line guided by the single's velocity vectors at the beginning of the encounter (as in section 6.3.3, we average the velocity vectors over N_e time instants to alleviate the impact of orientation noise). The impact parameter can be considered to indicate how close the single and the dyad would have approached each other without collision avoidance. We illustrate the computation of the impact parameter in fig. 6.5.

Let $\hat{\mathbf{v}}_{i_0}$ be the average velocity vector of the single over the first N_e time instants of the encounter,

$$\hat{\mathbf{v}}_{i_0} = \frac{1}{N_e} \sum_{k=0}^{N_e-1} \hat{\mathbf{v}}_i(t_k). \tag{6.14}$$

We can compute r_b as

$$r_b = \frac{||\hat{\mathbf{v}}_{i_0} \times \hat{\mathbf{p}}_i(t_0)||}{||\hat{\mathbf{v}}_{i_0}||}. \tag{6.15}$$

As detailed in [3], we scale the impact parameter by the dyad's width (i.e. the average distance between dyad members with that interaction level) to obtain a dimensionless measure $\bar{r}_b$ that better captures the relative distance between the single and the dyad members. In particular, an $\bar{r}_b$ value smaller than 0.5 indicates that the single would have passed through the dyad.

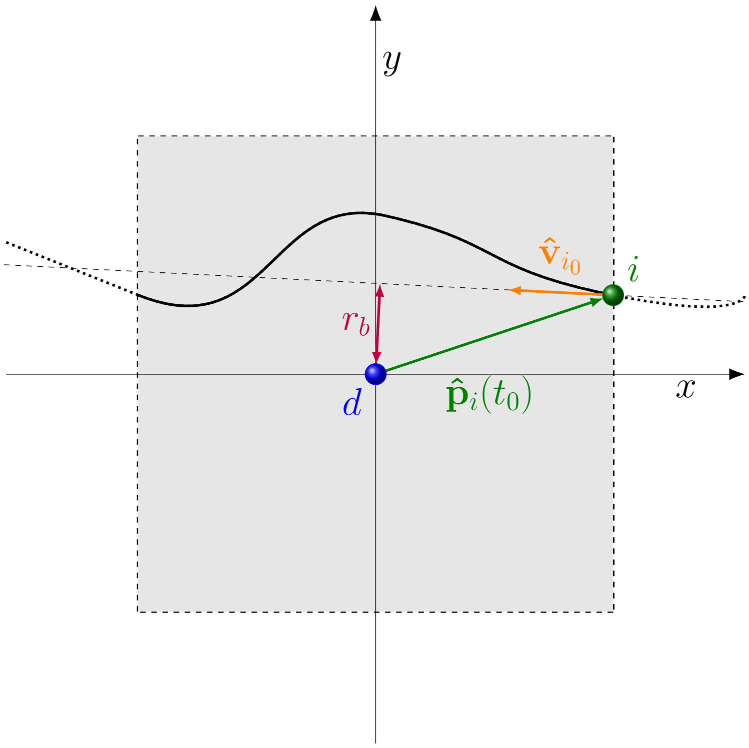

Figure 6.5: Single i in green approaches the dyad d in blue (static and centered at the origin) in a reference frame that moves with the dyad. The gray area represents the 4 m window around the dyad. The (transformed) trajectory of the single inside the box is represented in thick black. The impact parameter r_b indicates the distance between the dyad and the line guided by the single's velocity vectors at the beginning of the encounter.

6.4 Results

6.4.1 Undisturbed situations

While pedestrians typically aim to minimise travel distance by choosing the straightest path possible, expecting them to walk in a perfectly straight line is unrealistic, even in the absence of other pedestrians. Therefore, we begin by examining the deviation of singles and dyads in 4 m long undisturbed segments, arguing that these segments provide a baseline for expected deviation in the absence of encounters.

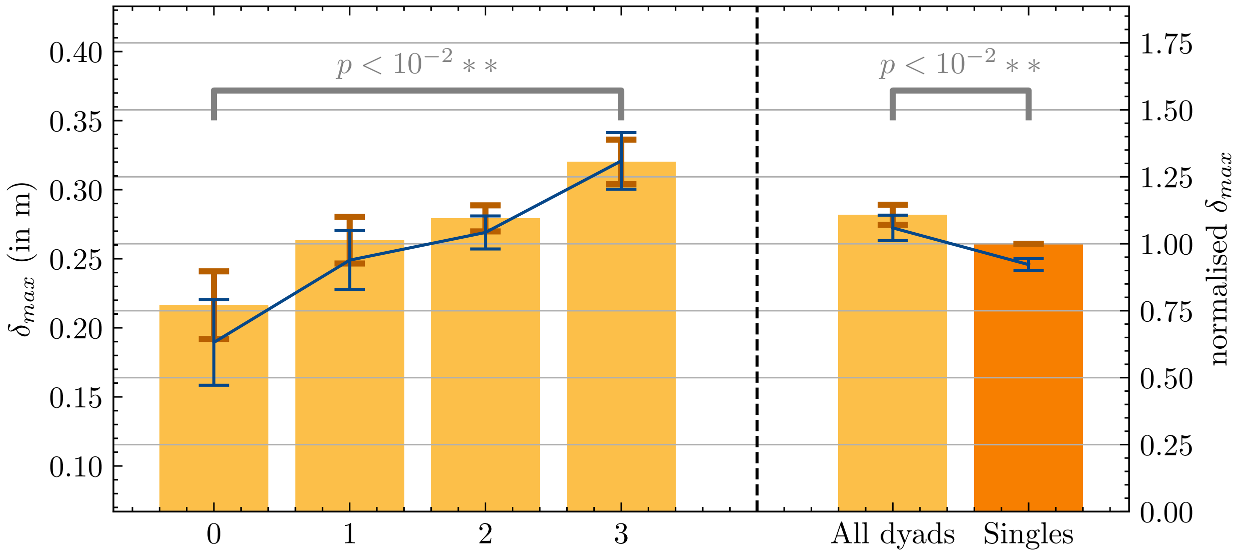

Figure 6.6: Lockstep maximum deviation δ_{max} in undisturbed situations. The bar plot shows the ratio of the measure to the deviation value for the singles (right axis). The error bars represent the standard error of the mean. The Kruskal–Wallis p-value for the difference in means between the levels of interaction for the dyads and the Welch T-test p-value for the difference in means between the dyads and the singles are also shown.

In figs. 6.6 to 6.8, we display the deviation amounts in terms of various deviation measures (see section 6.3.5). Additionally, we present the normalised values, obtained by dividing the average deviation of each dyad category (or singles) by the average deviation of singles. This normalisation facilitates a straightforward comparison between dyads and singles. Furthermore, we include the Kruskal–Wallis H test p-value for assessing the difference in means among dyads with varying interaction levels, as well as the Welch T-test p-value for comparing the means between singles and all dyads [206, 207]. The significance level is set to

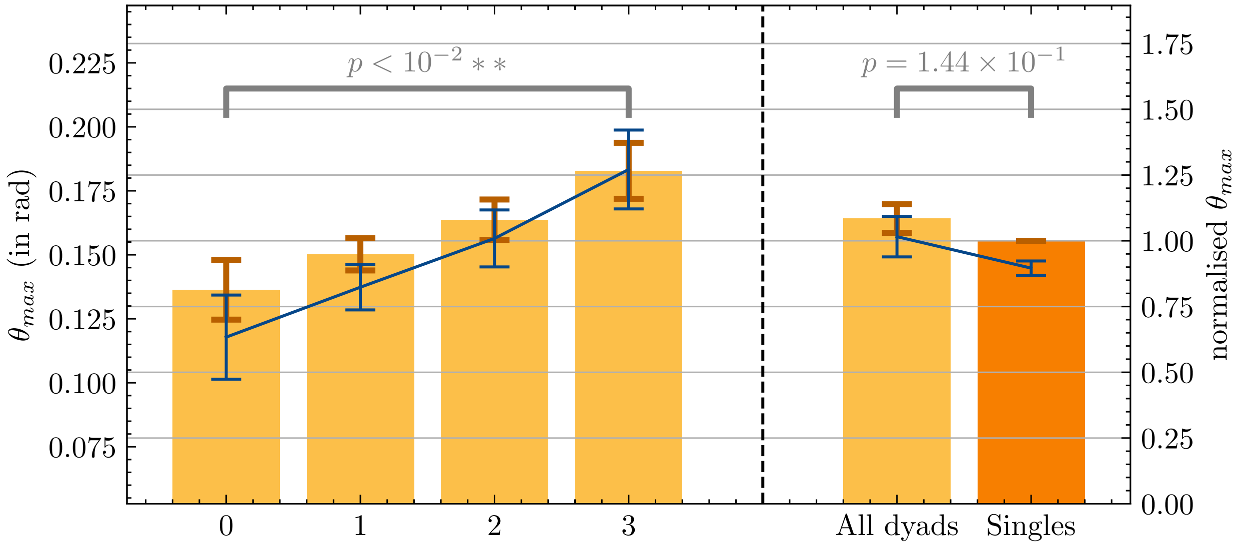

Figure 6.7: The line plot shows the raw values of θ_{max} (left axis). The bar plot shows the ratio of the measure to the deviation value for the singles (right axis). The error bars represent the standard error of the mean. The Kruskal–Wallis p-value for the difference in means between the levels of interaction for the dyads and the Welch T-test p-value for the difference in means between the dyads and the singles are also shown.

0.05 for all tests, and p-values below this threshold are reported in bold in the tables. In the figures, the significance level is indicated by the following symbols: $*$ for $p < 0.05$, $**$ for $p < 0.01$, $***$ for $p < 0.001$ and $****$ for $p < 0.0001$.

The initial noteworthy observation from figs. 6.6 to 6.8 is that deviation is systematically higher for dyads compared to singles, and significantly so for the lockstep maximum deviation δ_{max} (with $H(3) = 16.24$, $p < 10^{-2}$). However, to accurately interpret this observation, it is essential to compare deviations among dyads with varying interaction levels. Examining the breakdown of normalised deviations according to the interaction level of the dyad, we observe a trend where the interaction level correlates with an increase in deviation. Interestingly, non-interacting dyads tend to have smaller deviations than singles, while interacting dyads exhibit comparable or higher deviations.

6.4.2 Deviations during encounters

We now focus on encounter situations, where dyads and singles pass each other frontally at a distance less than 4 m [148, 104, 105]. The line plots of figs. 6.9 to 6.11 show the deviation

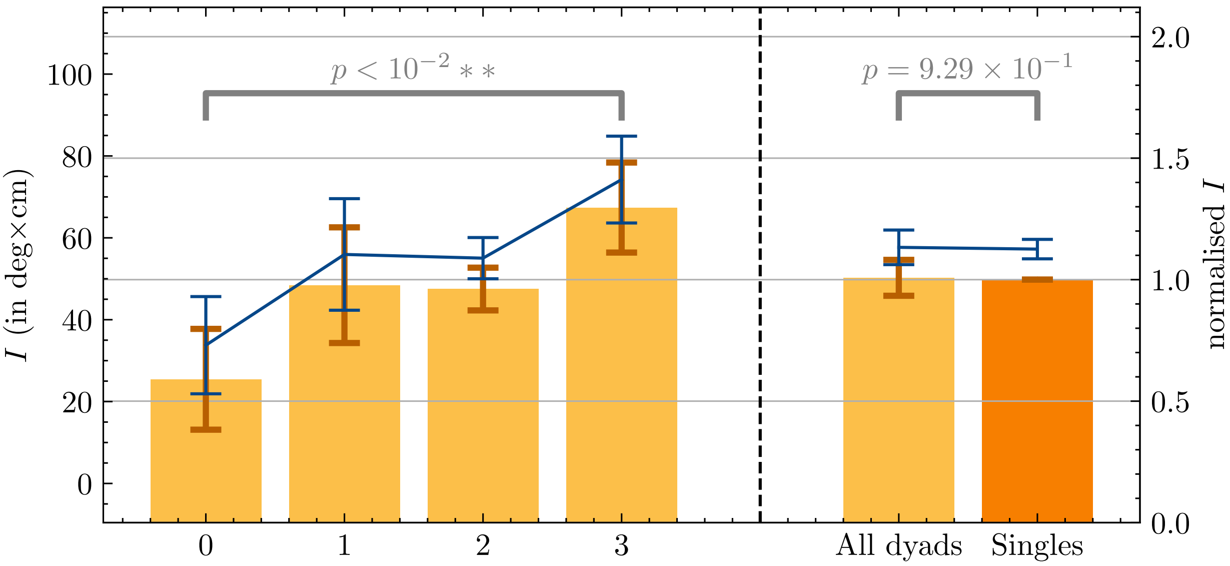

Figure 6.8: Turn intensity I in undisturbed situations. The line plot shows the raw values of I (left axis). The bar plot shows the ratio of the measure to the deviation value for the singles (right axis). The error bars represent the standard error of the mean. The Kruskal–Wallis p-value for the difference in means between the levels of interaction for the dyads and the Welch T-test p-value for the difference in means between the dyads and the singles are also shown.

amounts for both singles and dyads. It is crucial to emphasise that, when reporting deviations in these encounter scenarios, we categorise not only the values of dyads but also those of singles, with respect to the level of social interaction of the dyad involved in that encounter.

We notice that singles tend to deviate more when encountering dyads with medium or high interaction levels (i.e. levels 2, 3) compared to when they encounter non- or weakly interacting dyads (i.e. levels 0, 1). However, this tendency lacks statistical significance ($H(3) = 0.33$, $p = 0.93$ for δ_{max}, $H(3) = 0.94$, $p = 0.41$ for θ_{max} and $H(3) = 0.99$, $p = 0.11$ for I). Conversely, the variation in dyad deviation is statistically significant ($H(3) = 8.99$, $p = 2.94 \times 10^{-2}$ for δ_{max}, $H(3) = 11.14$, $p = 1.10 \times 10^{-2}$ for θ_{max} and $H(3) = 10.20$, $p = 1.60 \times 10^{-2}$ for I), but no clear pattern emerges, as dyads at interaction levels 0 and 3 deviate more than at levels 1 and 2. Finally, at all interaction levels, the deviations are notably asymmetric, with singles deviating more than dyads in a statistically significant manner.

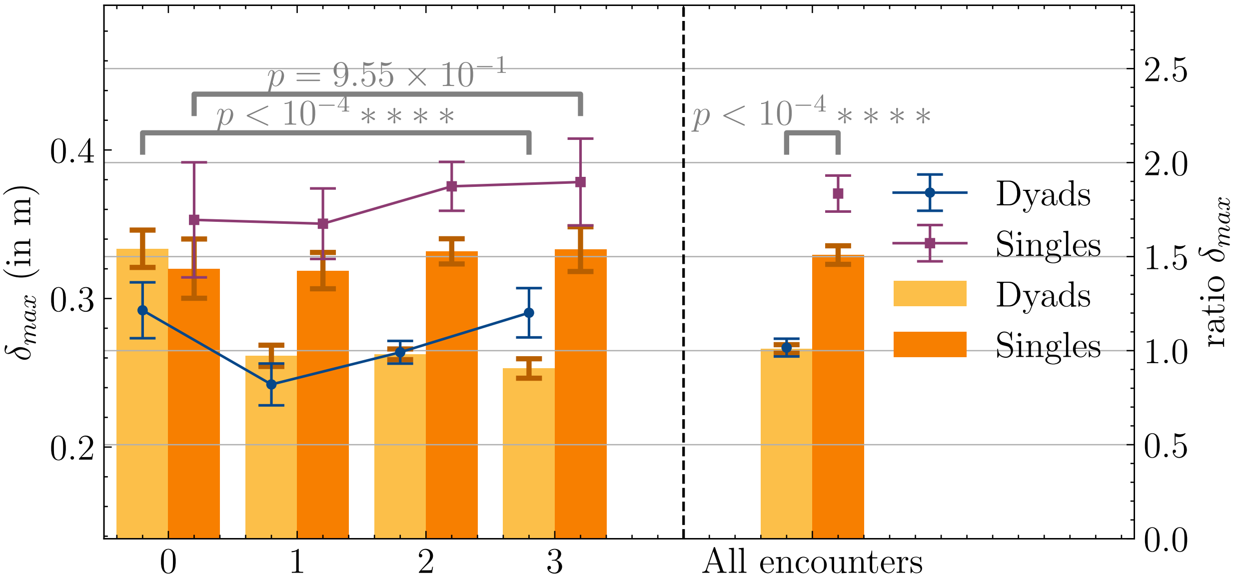

Figure 6.9: Lockstep maximum deviation δ_{max} during encounters. The line plot shows the raw values of the measure for dyads and singles (left axis). The bar plot shows the ratio of the measure in encounters to the undisturbed value for dyads and singles (right axis). The error bars represent the standard error of the mean. The Kruskal–Wallis p-values for the difference in means between the ratios of dyads (resp. singles) with respect to varying intensities of interaction and the Welch T-test p-value for the difference in means between the ratios of all dyads and singles are also shown.

6.4.3 Comparison of deviations during encounters and undisturbed situations

The conclusions drawn from the raw values become clearer when juxtaposed with undisturbed situations. To facilitate this comparison, figs. 6.9 to 6.11 also provide the ratio of average deviations during encounters to those observed in undisturbed scenarios, depicted as bar plots.

For singles, deviation increases when encountering dyads compared to undisturbed scenarios, with ratios consistently greater than 1. A similar increase is noted for dyads with 0 interaction level, whereas higher interaction levels show ratios close to 1, suggesting minimal change. For dyads, we observe a decrease in the ratios with increasing interaction levels, with statistically significant differences between these interaction levels (Kruskal–Wallis p-values of $H(3) = 42.92$, $p < 10^{-4}$ for δ_{max}, $H(3) = 49.83$, $p < 10^{-4}$ for θ_{max} and $H(3) = 32.84$,

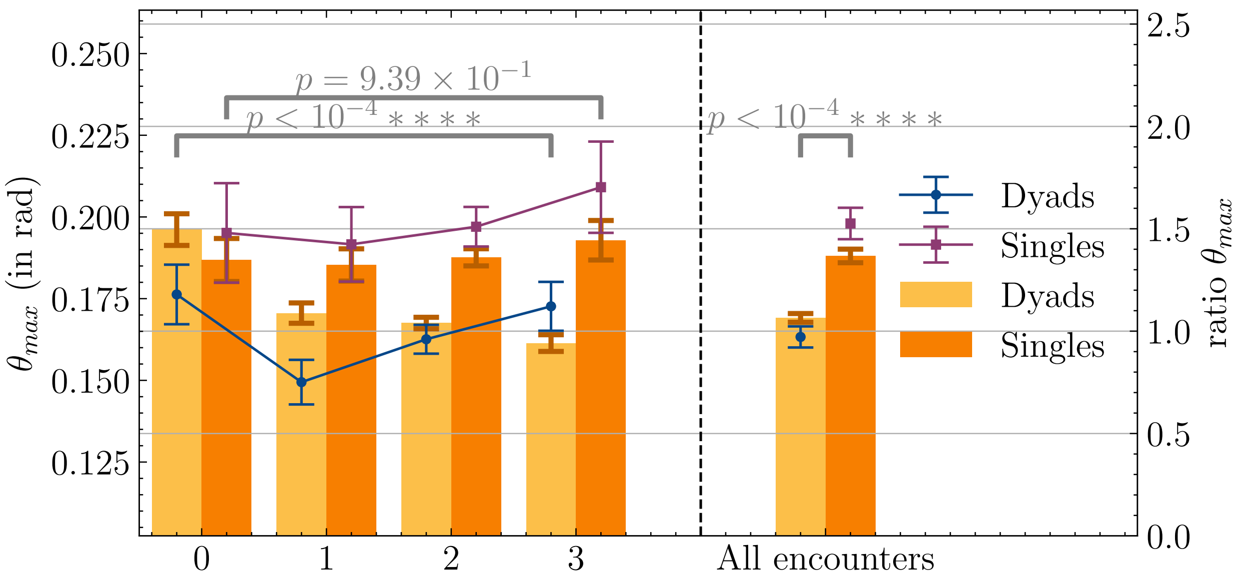

Figure 6.10: Maximum cumulative turning angle θ_{max} during encounters. The line plot shows the raw values of the measure for dyads and singles (left axis). The bar plot shows the ratio of the measure in encounters to the undisturbed value for dyads and singles (right axis). The error bars represent the standard error of the mean. The Kruskal–Wallis p-values for the difference in means between the ratios of dyads (resp. singles) with respect to varying intensities of interaction and the Welch T-test p-value for the difference in means between the ratios of all dyads and singles are also shown.

$p < 10^{-4}$ for I). Additionally, a statistically significant difference was evident between the deviation ratios of singles and dyads after averaging across all interaction levels for all measures (Welch T-test p-values of $t(875.45) = 9.18$, $p < 10^{-4}$ for δ_{max}, $t(1111.56) = 7.67$, $p < 10^{-4}$ for θ_{max} and $t(806.62) = 6.06$, $p < 10^{-4}$ for I).

These findings are further clarified by tables 6.2 to 6.4, which provide Welch T-test p-values for the difference between undisturbed situations and encounters for both singles and dyads across all interaction levels. Upon averaging over different interaction levels, both singles and dyads exhibited a statistically significant difference between undisturbed and encounter scenarios. However, while the discrepancy remained true for singles regardless of the interaction level of the encountered dyad, only dyads with an interaction level of 0 exhibit a distinct behaviour in encounters compared to undisturbed situations across all three deviation measures.

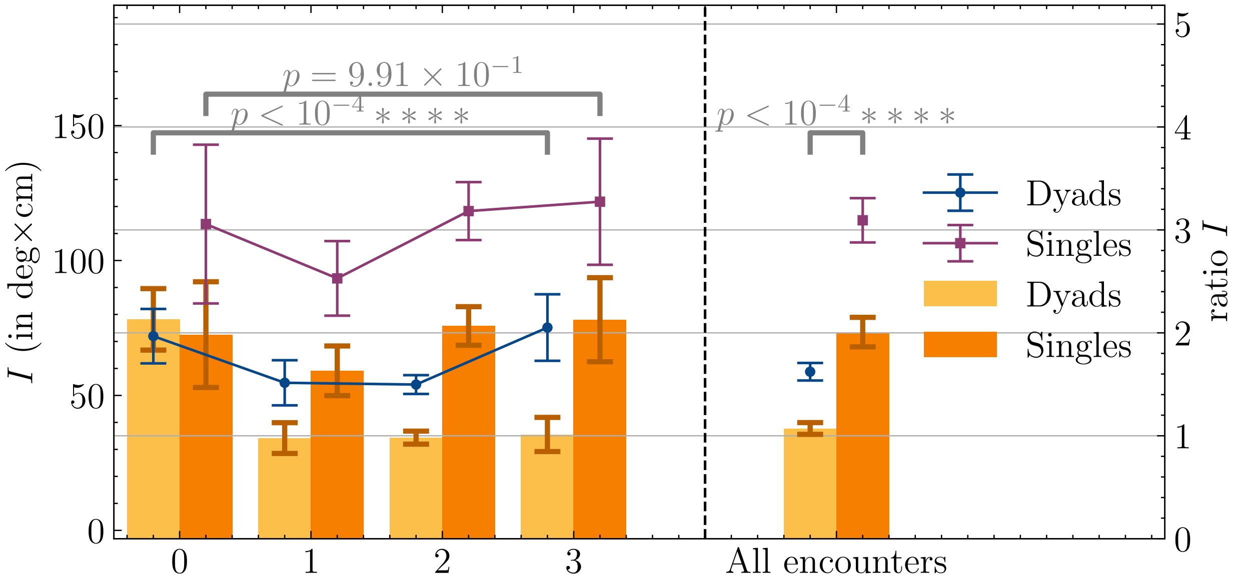

Figure 6.11: Turn intensity I during encounters. The line plot shows the raw values of the measure for dyads and singles (left axis). The bar plot shows the ratio of the measure in encounters to the undisturbed value for dyads and singles (right axis). The error bars represent the standard error of the mean. The Kruskal–Wallis p-values for the difference in means between the ratios of dyads (resp. singles) with respect to varying intensities of interaction and the Welch T-test p-value for the difference in means between the ratios of all dyads and singles are also shown.

Table 6.2: Comparison of lockstep maximum deviation between undisturbed situations and encounters. Welch T-test p-values for the difference in means of the lockstep maximum deviation δ_{max} between singles (resp. dyads) in undisturbed situations and singles (resp. dyads) during encounters. Values in bold indicate statistical significance ($p < 0.05$).

Intensity of interaction	Singles	Dyads
0	$\mathbf{9.23 \times 10^{-3}}$	$\mathbf{9.54 \times 10^{-3}}$
1	$< \mathbf{10^{-4}}$	7.91×10^{-1}
2	$< \mathbf{10^{-4}}$	7.14×10^{-1}
3	$< \mathbf{10^{-4}}$	2.52×10^{-1}
All	$< \mathbf{10^{-4}}$	$\mathbf{6.69 \times 10^{-4}}$

Table 6.3: Comparison of maximum cumulative turning angle between undisturbed situations and encounters. Welch T-test p-values for the difference in means of the lockstep maximum deviation θ_{max} between singles (resp. dyads) in undisturbed situations and singles (resp. dyads) during encounters. Values in bold indicate statistical significance ($p < 0.05$).

Intensity of interaction	Singles	Dyads
0	$\mathbf{2.35 \times 10^{-3}}$	$\mathbf{5.12 \times 10^{-3}}$
1	$\mathbf{1.38 \times 10^{-4}}$	2.84×10^{-1}
2	$< \mathbf{10^{-4}}$	6.07×10^{-1}
3	$< \mathbf{10^{-4}}$	5.36×10^{-1}
All	$< \mathbf{10^{-4}}$	$\mathbf{3.27 \times 10^{-4}}$

Table 6.4:
Welch T-test p-values for the difference in means of the turn intensity I between undisturbed singles (resp. dyads) and singles (resp. dyads) during encounters. Values in bold indicate statistical significance ($p < 0.05$).

Intensity of interaction	Singles	Dyads
0	6.59×10^{-2}	$\mathbf{2.04 \times 10^{-2}}$
1	$\mathbf{1.20 \times 10^{-2}}$	9.38×10^{-1}
2	$< \mathbf{10^{-4}}$	8.70×10^{-1}
3	$\mathbf{7.48 \times 10^{-3}}$	9.55×10^{-1}
All	$< \mathbf{10^{-4}}$	$< \mathbf{10^{-4}}$

6.4.4 Examination in light of the impact parameter

As discussed in section 6.3.6, the impact parameter r_b is used to assess how close a single would pass a dyad without any collision avoidance behaviour involved. In particular, $\bar{r}_b$ serves as a dimensionless measure for the initial risk of collision, representing the distance between the single and the dyad relative to the dyad's width (i.e. the average distance between dyad members with that interaction level). We classified $\bar{r}_b$ into four equally sized bins: a value of $\bar{r}_b$ smaller than 1 indicates that the single is on track to pass through or collide with the dyad. Values between 1 and 2 indicate proximity to the dyad but no imminent collision.

Between 2 and 3, the single is further away from the dyad, likely requiring minimal deviation to pass comfortably. Finally, a value of $\bar{r}_b$ greater than 3 indicates that the single is far from the dyad and does not need to deviate.

In figs. 6.12 to 6.14, we illustrate the ratio of the average deviation during encounters to the average deviation in undisturbed situations for singles and dyads with respect to the normalised impact parameter $\bar{r}_b$ for each measure. We also provide the Welch T-test p-values for the difference in the ratio between dyads with low interaction levels (0 and 1) versus those with high interaction levels (2 and 3) for each bin of $\bar{r}_b$.

We classified encounters into two groups based on dyads' interaction levels: one with levels 0 and 1, and another for levels 2 and 3. This approach balances the number of data points, ensuring comparable sample sizes. We deem that this categorization is reasonable as it allows us to contrast low and high interaction levels.

For all deviation measure, both for singles and for dyads, we notice that in the fourth bins of $\bar{r}_b$, the ratios are very close to 1, regardless of the interaction level, indicating no effect of the encounter. At lower values of $\bar{r}_b$, singles and, to a lesser extent, dyads with 0–1 interaction levels show ratios greater than 1. Conversely, ratios for dyads with 2–3 interaction levels remain close to 1, confirming that they are largely unaffected by encounters regardless of collision risk.

Delving deeper into the interaction level effect, we observe that for singles the ratios are higher when encountering dyads with interaction levels 2–3 compared with with 0–1 levels. This difference is particularly pronounced in the first bin, likely reflecting the "intrusion" phenomenon reported previously in [3], where singles may choose to pass through non- or weakly interacting dyads instead of deviating. By contrast, the difference in the third bin could be attributed to the fact that for such a value of $\bar{r}_b$ there is no need of avoidance if, as with 0–1 interaction levels, the dyad moves straight (resulting in a ratio around 1). However, when encountering dyads with interaction levels 2–3, singles may need to deviate more, even for such values of $\bar{r}_b$, due to the more unpredictable, "wandering" behaviour of the interacting dyads.

For the dyads, in accordance with the previous results, we observe that the ratio of the lower interaction levels (0–1) is systematically higher for higher interaction levels (2–3) across all measures and all values of $\bar{r}_b$. Finally, the difference in the ratio between the two dyad categories is statistically significant in the second bin of $\bar{r}_b$ (i.e. where the single is close to the dyad but not on a collision course) for all three measures. The more pronounced

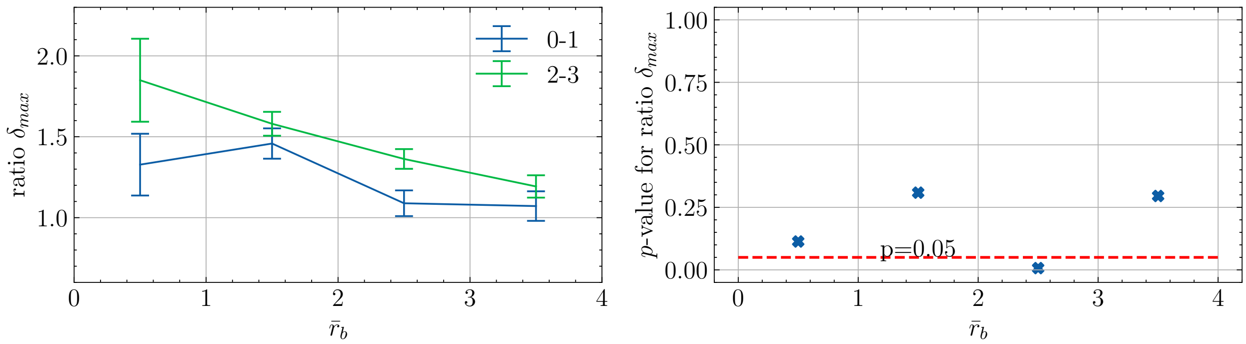

(a) Singles

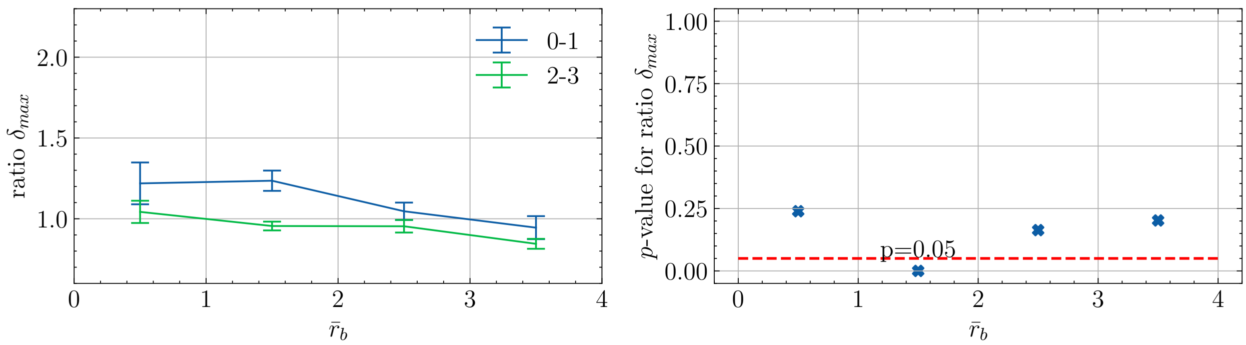

(b) Dyads

Figure 6.12: Lockstep maximum deviation and impact parameter. Ratio of the value of the lockstep maximum deviation of (a) singles and (b) dyads in encounters to the undisturbed value for the binned normalised impact parameter $\bar{r}_b$. The ratios are shown separately for encounters involving dyads with a low (0–1, in blue) and high (2–3, in green) interaction level. The error bars represent the standard error of the mean. The p-values for the difference in means between 0–1 and 2–3 are also shown. The red dashed line represents the significant threshold of $p = 0.05$.

difference observed in the second bin, compared to the first, may again be attributed to the intrusion phenomenon, which could attenuate the amount of avoidance performed by dyads in the first bin of $\bar{r}_b$, but not in the second.

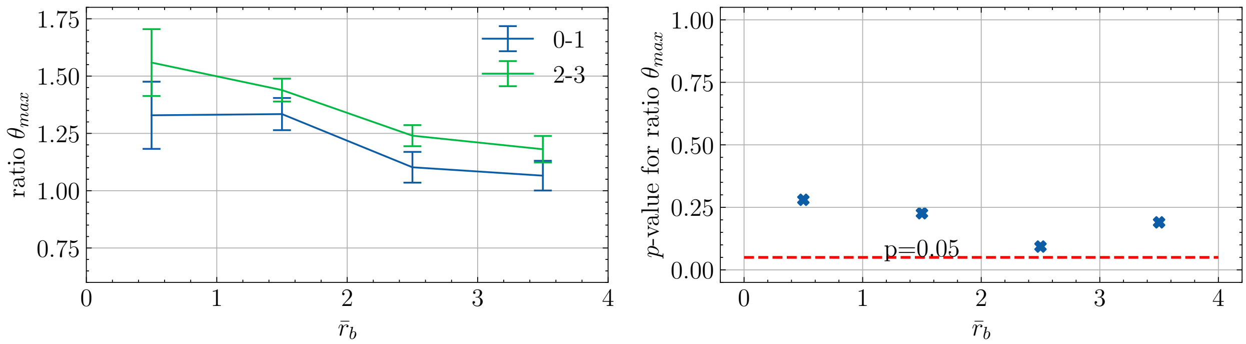

(a) Singles

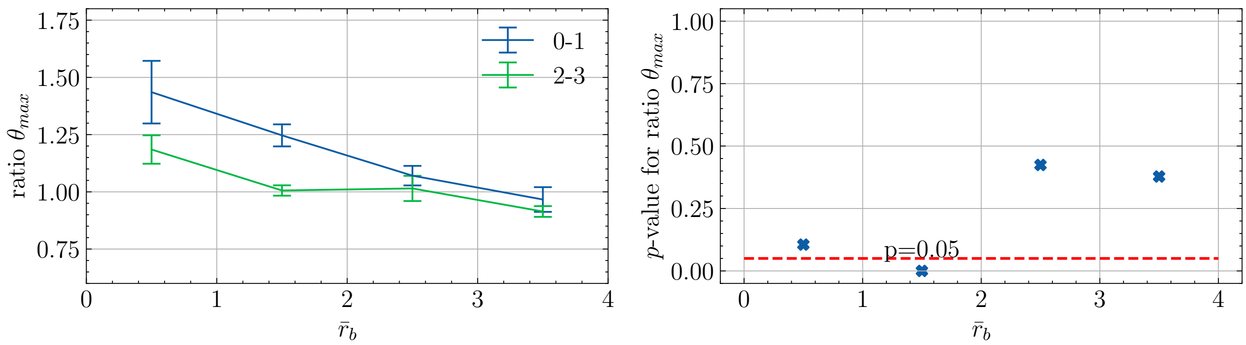

(b) Dyads

Figure 6.13: Maximum cumulative turning angle and impact parameter. Ratio of the value of the maximum cumulative turning angle of (a) singles and (b) dyads in encounters to the undisturbed value for the binned normalised impact parameter $\bar{r}_b$. The ratios are shown separately for encounters involving dyads with a low (0–1, in blue) and high (2–3, in green) interaction level. The error bars represent the standard error of the mean. The p-values for the difference in means between 0–1 and 2–3 are also shown. The red dashed line represents the significant threshold of $p = 0.05$.

6.5 Discussion

In undisturbed situations, non- and weakly interacting deviate significantly less than singles (see figs. 6.6 to 6.8). This indicates that dyads maintain a straighter trajectory compared to singles, potentially owing to their tendency to remain physically close, thereby constraining deviations from the intended path. Using a physical analogy, the inertia of systems composed of the two members is likely greater than that of singles, which would make the dyads more stable.

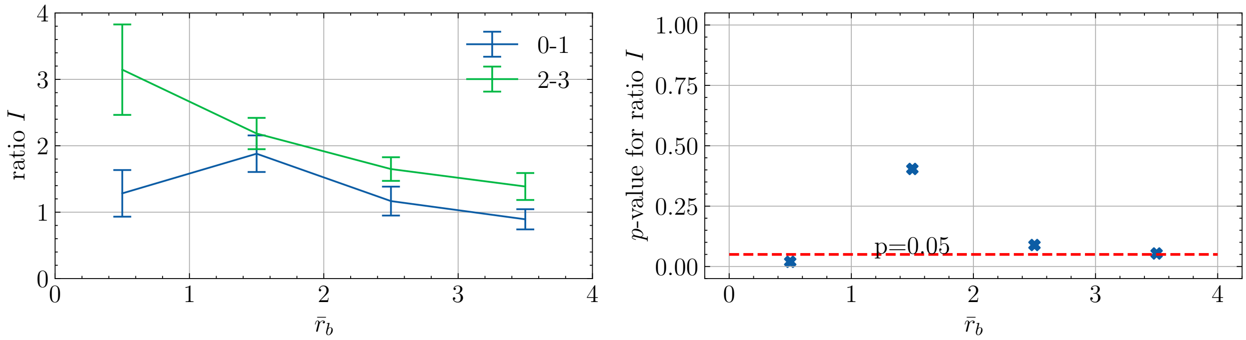

(a) Singles

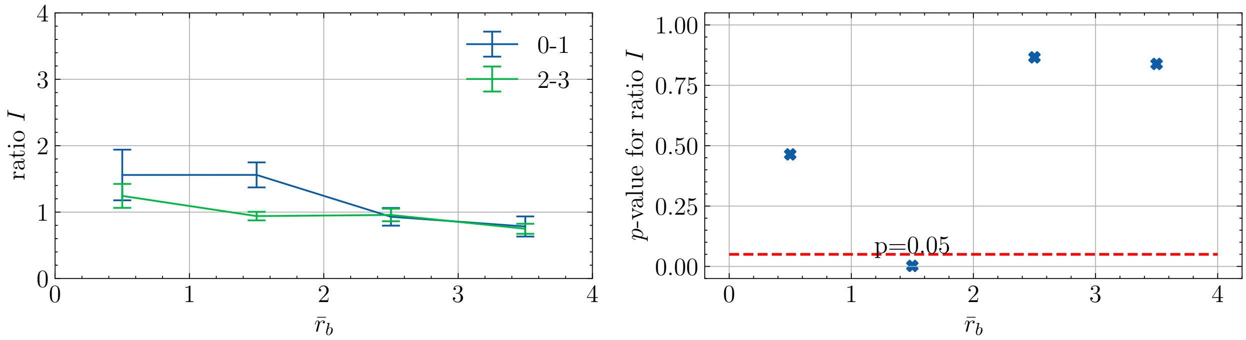

(b) Dyads

Figure 6.14: Turn intensity and impact parameter. Ratio of the value of the turn intensity of (a) singles and (b) dyads in encounters to the undisturbed value for the binned normalised impact parameter $\bar{r}_b$. The ratios are shown separately for encounters involving dyads with a low (0–1, in blue) and high (2–3, in green) interaction level. The error bars represent the standard error of the mean. The p-values for the difference in means between 0–1 and 2–3 are also shown. The red dashed line represents the significant threshold of $p = 0.05$.

In addition, awareness of the environmental changes is thought to be linked to dyad's interaction level. It seems reasonable to assume that non- or weakly interacting dyads in undisturbed situations are more attentive to their surroundings, since they do not need to allocate much attention towards social interactions. Consequently, in undisturbed scenarios, these dyads were more likely to choose efficient, straight paths compared to interacting dyads (see figs. 6.6 to 6.8), which may deviate owing to social engagement (interactions).

During encounters, the fact that all dyads deviate significantly less than the singles suggests an asymmetry in avoidance behaviour, with dyads contributing less (see figs. 6.9

to 6.11). In addition, the deviation ratio of non-interacting dyads was significantly higher than that of interacting dyads, suggesting that interaction levels affect dyads' environmental awareness. This is further supported by the fact that the deviation of the singles increases with the dyad's interaction level (see figs. 6.9 to 6.11), although this increase is not statistically significant. This suggests that singles anticipate the reduced involvement of dyads in human–human collision avoidance and adjust their deviations accordingly.

Furthermore, the impact parameter analysis provides further insights into the dynamics of the encounters. The patterns observed in the ratios of deviation during encounters compared to undisturbed situations for singles and dyads with respect to the impact parameter (see figs. 6.12 to 6.14) suggest that the initial collision risk influences the deviation of both singles and dyads. A low impact parameter implies a collision course between the dyad and the single, while higher values suggest safer passing paths. Singles displayed straighter trajectories when on a collision course with non- or weakly interacting dyads, likely owing to a higher rate of intrusion, as observed previously [3]. For dyads, the difference between high and low interaction levels is most pronounced when the single and dyad are set to pass close to each other (second bin), with low interaction level dyads showing significantly higher deviations than their high interaction level counterparts. We hypothesise that this reflects the heightened environmental awareness of low interaction level dyads, making them more responsive to the presence of individuals.

6.6 Conclusion

Over the last few decades, numerous human–human collision avoidance models have emerged, offering insights into various aspects of pedestrian behaviour [208, 74]. Despite this extensive body of work, most microscopic models predominantly focus on one-on-one collision avoidance scenarios, often neglecting the dynamics involving groups [209]. This oversight is notable considering that groups comprise a substantial portion of crowds in real-world settings [138, 64]. Therefore, investigating how groups and singles interact during collision avoidance is important for a more comprehensive understanding of pedestrian behaviour. Our study addresses this gap by investigating how groups and singles navigate and avoid collisions in crowded environments, offering new insights into this less explored aspect of pedestrian behaviour. In particular, by analysing ecological data and considering various deviation measures, this chapter presents findings on the stability and deviation dynamics of dyads and singles.

First, our analysis of the behaviour of singles and dyads in undisturbed scenarios reveals that the intensity of social interaction within dyads significantly impacts their deviation from the intended path. Non-interacting dyads tend to display smaller deviations compared to single pedestrians, whereas interacting dyads exhibit similar or even larger deviations. This suggests that higher social interaction levels may reduce a dyad's attentiveness to their surroundings, thereby affecting their ability to maintain a straight trajectory.

During encounters, our findings show that single pedestrians are the primary contributors to collision avoidance. They appear to adapt their path deviations based on the social interaction level within the encountered dyad. For instance, when facing highly interacting dyads, single pedestrians often make larger deviations, potentially to avoid interfering with the ongoing interaction between the two group members. This suggests that they are sensitive to the social dynamics of others and modify their behaviour accordingly. Most of the additional measures employed in our analysis [203] support this trend although none reached statistical significance.

Moreover, dyads engaged in social interaction demonstrate reduced responsiveness in collision avoidance situations. Our study indicates that they are less likely to adjust their paths in response to an approaching individual. This reduced responsiveness may result from a focus shift toward their social interaction, making them less aware of potential collisions and more reliant on the single pedestrian to take evasive actions.

Finally, we observed significant behavioural differences in path deviations based on the perceived collision risk. Pedestrians, whether walking alone or in groups, exhibit more pronounced deviations when the collision risk is high. By comparing the deviations of non- or weakly interacting dyads with those of highly interacting dyads, we observe that the level of social interaction within a group plays an important role in shaping their deviation behaviour. This effect is particularly evident when singles are on a path that brings them close to the dyads, although not directly on a collision course. In such situations, interacting dyads exhibit less deviation, suggesting that they are less responsive to the presence of nearby singles. Conversely, singles tend to deviate more when encountering highly interacting dyads, potentially to avoid disrupting their social interaction and to account for the dyad's reduced responsiveness. This risk-based adjustment is considered an adaptive behaviour, enabling pedestrians to navigate safely in crowded or unpredictable environments.

Nonetheless, our results are not definitive enough to presume a “Theory of Mind” effect (i.e. singles’ awareness of the dyad’s inner state). Singles may simply be dynamically reacting to the dyad’s limited response.

This chapter offers valuable insights into group-single collision avoidance, emphasising human factors that influence pedestrian behaviour. The observed differences in deviation patterns based on social interaction levels potentially relate to attentional demands and decision-making processes in navigation. These findings have practical implications for urban planning, crowd management, and smart systems. They can inform the development of more efficient pedestrian flow strategies and enhance urban space design for greater safety and functionality. Furthermore, the results can support the development of intelligent systems for autonomous vehicles and robots, enabling safer, more seamless interactions with pedestrians in smart environments.

While previous research has suggested that utilising angular variables [134, 194] or velocity adjustments [113, 210] to assess deviations from the intended path could be promising, we faced difficulties in this area. As discussed in section 6.3.1, the trajectory data we utilised may not be suitable for computing acceleration, making certain measures (such as the suddenness of turn, the energy curvature or the sinuosity) less effective in capturing deviations compared to others. While controlled experiments can employ various wearable sensors to accurately register position or acceleration [211, 212] implementing such methods in real-world settings poses challenges. Environmental sensors may be sparse or susceptible to measurement noise and clutter, complicating the derivation of accurate values in natural environments.

Future research should explore how deviation evolves over time, e.g. incorporating factors like the time or distance to the predicted collision point [140, 198]. Another aspect of pedestrian dynamics that is worth investigating is the behaviour of overtaking or following others, whether they are singles or groups. Given the typically faster and more flexible nature of singles compared to groups, it is reasonable to expect they would overtake more frequently than groups. Moreover, singles may tend to overtake groups more frequently than other singles, owing to their greater speed and maneuverability. Interestingly, singles’ decision to overtake groups may not necessarily depend on the social relationships or interactions within the group, as singles approaching from behind often have limited visibility of the group’s social features or intentions.

Furthermore, it would be interesting to investigate how the findings of this chapter might scale to triads or even larger groups. Interaction dynamics in larger groups is obviously more complex, and defining the interaction level would be particularly challenging. Force-based models suggest that larger groups should exert a stronger collective repulsive force (owing to the additive nature of the individual forces) on a single pedestrian, potentially leading to more pronounced deviations. Moreover, the broader physical span of a larger group may also increase the degree of deviation required for singles to avoid it. However, large groups tend to have a less stable structure than smaller ones, often breaking into smaller subgroups [125]. A single pedestrian approaching a large group might opt to pass between two subgroups without significantly deviating or disrupting their internal interactions. Such analysis might require defining sophisticated nested interaction levels to adequately capture the complexity of group dynamics.

Finally, the geometry considered in this chapter (i.e. a straight corridor) is a simple case that does not capture all the complexities of real-world environments. Extending the study to more complex geometries, such as spaces in which even undisturbed pedestrians may be expected to walk in curved paths, like those studied in [176], would be beneficial. This would require a more sophisticated approach to handle the intended paths of pedestrians, as these are likely to be more complex than the straight lines that we considered in this chapter.

Chapter 7

Conclusion

This thesis has explored the intricate interplay between social factors and pedestrian dynamics, focusing on how two-person groups interact with individual pedestrians in collision scenarios. Across the chapters, the findings provide a detailed picture of how social relationships and interaction intensity shape pedestrian behavior.

In Chapter 2, we addressed the challenge of recognizing gestures in mobile interaction settings where pedestrians' arm movements are influenced by their walking activity. A novel method was proposed to decouple these inherent oscillatory movements from intentional gestures by using a pitch detection technique to model the oscillatory motion as a sinusoidal waveform, with deviations from this model indicating gesture actions. The approach achieved an accuracy of 0.80 and demonstrated significant advantages, including its noninvasive nature and robustness to variations in camera view angle and distance.

In Chapter 3, we examined the effect of the intensity of interaction within dyads on their collision avoidance behavior with non-group pedestrians. The findings revealed that the magnitude of the mutual deviation increased as the dyad's level of interaction intensified, highlighting a clear relationship between social interaction and collision avoidance dynamics. Furthermore, the probability of a non-group pedestrian intruding into a dyad decreased with higher levels of dyadic interaction, suggesting that stronger social engagement creates an implicit barrier discouraging intrusion.

In Chapter 4, the thesis extended the analysis to include an analysis of the influence of the group's social. The study demonstrated that the minimum distance during encounters increases with interaction intensity, reaching higher values for closely bonded groups like couples and friends. Conversely, individuals were found to be more likely to intrude into loosely interacting groups, such as families or colleagues, often passing at distances comparable to the group's internal spacing. A novel potential-based approach, inspired by classical mechanics, highlighted that the intensity of collision avoidance grows more rapidly for strongly bonded groups, reflecting social norms. The results underscored the importance of considering social relationships in pedestrian behavior research and when calibrating collision avoidance models.

In Chapter 5, the thesis presented a preliminary analysis of frontal encounters between dyads and individuals, focusing on quantifying each participant's role in collision avoidance based on their deviation from their intended path. The findings revealed significant differences in the deviation between group members and individuals during these encounters, with the greatest contrast observed when the interaction intensity within the dyad was high. The study also found that higher interaction levels between dyad members led to more substantial deviations in the trajectories of encountered individuals.

In Chapter 6, we confirmed these findings and extended them by using various measures to quantify deviations during encounters and computing baseline deviations in undisturbed situations. The results confirmed that singles are the primary contributors to collision avoidance, adjusting their paths based on the social interaction level of the encountered dyad. Conversely, dyads were less responsive to potential collisions, likely due to their focus on social interaction, making them less attuned to their environment. An impact parameter analysis further elucidated the dynamics of encounters, showing that the initial collision risk influences the deviation of both singles and dyads.

While this thesis advances our understanding of social factors in pedestrian behavior, it also opens new avenues for research. Future studies should broaden the scope by incorporating more diverse populations to assess how factors such as age, culture (i.e. not limited to Japanese pedestrians), or gender influence pedestrian dynamics. Larger group sizes could also be explored to uncover how subgroup interactions and social hierarchies affect movement. Regarding gesture recognition, further research could investigate the integration of machine learning techniques to enhance the accuracy and robustness of gesture detection in mobile settings, exploring the possibility of real-time gesture recognition in dynamic environments. Issues of privacy and data security should also be addressed to ensure the ethical use such technologies based on video data.

Building predictive models that account for social factors and individual differences could further enhance our ability to design pedestrian-friendly spaces. Additionally, these findings have implications for robotics and artificial intelligence, suggesting that socially aware navigation systems could benefit from incorporating insights into human interaction patterns.

By addressing these challenges, future research can build upon the foundation laid by this thesis, deepening our understanding of the dynamic relationship between social factors and pedestrian movement in complex environments.

Acknowledgement

I would like to express my deepest gratitude to my supervisor, Dr. Zeynep Yücel, for her unwavering support, guidance, and encouragement throughout my doctoral studies. Her expertise, patience, and commitment have been invaluable in shaping my research and academic development. I am especially grateful for the opportunity she provided to work in Japan during my master's studies, an experience that greatly influenced my academic path and personal growth. Her continued belief in my potential gave me the chance to return to Japan to pursue my PhD, an opportunity that has been transformative in my life.

I would also like to extend my heartfelt thanks to my co-supervisor, Prof. Akito Monden, for his insightful feedback, encouragement, and continuous support, which have enriched both my work and my learning experience.

I am deeply grateful to the members of my doctoral committee, Prof. Norikazu Takahashi and Assoc. Prof. Koichi Takeuchi, for their valuable feedback and suggestions which have significantly enhanced the quality of this thesis.

I would like to express my sincere thanks to Dr. Francesco Zanlungo for the many insightful discussions and valuable guidance they provided throughout my research. Our conversations not only enhanced my understanding of key concepts but also inspired me to think more critically, significantly enriching the development of my work.

I would like to sincerely thank Prof. Bernard Chenevier for fostering the connection between Grenoble and Okayama and for offering opportunities for students to participate in exchange programs and internships. It was through this initiative that I had the chance to come to Japan for the first time, an experience that sparked my desire to return and ultimately led to my decision to stay here.

I would like to thank all members of the Human Behavior Understanding Lab and the Software Measurement and Analytics Lab for their support, camaraderie, and stimulating discussions. A special thank you goes to the students and colleagues who patiently helped me navigate the complexities of the Japanese language and culture. Your kindness and willingness to teach not only made my academic journey smoother but also enriched my personal experiences in Japan.

I am grateful to my friend, Romain, whose wisdom as an experienced PhD holder offered me reassurance and invaluable perspective during moments of doubt. Our thought-provoking discussions about biology–while far from the scope of my research–were a constant source of fascination, reminding me of the broader beauty of scientific inquiry.

To my parents, Laurent and Marie-Bénédicte, thank you for your unconditional love, patience, and unwavering belief in me. Your constant support has been my foundation throughout this journey, giving me the strength and confidence to persevere. I am deeply grateful for the sacrifices you have made and the values you have instilled in me, which have profoundly shaped the person I am today.

To my siblings, Hortense, Louis-Etienne, and Joseph, thank you for your encouragement and for always being there for me, even from across continents. Your presence and support have been a source of comfort and joy every step of the way.

To my wife, Serina, my deepest gratitude goes to you for your constant support, patience, and love. Your belief in me, even during the most challenging moments, gave me the strength to persevere.

I gratefully acknowledge the support of the Japan Society for the Promotion of Science (JSPS) for funding my doctoral studies through the Research Fellowship for Young Scientists. This financial support provided me with the resources and opportunities to focus on my research and to engage in meaningful academic exchanges. I am truly honored to have been a recipient of this prestigious fellowship, which significantly contributed to the successful completion of this work.

Finally, I would like to extend my heartfelt thanks to everyone who has contributed, directly or indirectly, to the completion of this thesis. Each one of you has played an essential role in my journey, and I am truly grateful for your support and encouragement. Thank you.

References

[1] I. von Sivers, A. Templeton, F. Künzner, G. Köster, J. Drury, A. Philippides, T. Neckel, and H. J. Bungartz, "Modelling social identification and helping in evacuation simulation," *Safety Science*, vol. 89, pp. 288–300, 2016.

[2] J. Adrian, A. Seyfried, and A. Sieben, "Crowds in front of bottlenecks at entrances from the perspective of physics and social psychology," *Journal of the Royal Society Interface*, vol. 17, no. 165, p. 20190871, 2020.

[3] M. Shiomi, F. Zanlungo, K. Hayashi, and T. Kanda, "Towards a Socially Acceptable Collision Avoidance for a Mobile Robot Navigating Among Pedestrians Using a Pedestrian Model," *International Journal of Social Robotics*, vol. 6, no. 3, pp. 443–455, 2014.

[4] F. Camara, N. Bellotto, S. Cosar, F. Weber, D. Nathanael, M. Althoff, J. Wu, J. Ruenz, A. Dietrich, G. Markkula, A. Schieben, F. Tango, N. Merat, and C. Fox, "Pedestrian models for autonomous driving part ii: High-level models of human behavior," *IEEE Transactions on Intelligent Transportation Systems*, vol. 22, no. 9, pp. 5453–5472, 2021.

[5] S. H. Scott and D. A. Winter, "Biomechanical model of the human foot: Kinematics and kinetics during the stance phase of walking," *Journal of Biomechanics*, vol. 26, no. 9, pp. 1091–1104, 1993.

[6] F. E. Zajac, R. R. Neptune, and S. A. Kautz, "Biomechanics and muscle coordination of human walking: Part i: Introduction to concepts, power transfer, dynamics and simulations," *Gait & Posture*, vol. 16, no. 3, pp. 215–232, 2002.

[7] S. Hoogendoorn and P. Bovy, "Pedestrian route-choice and activity scheduling theory and models," *Transportation Research Part B: Methodological*, vol. 38, no. 2, pp. 169–190, 2004.

[8] F. Zanlungo, "A collision-avoiding mechanism based on a theory of mind," *Advances in Complex Systems*, vol. 10, pp. 363–371, 2007.

[9] A. Corbetta and F. Toschi, "Physics of Human Crowds," *Annual Review of Condensed Matter Physics*, vol. 14, no. 1, pp. 311–333, 2023.

[10] D. Helbing and P. Molnar, "Social force model for pedestrian dynamics," *Physical Review E*, vol. 51, no. 5, pp. 4282–4286, 1995.

[11] S. Bandini, L. Crociani, A. Gorrini, and G. Vizzari, "An agent-based model of pedestrian dynamics considering groups: A real world case study," in *IEEE Conference on Intelligent Transportation Systems*, pp. 572–577, IEEE, 2014.

[12] A. Alahi, K. Goel, V. Ramanathan, A. Robicquet, L. Fei-Fei, and S. Savarese, "Social LSTM: Human trajectory prediction in crowded spaces," in *IEEE/CVF Conference on Computer Vision and Pattern Recognition*, 2016.

[13] A. Gupta, J. Johnson, L. Fei-Fei, S. Savarese, and A. Alahi, "Social gan: Socially acceptable trajectories with generative adversarial networks," in *IEEE/CVF Conference on Computer Vision and Pattern Recognition*, pp. 2255–2264, IEEE, 2018.

[14] F. Zanlungo, T. Ikeda, and T. Kanda, "Potential for the dynamics of pedestrians in a socially interacting group," *Physical Review E*, vol. 89, p. 012811, 2014.

[15] Z. Yücel, F. Zanlungo, and M. Shiomi, "Modeling the impact of interaction on pedestrian group motion," *Advanced Robotics*, vol. 32, no. 3, pp. 137–147, 2018.

[16] J. L. Tracy, D. Randles, and C. M. Steckler, "The nonverbal communication of emotions," *Current Opinion in Behavioral Sciences*, vol. 3, pp. 25–30, 2015.

[17] S. Goldin-Meadow, "Using our hands to change our minds," *WIREs Cognitive Science*, vol. 8, no. 1-2, p. e1368, 2017.

[18] M. Karam, *A framework for research and design of gesture-based human-computer interactions*. PhD thesis, University of Southampton, 2006.

[19] W. Pouw and A. B. Hostetter, "Gesture as predictive action," *Reti, saperi, linguaggi*, vol. 3, no. 1, pp. 57–80, 2016.

[20] J. J. Lee, C. Breazeal, and D. DeSteno, "Role of speaker cues in attention inference," *Frontiers in Robotics and AI*, vol. 4, p. 47, 2017.

[21] R. A. Gordon and D. Druckman, "Nonverbal behaviour as communication: Approaches, issues, and research," in *The handbook of communication skills*, pp. 81–134, Routledge, 2018.

[22] C. Breazeal, C. D. Kidd, A. L. Thomaz, G. Hoffman, and M. Berlin, "Effects of nonverbal communication on efficiency and robustness in human-robot teamwork," in *IEEE/RSJ International Conference on Intelligent Robots and Systems*, pp. 708–713, IEEE, 2005.

[23] S. S. Rautaray and A. Agrawal, "Vision based hand gesture recognition for human computer interaction: A survey," *Artificial Intelligence Review*, vol. 43, no. 1, pp. 1–54, 2015.

[24] G. Saponaro, L. Jamone, A. Bernardino, and G. Salvi, "Interactive robot learning of gestures, language and affordances," in *GLU*, pp. 83–87, 2017.

[25] S. Sheikholeslami, A. Moon, and E. A. Croft, "Cooperative gestures for industry: Exploring the efficacy of robot hand configurations in expression of instructional gestures for human–robot interaction," *The International Journal of Robotics Research*, vol. 36, no. 5-7, pp. 699–720, 2017.

[26] Consortium for the Physics and Psychology of Human Crowd Dynamics, "A glossary for research on human crowd dynamics," *Collective Dynamics*, vol. 4, pp. 1–13, 2019.

[27] Z. Yücel, F. Zanlungo, and M. Shiomi, "Walk the talk: Gestures in mobile interaction," in *ICSR*, pp. 220–230, 2017.

[28] P. S. Katz, "Evolution of central pattern generators and rhythmic behaviours," *Philosophical Transactions of the Royal Society B*, vol. 371, no. 1685, p. 20150057, 2016.

[29] P. Meyns, S. M. Bruijn, and J. Duysens, "The how and why of arm swing during human walking," *Gait & Posture*, vol. 38, no. 4, pp. 555–562, 2013.

[30] R. E. Van Emmerik, J. Hamill, and W. J. McDermott, "Variability and coordinative function in human gait," *Quest*, vol. 57, no. 1, pp. 102–123, 2005.

[31] M. Punt, S. M. Bruijn, H. Wittink, and J. H. van Dieën, "Effect of arm swing strategy on local dynamic stability of human gait," *Gait & posture*, vol. 41, no. 2, pp. 504–509, 2015.

[32] G. Di Scala, M. Dupuy, E. Guillaud, E. Doat, E. Barse, B. Dillhareguy, F. Jean, M. Audiffren, J. Cazalets, and S. Chanraud, "Efficiency of sensorimotor networks: Posture and gait in young and older adults," *Experimental Aging Research*, pp. 1–16, 2019.

[33] C. Simon-Martinez, G. L. dos Santos, E. Jaspers, R. Vanderschueren, L. Mailleux, K. Klingels, E. Ortibus, K. Desloovere, and H. Feys, "Age-related changes in upper limb motion during typical development," *PLOS ONE*, vol. 13, no. 6, p. e0198524, 2018.

[34] F. Solera, S. Calderara, E. Ristani, C. Tomasi, and R. Cucchiara, "Tracking social groups within and across cameras," *IEEE Transactions on Circuits and Systems for Video Technology*, 2017.

[35] J. P. Ferreira, M. M. Crisostomo, and A. P. Coimbra, "Human gait acquisition and characterization," *IEEE Transactions on Instrumentation and Measurement*, vol. 58, no. 9, pp. 2979–2988, 2009.

[36] S. Meng, S. Jin, J. Li, K. Hashimoto, S. Guo, and S. Dai, "The analysis of human walking stability using zmp in sagittal plane," in *IEEE International Conference on Cybernetics and Intelligent Systems (CIS) and IEEE Conference on Robotics, Automation and Mechatronics (RAM)*, pp. 496–501, IEEE, 2017.

[37] V. De-León-Gómez, Q. Luo, A. Kalouguine, J. A. Pámanes, Y. Aoustin, and C. Chevallereau, "An essential model for generating walking motions for humanoid robots," *Robotics and Autonomous Systems*, vol. 112, pp. 229–243, 2019.

[38] L. Y. Vorochaeva, A. S. Yatsun, and S. F. Jatsun, "Controlling a quasistatic gait of an exoskeleton on the basis of the expert system," *Trudy SPIIRAN*, vol. 52, pp. 70–94, 2017.

[39] A. Gorobtsov, A. Andreev, A. Markov, A. Skorikov, and P. Tarasov, "Features of

solving the inverse dynamic method equations for the synthesis of stable walking robots controlled motion," *SPIIRAS Proceedings*, vol. 18, pp. 85–122, 2019.

[40] M. Salem, S. Kopp, I. Wachsmuth, K. Rohlfing, and F. Joublin, "Generation and evaluation of communicative robot gesture," *IJSR*, no. 2, pp. 201–217, 2012.

[41] P. Haddington, L. Mondada, and M. Nevile, *Interaction and mobility: Language and the body in motion*, vol. 20. Walter de Gruyter, 2013.

[42] E. Bochinski, V. Eiselein, and T. Sikora, "Training a convolutional neural network for multi-class object detection using solely virtual world data," in *IEEE Conference on Advanced Video and Signal Based Surveillance*, pp. 278–285, IEEE, 2016.

[43] J. Berclaz, F. Fleuret, E. Turetken, and P. Fua, "Multiple object tracking using k-shortest paths optimization," *IEEE Transactions on Pattern Analysis and Machine Intelligence*, vol. 33, no. 9, pp. 1806–1819, 2011.

[44] F. Zanlungo, Z. Yücel, D. Brščić, T. Kanda, and N. Hagita, "Intrinsic group behaviour: Dependence of pedestrian dyad dynamics on principal social and personal features," *PLOS ONE*, vol. 12, no. 11, p. e0187253, 2017.

[45] H. Riemenschneider, "YACVID." `http://yacvid.hayko.at/`, 2018.

[46] E. Ristani, F. Solera, R. Zou, R. Cucchiara, and C. Tomasi, "Performance measures and a data set for multi-target, multi-camera tracking," in *European Conference on Computer Vision*, pp. 17–35, 2016.

[47] D. McNeill, *Hand and mind: What gestures reveal about thought.* University of Chicago Press, 1992.

[48] K. Krippendorff, *Content analysis: An introduction to its methodology.* Sage, 2018.

[49] K. Krippendorff, "Reliability in content analysis: Some common misconceptions and recommendations," *Human Communication Research*, vol. 30, no. 3, pp. 411–433, 2004.

[50] Z. Cao, T. Simon, S.-E. Wei, and Y. Sheikh, "Realtime multi-person 2D pose estimation using part affinity fields," in *IEEE/CVF Conference on Computer Vision and Pattern Recognition*, pp. 7291–7299, 2017.

[51] E. Ristani, F. Solera, R. S. Zou, R. Zou, Cucchiara, and C. T. Tomasi, "DukeMTMC Project." `http://vision.cs.duke.edu/DukeMTMC/`, 2018.

[52] M. Ross, H. Shaffer, A. Cohen, R. Freudberg, and H. Manley, "Average magnitude difference function pitch extractor," *IEEE Transactions on Aerospace and Electronic Systems*, vol. 22, no. 5, pp. 353–362, 1974.

[53] S. Yan, Y. Xiong, and D. Lin, "Spatial temporal graph convolutional networks for skeleton-based action recognition," in *AAAI conference on artificial intelligence*, 2018.

[54] C. McPhail and R. T. Wohlstein, "Using film to analyze pedestrian behavior," *Sociological Methods and Research*, vol. 10, no. 3, pp. 347–375, 1982.

[55] W. Xie, E. W. M. Lee, T. Li, M. Shi, R. Cao, and Y. Zhang, "A study of group effects in pedestrian crowd evacuation: Experiments, modelling and simulation," *Safety Science*, vol. 133, p. 105029, 2021.

[56] I. von Sivers, A. Templeton, F. Künzner, G. Köster, J. Drury, A. O. Philippides, T. Neckel, and H.-J. Bungartz, "Modelling social identification and helping in evacuation simulation," *Safety Science*, vol. 89, pp. 288–300, 2016.

[57] C. von Krüchten and A. Schadschneider, "Empirical study on social groups in pedestrian evacuation dynamics," *Physica A: Statistical Mechanics and its Applications*, vol. 475, pp. 129–141, 2017.

[58] Y. Hu, J. Zhang, W. Song, and N. W. F. Bode, "Social groups barely change the speed-density relationship in unidirectional pedestrian flow, but affect operational behaviours," *Safety Science*, vol. 139, p. 105259, 2021.

[59] F. Zanlungo, L. Crociani, Z. Yücel, and T. Kanda, "The effect of social groups on the dynamics of bi-directional pedestrian flow: A numerical study," in *Traffic and Granular Flow 2019*, pp. 307–313, Springer International Publishing, 2020.

[60] B. Zhang, Y. Gao, Y. Han, S. Liang, Q. Chen, and Z. Yu, "Walking characteristics and collision avoidance strategy in bidirectional pedestrian flow: a study focused on the influence of social groups," *Journal of Statistical Mechanics: Theory and Experiment*, vol. 2022, no. 7, p. 073405, 2022.

[61] B. Zhang, W. Chen, X. Ma, P. Qiu, and F. Liu, "Experimental study on pedestrian behavior in a mixed crowd of individuals and groups," *Physica A: Statistical Mechanics and its Applications*, vol. 556, p. 124814, 2020.

[62] Y. Hu, J. Zhang, H. Xiao, S. Cao, X. Ren, X. Liang, H. Li, and W. Song, "Experimental study and analysis on behaviours and strategies of social groups and individuals," *Safety Science*, vol. 127, p. 104736, 2020.

[63] D. Brščić, T. Kanda, T. Ikeda, and T. Miyashita, "Person tracking in large public spaces using 3-d range sensors," *IEEE Transactions on Human-Machine Systems*, vol. 43, no. 6, pp. 522–534, 2013.

[64] M. Moussaïd, N. Perozo, S. Garnier, D. Helbing, and G. Theraulaz, "The walking behaviour of pedestrian social groups and its impact on crowd dynamics," *PLOS ONE*, vol. 5, no. 4, p. e10047, 2010.

[65] M. Schultz, L. Rößger, H. Fricke, and B. Schlag, "Group dynamic behavior and psychometric profiles as substantial driver for pedestrian dynamics," in *Pedestrian and Evacuation Dynamics*, pp. 1097–1111, Springer International Publishing, 2013.

[66] M. Costa, "Interpersonal distances in group walking," *Journal of Nonverbal Behavior*, vol. 34, no. 1, pp. 15–26, 2009.

[67] F. Zanlungo, D. Brščić, and T. Kanda, "Spatial-size scaling of pedestrian groups under growing density conditions," *Physical Review E*, vol. 91, no. 6, 2015.

[68] L. Fu, S. Cao, Y. Shi, S. Chen, P. Yang, and J. Fang, "Walking behavior of pedestrian social groups on stairs: A field study," *Safety Science*, vol. 117, pp. 447–457, 2019.

[69] L. Fu, Y. Liu, P. Yang, Y. Shi, Y. Zhao, and J. Fang, "Dynamic analysis of stepping behavior of pedestrian social groups on stairs," *Journal of Statistical Mechanics: Theory and Experiment*, vol. 2020, no. 6, p. 063403, 2020.

[70] L. Fu, Q. Shi, H. Qin, Y. Zhang, and Y. Shi, "Analysis of movement behavior of pedestrian social groups through a bottleneck," *Physica A: Statistical Mechanics and its Applications*, vol. 608, p. 128257, 2022.

[71] Y. Zhang, J. Pettre, X. Qin, S. Donikian, and Q. Peng, "A local behavior model for small pedestrian groups," in *International Conference on Computer-Aided Design and Computer Graphics*, pp. 275–281, IEEE, 2011.

[72] A. Gorrini, L. Crociani, C. Feliciani, P. Zhao, K. Nishinari, and S. Bandini, "Social groups and pedestrian crowds: Experiment on dyads in a counter flow scenario," *arXiv preprint arXiv:1610.08325*, 2016.

[73] F. Zanlungo and T. Kanda, "A mesoscopic model for the effect of density on pedestrian group dynamics," *Europhysics Letters*, vol. 111, no. 3, p. 38007, 2015.

[74] I. Karamouzas, B. Skinner, and S. J. Guy, "Universal power law governing pedestrian interactions," *Physical Review Letters*, vol. 113, no. 23, 2014.

[75] G. Vizzari, L. Manenti, and L. Crociani, "Adaptive pedestrian behaviour for the preservation of group cohesion," *Complex Adaptive Systems Modeling*, vol. 1, no. 1, 2013.

[76] G. Köster, M. Seitz, F. Treml, D. Hartmann, and W. Klein, "On modelling the influence of group formations in a crowd," *Contemporary Social Science*, vol. 6, no. 3, pp. 397–414, 2011.

[77] Z. Yücel, F. Zanlungo, C. Feliciani, A. Gregorj, and T. Kanda, "Identification of social relation within pedestrian dyads," *PLOS ONE*, vol. 14, no. 10, p. e0223656, 2019.

[78] F. Zanlungo, Z. Yücel, and T. Kanda, "Intrinsic group behaviour II: On the dependence of triad spatial dynamics on social and personal features; and on the effect of social interaction on small group dynamics," *PLOS ONE*, vol. 14, no. 12, p. e0225704, 2019.

[79] X. Wei, W. Lv, W. Song, and X. Li, "Survey study and experimental investigation on the local behavior of pedestrian groups," *Complexity*, vol. 20, no. 6, pp. 87–97, 2015.

[80] A. K.-F. Lui, Y.-H. Chan, and M.-F. Leung, "Modelling of destinations for data-driven pedestrian trajectory prediction in public buildings," in *IEEE International Conference on Big Data*, pp. 1709–1717, Institute of Electrical and Electronics Engineers (IEEE), 2021.

[81] H. Kidokoro, T. Kanda, D. Brščić, and M. Shiomi, "Simulation-based behavior planning to prevent congestion of pedestrians around a robot," *IEEE Transactions on Robotics*, vol. 31, no. 6, pp. 1419–1431, 2015.

[82] M. Fahad, Z. Chen, and Y. Guo, "Learning how pedestrians navigate: A deep inverse reinforcement learning approach," in *IEEE/RSJ International Conference on Intelligent Robots and Systems*, pp. 819–826, Institute of Electrical and Electronics Engineers (IEEE), 2018.

[83] T. Ono and T. Kanamaru, "Prediction of pedestrian trajectory based on long short-term memory of data," in *International Conference on Control, Automation and Systems*, pp. 1676–1679, Institute of Electrical and Electronics Engineers (IEEE), 2021.

[84] R. Akabane and Y. Kato, "Pedestrian trajectory prediction using pre-trained machine learning model for human-following mobile robot," in *IEEE International Conference on Big Data*, pp. 3453–3458, Institute of Electrical and Electronics Engineers (IEEE), 2020.

[85] S. H. Kiss, K. Katuwandeniya, A. Alempijevic, and T. Vidal-Calleja, "Constrained gaussian processes with integrated kernels for long-horizon prediction of dense pedestrian crowd flows," *IEEE Robotics and Automation Letters*, vol. 7, no. 3, pp. 7343–7350, 2022.

[86] N. W. Bode, S. Holl, W. Mehner, and A. Seyfried, "Disentangling the impact of social groups on response times and movement dynamics in evacuations," *PLOS ONE*, vol. 10, no. 3, p. e0121227, 2015.

[87] R. Lovreglio, E. Ronchi, and D. Nilsson, "An evacuation decision model based on perceived risk, social influence and behavioural uncertainty," *Simulation Modelling Practice and Theory*, vol. 66, pp. 226–242, 2016.

[88] C. Von Krüchten and A. Schadschneider, "Empirical study on social groups in pedestrian evacuation dynamics," *Physica A: Statistical Mechanics and its Applications*, vol. 475, pp. 129–141, 2017.

[89] C. Feliciani, I. Zuriguel, A. Garcimartín, D. Maza, and K. Nishinari, "Systematic experimental investigation of the obstacle effect during non-competitive and extremely competitive evacuations," *Scientific Reports*, vol. 10, no. 1, 2020.

[90] H. Gayathri, P. Aparna, and A. Verma, "A review of studies on understanding crowd

dynamics in the context of crowd safety in mass religious gatherings," *International Journal of Disaster Risk Reduction*, vol. 25, pp. 82–91, 2017.

[91] I. Karamouzas and M. Overmars, "Simulating and evaluating the local behavior of small pedestrian groups," *IEEE Transactions on Visualization and Computer Graphics*, vol. 18, no. 3, pp. 394–406, 2011.

[92] I. von Sivers, F. Künzner, and G. Köster, "Pedestrian evacuation simulation with separated families," in *Pedestrian and Evacuation Dynamics*, 2016.

[93] L. He, J. Pan, W. Wang, and D. Manocha, "Proxemic group behaviors using reciprocal multi-agent navigation," in *IEEE International Conference on Robotics and Automation*, pp. 292–297, IEEE, 2016.

[94] Y. Feng and D. Li, "An empirical study and a conceptual model on heterogeneity of pedestrian social groups for friend-group and family-group," in *Pedestrian and Evacuation Dynamics*, pp. 402–407, University of Science and Technology of China Press, 2016.

[95] M. J. Seitz, A. Templeton, J. Drury, G. Köster, and A. Philippides, "Parsimony versus reductionism: How can crowd psychology be introduced into computer simulation?," *Review of General Psychology*, vol. 21, no. 1, pp. 95–102, 2017.

[96] U. Chattaraj, A. Seyfried, and P. Chakroborty, "Comparison of pedestrian fundamental diagram across cultures," *Advances in complex systems*, vol. 12, no. 03, pp. 393–405, 2009.

[97] F. Zanlungo, T. Ikeda, and T. Kanda, "Social force model with explicit collision prediction," *EPL (Europhysics Letters)*, vol. 93, no. 6, p. 68005, 2011.

[98] R. P. Feynman, R. B. Leighton, and M. Sands, *The Feynman Lectures on Physics (Vol. I)*. New York: Addison-Wesley, 1965.

[99] ATR, "Pedestrian group dataset," 2015.

[100] D. Brščić, T. Kanda, T. Ikeda, and T. Miyashita, "Person tracking in large public spaces using 3-D range sensors," *IEEE Transactions on Human-Machine Systems*, vol. 43, no. 6, pp. 522–534, 2013.

[101] D. F. Glas, F. Ferreri, T. Miyashita, H. Ishiguro, and N. Hagita, "Automatic calibration of laser range finder positions for pedestrian tracking based on social group detections," *Advanced Robotics*, vol. 28, no. 9, pp. 573–588, 2014.

[102] D. B. Bugental, "Acquisition of the algorithms of social life: A domain-based approach," *Psychological Bulletin*, vol. 126, no. 2, pp. 187–219, 2000.

[103] M. L. Knapp, J. A. Hall, and T. G. Horgan, *Nonverbal Communication in Human Interaction*. Cengage Learning, 2013.

[104] M. E. Cinelli and A. E. Patla, "Locomotor avoidance behaviours during a visually guided task involving an approaching object," *Gait & Posture*, vol. 28, no. 4, pp. 596–601, 2008.

[105] K. Kitazawa and T. Fujiyama, "Pedestrian vision and collision avoidance behavior: Investigation of the information process space of pedestrians using an eye tracker," in *Pedestrian and Evacuation Dynamics*, pp. 95–108, Springer Berlin Heidelberg, 2009.

[106] L. D. Landau and E. M. Lifshitz, *Mechanics: Volume 1 (Course of Theoretical Physics Series)*. Oxford: Pergamon Press, 1960.

[107] M. Blau, *Lecture notes on general relativity*. Albert Einstein Center for Fundamental Physics, 2011.

[108] B. C. Hall, *Quantum Theory for Mathematicians*, vol. 267. Springer New York, NY, 2013.

[109] F. Zanlungo, T. Ikeda, and T. Kanda, "A microscopic "social norm" model to obtain realistic macroscopic velocity and density pedestrian distributions," *PLOS ONE*, vol. 7, no. 12, p. e50720, 2012.

[110] C. A. Pouw, F. Toschi, F. van Schadewijk, and A. Corbetta, "Monitoring physical distancing for crowd management: Real-time trajectory and group analysis," *PLOS ONE*, vol. 15, no. 10, p. e0240963, 2020.

[111] F. Rojas, F. Tarnogol, and H. S. Yang, "Dynamic social formations of pedestrian groups navigating and using public transportation in a virtual city," *The Visual Computer*, vol. 32, no. 3, pp. 335–345, 2016.

[112] A. Templeton, J. Drury, and A. Philippides, "From mindless masses to small groups: Conceptualizing collective behavior in crowd modeling," *Review of General Psychology*, vol. 19, no. 3, pp. 215–229, 2015.

[113] M. Huber, Y.-H. Su, M. Krüger, K. Faschian, S. Glasauer, and J. Hermsdörfer, "Adjustments of speed and path when avoiding collisions with another pedestrian," *PLOS ONE*, vol. 9, no. 2, p. e89589, 2014.

[114] A. N. Alhawsawi, M. Sarvi, E. Felemban, A. Rajabifard, and J. Wang, "Understanding the characteristics of pedestrians when passing obstacles of different sizes: An experimental study," *Collective Dynamics*, vol. 6, p. 1–23, 2021.

[115] S. Cao, Y. Li, J. Ni, and X. Wu, "Gait analysis and avoidance mechanism of pedestrians under the quantitative control of visibility," *Transportmetrica A: Transport Science*, vol. 20, no. 2, p. 2152300, 2024.

[116] Z. Zhou, Y. Cai, R. Ke, and J. Yang, "A collision avoidance model for two-pedestrian groups: Considering random avoidance patterns," *Physica A: Statistical Mechanics and its Applications*, vol. 475, pp. 142–154, 2017.

[117] Q.-L. Wang, Y. Chen, H.-R. Dong, M. Zhou, and B. Ning, "A new collision avoidance model for pedestrian dynamics," *Chinese Physics B*, vol. 24, no. 3, p. 038901, 2015.

[118] I. Karamouzas, P. Heil, P. van Beek, and M. H. Overmars, "A Predictive Collision Avoidance Model for Pedestrian Simulation," in *Motion in Games* (A. Egges, R. Geraerts, and M. Overmars, eds.), Lecture Notes in Computer Science, (Berlin, Heidelberg), pp. 41–52, Springer, 2009.

[119] A. Corbetta, J. A. Meeusen, C.-m. Lee, R. Benzi, and F. Toschi, "Physics-based modeling and data representation of pairwise interactions among pedestrians," *Physical Review E*, vol. 98, no. 6, p. 062310, 2018.

[120] A. Corbetta, L. Schilders, and F. Toschi, "High-Statistics Modeling of Complex Pedestrian Avoidance Scenarios," in *Crowd Dynamics, Volume 2: Theory, Models, and Applications* (L. Gibelli, ed.), Modeling and Simulation in Science, Engineering and Technology, pp. 33–53, Springer International Publishing, 2020.

[121] A. Gregorj, Z. Yücel, F. Zanlungo, C. Feliciani, and T. Kanda, "Social aspects of collision avoidance: a detailed analysis of two-person groups and individual pedestrians," *Scientific Reports*, vol. 13, no. 1, p. 5756, 2023.

[122] A. Gregorj, Z. Yücel, F. Zanlungo, and T. Kanda, "On the influence of group social interaction on intrusive behaviours," in *Traffic and Granular Flow '22* (K. R. Rao, A. Seyfried, and A. Schadschneider, eds.), (Singapore), pp. 117–124, Springer Nature Singapore, 2024.

[123] A. Gregorj, Z. Yücel, F. Zanlungo, C. Feliciani, and T. Kanda, "On the influence of group social relation on the dynamics of pedestrians outside the group," in *Pedestrian and Evacuation Dynamics*, 2021, abstract.

[124] G. Turchetti, F. Zanlungo, and B. Giorgini, "Dynamics and thermodynamics of a gas of automata," *Europhysics Letters*, vol. 78, no. 5, p. 58003, 2007.

[125] F. Zanlungo and T. Kanda, "Do walking pedestrians stabily interact inside a large group? analysis of group and sub-group spatial structure," in *Proceedings of the Annual Meeting of the Cognitive Science Society*, vol. 35, 2013.

[126] M. Baqui and R. Löhner, "Pedpiv: Pedestrian velocity extraction from particle image velocimetry," *IEEE Transactions on Intelligent Transportation Systems*, vol. 21, no. 2, pp. 580–589, 2019.

[127] E. Ronchi, "Developing and validating evacuation models for fire safety engineering," *Fire Safety Journal*, vol. 120, p. 103020, 2021.

[128] J. Francis, B. Giles-Corti, L. Wood, and M. Knuiman, "Creating sense of community: The role of public space," *Journal of Environmental Psychology*, vol. 32, no. 4, pp. 401–409, 2012.

[129] S. Ferrer, T. Ruiz, and L. Mars, "A qualitative study on the role of the built environment for short walking trips," *Transportation Research Part F: Traffic Psychology and Behaviour*, vol. 33, pp. 141–160, 2015.

[130] W. W. Braham, J. M. Lee, E. Oskierko-Jeznacki, B. Silverman, and N. Khansari, "Spatial concentration of urban assets in the Philadelphia region: An emergy synthesis," *Ecological Modelling*, vol. 401, pp. 52–68, 2019.

[131] A. E. Patla and M. Greig, “Any way you look at it, successful obstacle negotiation needs visually guided on-line foot placement regulation during the approach phase,” *Neuroscience Letters*, vol. 397, no. 1-2, pp. 110–114, 2006.

[132] J. J. Fruin, “Designing for pedestrians: A level-of-service concept,” *Highway Research Record*, pp. 1–15, 1971.

[133] K. W. Rio, G. C. Dachner, and W. H. Warren, “Local interactions underlying collective motion in human crowds,” *Proceedings of the Royal Society B: Biological Sciences*, vol. 285, no. 1878, p. 20180611, 2018.

[134] H. Murakami, C. Feliciani, Y. Nishiyama, and K. Nishinari, “Mutual anticipation can contribute to self-organization in human crowds,” *Science Advances*, vol. 7, no. 12, p. eabe7758, 2021.

[135] E. Papadimitriou, G. Yannis, and J. Golias, “A critical assessment of pedestrian behaviour models,” *Transportation Research Part F: Traffic Psychology and Behaviour*, vol. 12, no. 3, pp. 242–255, 2009.

[136] R. Löhner, “On the modeling of pedestrian motion,” *Applied Mathematical Modelling*, vol. 34, no. 2, pp. 366–382, 2010.

[137] A. Gregorj, Z. Yücel, F. Zanlungo, and T. Kanda, “Asymmetries in Group-Individual Collision Avoidance due to Social Factors,” *Collective Dynamics*, vol. 9, pp. 1–9, 2024.

[138] M. Schultz, L. Rößger, H. Fricke, and B. Schlag, “Group dynamic behavior and psychometric profiles as substantial driver for pedestrian dynamics,” in *Pedestrian and Evacuation Dynamics 2012* (U. Weidmann, U. Kirsch, and M. Schreckenberg, eds.), pp. 1097–1111, Springer International Publishing, 2014.

[139] M. Costa, “Interpersonal distances in group walking,” *J Nonverbal Behav*, vol. 34, no. 1, pp. 15–26, 2010.

[140] T. M. Bhojwani, S. D. Lynch, M. A. Bühler, and A. Lamontagne, “Impact of dual tasking on gaze behaviour and locomotor strategies adopted while circumventing virtual pedestrians during a collision avoidance task,” *Experimental Brain Research*, vol. 240, no. 10, pp. 2633–2645, 2022.

[141] A. Shumway-Cook, A. E. Patla, A. Stewart, L. Ferrucci, M. A. Ciol, and J. M. Guralnik, "Environmental demands associated with community mobility in older adults with and without mobility disabilities," *Physical Therapy*, vol. 82, no. 7, pp. 670–681, 2002.

[142] A. E. Patla and A. Shumway-Cook, "Dimensions of mobility: defining the complexity and difficulty associated with community mobility," *Journal of Aging and Physical Activity*, vol. 7, no. 1, pp. 7–19, 1999.

[143] P. Cisek and A. Pastor-Bernier, "On the challenges and mechanisms of embodied decisions," *Philosophical Transactions of the Royal Society B: Biological Sciences*, vol. 369, no. 1655, p. 20130479, 2014.

[144] J. J. Gibson, *The Ecological Approach to Visual Perception.* Psychology Press, 2014.

[145] J. R. Busemeyer and J. T. Townsend, "Decision field theory: A dynamic-cognitive approach to decision making in an uncertain environment.," *Psychological Review*, vol. 100, no. 3, p. 432, 1993.

[146] P. Cisek, "Cortical mechanisms of action selection: The affordance competition hypothesis," *Philosophical Transactions of the Royal Society B: Biological Sciences*, vol. 362, no. 1485, pp. 1585–1599, 2007.

[147] J. E. Cutting, P. M. Vishton, and P. A. Braren, "How we avoid collisions with stationary and moving objects.," *Psychological Review*, vol. 102, no. 4, p. 627, 1995.

[148] M. Gérin-Lajoie, C. L. Richards, and B. J. McFadyen, "The negotiation of stationary and moving obstructions during walking: Anticipatory locomotor adaptations and preservation of personal space," *Motor Control*, vol. 9, no. 3, pp. 242–269, 2005.

[149] D. Marr, *Vision: A computational investigation into the human representation and processing of visual information.* MIT press, 2010.

[150] L. Itti and C. Koch, "A saliency-based search mechanism for overt and covert shifts of visual attention," *Vision Research*, vol. 40, no. 10-12, pp. 1489–1506, 2000.

[151] A. Torralba, A. Oliva, M. S. Castelhano, and J. M. Henderson, "Contextual guidance of eye movements and attention in real-world scenes: the role of global features in object search.," *Psychological Review*, vol. 113, no. 4, p. 766, 2006.

[152] A. E. Patla, "Understanding the roles of vision in the control of human locomotion," *Gait & Posture*, vol. 5, no. 1, pp. 54–69, 1997.

[153] A. E. Patla, S. S. Tomescu, M. Greig, and A. Novak, "Gaze fixation patterns during goal-directed locomotion while navigating around obstacles and a new route-selection model," in *Eye Movements* (R. P. G. Van Gompel, M. H. Fischer, W. S. Murray, and R. L. Hill, eds.), pp. 677–696, Elsevier, 2007.

[154] M. R. Saeedpour-Parizi, S. E. Hassan, A. Azad, K. J. Baute, T. Baniasadi, and J. B. Shea, "Target position and avoidance margin effects on path planning in obstacle avoidance," *Scientific Reports*, vol. 11, no. 1, p. 15285, 2021.

[155] M. E. Cinelli and A. E. Patla, "Travel path conditions dictate the manner in which individuals avoid collisions," *Gait & Posture*, vol. 26, no. 2, pp. 186–193, 2007.

[156] J. M. Dabbs Jr and N. A. Stokes III, "Beauty is power: The use of space on the sidewalk," *Sociometry*, pp. 551–557, 1975.

[157] B. J. Van Basten, S. E. Jansen, and I. Karamouzas, "Exploiting motion capture to enhance avoidance behaviour in games," in *Motion in Games: Second International Workshop*, pp. 29–40, Springer, 2009.

[158] Y. Wu and H. Li, "Signalling security: An observational and game theory approach to inter-pedestrian psychology," *Transportation Research Part F: Traffic Psychology and Behaviour*, vol. 86, pp. 238–251, 2022.

[159] S. Baron-Cohen, A. M. Leslie, and U. Frith, "Does the autistic child have a "theory of mind"?," *Cognition*, vol. 21, no. 1, pp. 37–46, 1985.

[160] R. S. Hessels, A. J. van Doorn, J. S. Benjamins, G. A. Holleman, and I. T. Hooge, "Task-related gaze control in human crowd navigation," *Attention, Perception, & Psychophysics*, vol. 82, pp. 2482–2501, 2020.

[161] L. Nummenmaa, J. Hyönä, and J. K. Hietanen, "I'll walk this way: Eyes reveal the direction of locomotion and make passersby look and go the other way," *Psychological Science*, vol. 20, no. 12, pp. 1454–1458, 2009.

[162] S. Baron-Cohen, *Mindblindness: An essay on autism and theory of mind.* MIT press, 1997.

[163] Z. Yücel, A. A. Salah, Ç. Meriçli, T. Meriçli, R. Valenti, and T. Gevers, “Joint attention by gaze interpolation and saliency,” *IEEE Transactions on Cybernetics*, vol. 43, no. 3, pp. 829–842, 2013.

[164] C. Zhou, M.-C. Miao, X.-R. Chen, Y.-F. Hu, Q. Chang, M.-Y. Yan, and S.-G. Kuai, “Human-behaviour-based social locomotion model improves the humanization of social robots,” *Nature Machine Intelligence*, vol. 4, no. 11, pp. 1040–1052, 2022.

[165] A. D. Wilson and S. Golonka, “Embodied cognition is not what you think it is,” *Frontiers in Psychology*, vol. 4, p. 58, 2013.

[166] A. Kendon, *Conducting interaction: Patterns of behavior in focused encounters*, vol. 7. CUP Archive, 1990.

[167] F. Zanlungo, D. Brščić, and T. Kanda, “Spatial-size scaling of pedestrian groups under growing density conditions,” *Physical Review E*, vol. 91, no. 6, p. 062810, 2015.

[168] Z. Yücel, F. Zanlungo, T. Ikeda, T. Miyashita, and N. Hagita, “Deciphering the crowd: Modeling and identification of pedestrian group motion,” *Sensors*, vol. 13, no. 1, pp. 875–897, 2013.

[169] A. Dam, P. Oberoi, J. Pierson, M. Jeon, and R. N. C. Patrick, “Technological and social distractions at unsignalized and signalized campus crosswalks: A multi-stage naturalistic observation study,” *Transportation Research Part F: Traffic Psychology and Behaviour*, vol. 97, pp. 246–267, 2023.

[170] E. Bonabeau, “Agent-based modeling: Methods and techniques for simulating human systems,” *Proceedings of the National Academy of Sciences*, vol. 99, pp. 7280–7287, 2002.

[171] T. Bonnemain, M. Butano, T. Bonnet, I. Echeverría-Huarte, A. Seguin, A. Nicolas, C. Appert-Rolland, and D. Ullmo, “Pedestrians in static crowds are not grains, but game players,” *Physical Review E*, vol. 107, p. 024612, 2023.

[172] E. Cristiani, M. Menci, A. Malagnino, and G. G. Amaro, "An all-densities pedestrian simulator based on a dynamic evaluation of the interpersonal distances," *Physica A: Statistical Mechanics and its Applications*, vol. 616, p. 128625, 2023.

[173] I. Echeverría-Huarte and A. Nicolas, "Body and mind: Decoding the dynamics of pedestrians and the effect of smartphone distraction by coupling mechanical and decisional processes," *Transportation Research Part C: Emerging Technologies*, vol. 157, p. 104365, 2023.

[174] J. W. Bae, J. Kim, J. Yun, C. Kang, J. Choi, C. Kim, J. Lee, J. Choi, and J. W. Choi, "Sit dataset: Socially interactive pedestrian trajectory dataset for social navigation robots," in *Advances in Neural Information Processing Systems* (A. Oh, T. Naumann, A. Globerson, K. Saenko, M. Hardt, and S. Levine, eds.), vol. 36, pp. 24552–24563, Curran Associates, Inc., 2023.

[175] A. Wang, D. Sato, Y. Corzo, S. Simkin, A. Biswas, and A. Steinfeld, "Tbd pedestrian data collection: Towards rich, portable, and large-scale natural pedestrian data," 2024.

[176] G. G. M. van der Vleuten, F. Toschi, W. Schilders, and A. Corbetta, "Stochastic fluctuations of diluted pedestrian dynamics along curved paths," *Physical Review E*, vol. 109, p. 014605, 2024.

[177] X. Jia, C. Feliciani, D. Yanagisawa, and K. Nishinari, "Experimental study on the evading behavior of individual pedestrians when confronting with an obstacle in a corridor," *Physica A: Statistical Mechanics and its Applications*, vol. 531, p. 121735, 2019.

[178] A. Corbetta, C.-m. Lee, R. Benzi, A. Muntean, and F. Toschi, "Fluctuations around mean walking behaviors in diluted pedestrian flows," *Physical Review E*, vol. 95, p. 032316, 2017.

[179] T. Kanda and D. Brščić, "Data set: Pedestrian tracking with group annotations," 2015.

[180] D. F. Glas, T. Miyashita, H. Ishiguro, and N. Hagita, "Laser-based tracking of human position and orientation using parametric shape modeling," *Advanced robotics*, vol. 23, no. 4, pp. 405–428, 2009.

[181] M. Rosenberg, T. Zhang, P. Perona, and M. Meister, "Mice in a labyrinth show rapid learning, sudden insight, and efficient exploration," *eLife*, vol. 10, p. e66175, 2021.

[182] A. J. Calhoun, J. W. Pillow, and M. Murthy, "Unsupervised identification of the internal states that shape natural behavior," *Nature Neuroscience*, vol. 22, no. 12, pp. 2040–2049, 2019.

[183] C. Stringer, M. Pachitariu, N. Steinmetz, C. B. Reddy, M. Carandini, and K. D. Harris, "Spontaneous behaviors drive multidimensional, brainwide activity," *Science*, vol. 364, no. 6437, p. eaav7893, 2019.

[184] P. Sedgwick and N. Greenwood, "Understanding the Hawthorne effect," *BMJ*, vol. 351, 2015.

[185] J. McCambridge, J. Witton, and D. R. Elbourne, "Systematic review of the Hawthorne effect: New concepts are needed to study research participation effects," *Journal of Clinical Epidemiology*, vol. 67, no. 3, pp. 267–277, 2014.

[186] K. L. Leonard and M. C. Masatu, "Using the Hawthorne effect to examine the gap between a doctor's best possible practice and actual performance," *Journal of Development Economics*, vol. 93, no. 2, pp. 226–234, 2010.

[187] D. Schwartz, B. Fischhoff, T. Krishnamurti, and F. Sowell, "The Hawthorne effect and energy awareness," *Proceedings of the National Academy of Sciences*, vol. 110, no. 38, pp. 15242–15246, 2013.

[188] S. Farhan, M. A. Avalos, and N. J. Rosenblatt, "Variability of Spatiotemporal Gait Kinematics During Treadmill Walking: Is There a Hawthorne Effect?," *Journal of Applied Biomechanics*, vol. 39, no. 3, pp. 151–156, 2023.

[189] K. B. Friesen, Z. Zhang, P. G. Monaghan, G. D. Oliver, and J. A. Roper, "All eyes on you: How researcher presence changes the way you walk," *Scientific Reports*, vol. 10, no. 1, p. 17159, 2020.

[190] D. Mobbs, T. Wise, N. Suthana, N. Guzmán, N. Kriegeskorte, and J. Z. Leibo, "Promises and challenges of human computational ethology," *Neuron*, vol. 109, no. 14, pp. 2224–2238, 2021.

[191] J. L. Fleiss, B. Levin, and M. C. Paik, *Statistical Methods for Rates and Proportions*. Wiley, 2003.

[192] A. G. Knorr, L. Willacker, J. Hermsdörfer, S. Glasauer, and M. Krüger, "Influence of person-and situation-specific characteristics on collision avoidance behavior in human locomotion.," *Journal of Experimental Psychology: Human Perception and Performance*, vol. 42, no. 9, p. 1332, 2016.

[193] A.-H. Olivier, A. Marin, A. Crétual, A. Berthoz, and J. Pettré, "Collision avoidance between two walkers: Role-dependent strategies," *Gait & Posture*, vol. 38, no. 4, pp. 751–756, 2013.

[194] B. R. Fajen, "Guiding locomotion in complex, dynamic environments," *Frontiers in Behavioral Neuroscience*, vol. 7, p. 85, 2013.

[195] A. Savitzky and M. J. E. Golay, "Smoothing and differentiation of data by simplified least squares procedures.," *Analytical Chemistry*, vol. 36, no. 8, pp. 1627–1639, 1964.

[196] C. Kirtley, M. W. Whittle, and R. J. Jefferson, "Influence of walking speed on gait parameters," *Journal of Biomedical Engineering*, vol. 7, no. 4, pp. 282–288, 1985.

[197] H. Hediyeh, T. Sayed, M. H. Zaki, and G. Mori, "Pedestrian gait analysis using automated computer vision techniques," *Transportmetrica A: Transport Science*, vol. 10, no. 3, pp. 214–232, 2014.

[198] A.-H. Olivier, A. Marin, A. Crétual, and J. Pettré, "Minimal predicted distance: A common metric for collision avoidance during pairwise interactions between walkers," *Gait & Posture*, vol. 36, no. 3, pp. 399–404, 2012.

[199] T. Uetake, "Can we really walk straight?," *American Journal of Physical Anthropology*, vol. 89, no. 1, pp. 19–27, 1992.

[200] S. Ho, A. Mohtadi, K. Daud, U. Leonards, and T. C. Handy, "Using smartphone accelerometry to assess the relationship between cognitive load and gait dynamics during outdoor walking," *Scientific Reports*, vol. 9, no. 1, p. 3119, 2019.

[201] H. L. Hollingworth, "The central tendency of judgment," *The Journal of Philosophy, Psychology and Scientific Methods*, vol. 7, no. 17, pp. 461–469, 1910.

[202] M. Ballerini, N. Cabibbo, R. Candelier, A. Cavagna, E. Cisbani, I. Giardina, V. Lecomte, A. Orlandi, G. Parisi, A. Procaccini, *et al.*, "Interaction ruling animal collective behavior depends on topological rather than metric distance: Evidence from a field study," *Proceedings of the National Academy of Sciences*, vol. 105, no. 4, pp. 1232–1237, 2008.

[203] A. Gregorj, Z. Yücel, F. Zanlugo, and T. Kanda, "Ecological Data Reveal Imbalances in Collision Avoidance Due to Groups' Social Interaction."

[204] W. Daamen, S. Hoogendoorn, M. Campanella, and D. Versluis, "Interaction behavior between individual pedestrians," in *Pedestrian and Evacuation Dynamics 2012* (U. Weidmann, U. Kirsch, and M. Schreckenberg, eds.), pp. 1305–1313, Springer International Publishing, 2014.

[205] Y. Tao, A. Both, R. I. Silveira, K. Buchin, S. Sijben, R. S. Purves, P. Laube, D. Peng, K. Toohey, and M. Duckham, "A comparative analysis of trajectory similarity measures," *GIScience & Remote Sensing*, vol. 58, no. 5, pp. 643–669, 2021.

[206] W. H. Kruskal and W. A. Wallis, "Use of ranks in one-criterion variance analysis," *Journal of the American Statistical Association*, vol. 47, no. 260, pp. 583–621, 1952.

[207] B. L. Welch, "The generalization of Student's problem when several different population varlances are involved," *Biometrika*, vol. 34, no. 1-2, pp. 28–35, 1947.

[208] A. Seyfried, B. Steffen, and T. Lippert, "Basics of modelling the pedestrian flow," *Physica A: Statistical Mechanics and its Applications*, vol. 368, no. 1, pp. 232–238, 2006.

[209] A. Nicolas and F. H. Hassan, "Social groups in pedestrian crowds: Review of their influence on the dynamics and their modelling," *Transportmetrica A: Transport Science.*, vol. 19, no. 1, p. 1970651, 2023.

[210] H. Yamamoto, D. Yanagisawa, C. Feliciani, and K. Nishinari, "Body-rotation behavior of pedestrians for collision avoidance in passing and cross flow," *Transportation Research Part B: Methodological.*, vol. 122, pp. 486–510, 2019.

[211] T. Ikeda, H. Ishiguro, D. F. Glas, M. Shiomi, T. Miyashita, and N. Hagita, "Person identification by integrating wearable sensors and tracking results from environmental sensors," in *2010 IEEE International Conference on Robotics and Automation*, pp. 2637–2642, 2010.

[212] K. Kaji and N. Kawaguchi, "Estimating 3D pedestrian trajectories using stability of sensing signal," in *2016 International Conference on Indoor Positioning and Indoor Navigation (IPIN)*, pp. 1–8, 2016.

List of publications

[1] A. Gregorj, Z. Yücel, S. Harao, A. Monden, and M. Shiomi, "A signal processing perspective on human gait: decoupling walking oscillations and gestures," in *International Conference on Interactive Collaborative Robotics '19*, pp. 75–85, 2019.

[2] A. Gregorj, Z. Yücel, F. Zanlungo, and T. Kanda, "On the influence of group social interaction on intrusive behaviours," in *Traffic and Granular Flow '22* (K. R. Rao, A. Seyfried, and A. Schadschneider, eds.), (Singapore), pp. 117–124, Springer Nature Singapore, 2024.

[3] A. Gregorj, Z. Yücel, F. Zanlungo, C. Feliciani, and T. Kanda, "Social aspects of collision avoidance: a detailed analysis of two-person groups and individual pedestrians," *Scientific Reports*, vol. 13, p. 5756, 2023.

[4] A. Gregorj, Z. Yücel, F. Zanlungo, and T. Kanda, "Asymmetries in Group-Individual Collision Avoidance due to Social Factors," *Collective Dynamics*, vol. 9, pp. 1–9, 2024.